Species from feces:
Decoding the secrets of genetic resilience, microbiome shift and niche partitioning from droppings

Yue Shi

A dissertation

submitted in partial fulfillment of the

requirements for the degree of

Doctor of Philosophy

University of Washington

2019

Reading Committee:

Samuel K. Wasser, Chair

Noah Snyder-Mackler

Richard Olmstead

Program Authorized to Offer Degree:

Biology

University of Washington

Abstract

Species from feces:
Decoding the secrets of genetic resilience, microbiome shift and niche partitioning from droppings

Yue Shi

Chair of the Supervisory Committee:

Samuel K. Wasser

Department of Biology

Effective species recovery plans rely on adequate scientific data, being tailored to the species' natural history and keeping up with rapid socioeconomic changes. My dissertation focuses on two great conservation success stories, Tibetan antelope (*Pantholops hodgsonii*) on the Tibetan Plateau and gray wolf (*Canis lupus*) in Washington state. These two species have different needs in terms of recovery. Tibetan antelope have a unique natural history that we need to consider in order to help them recover to their maximal potential. Whereas, for wolves, as apex predators, their recoveries rely on restoring the full suite of trophic interactions in their ecosystem. I used noninvasive fecal sampling and molecular tools to study the natural history of Tibetan antelope and trophic interactions of wolves.

Chapter one shed light on how the movement of Tibetan antelope may be the genetic resilience mechanism in the face of dramatic population decline. It is crucial to ensure their migration routes remain unobstructed by growing human disturbances while continuing to enforce anti-poaching law enforcement efforts. Chapter two took a more in-depth look at their seasonal female migration, as it is synchronized with the perinatal period when substantial physiological changes take place. I characterized the maternal gut microbiome of Tibetan antelope and demonstrated its shift in microbiome composition during the transition from late pregnancy to the postpartum period. It is essential to build a baseline for the changes in microbiome during this critical transition period when both the females and offspring are most vulnerable. If increasing human activities disrupt their migration routes and reproductive cycles, we can have a better understanding of the impacts on their reproductive health.

Chapter three focused on characterizing the wolf-coyote interactions, how their interactions change over time and space, and how it might affect the local prey populations. I developed a dietary analysis protocol using fecal DNA and DNA metabarcoding to characterize their diet profiles with the fine-grained resolution. This protocol can be applied to other carnivore species to help understand the impacts of recovery of apex predators on the local ecosystems.

Acknowledgements

First, I would like to thank my advisor Samuel K. Wasser, who has provided me with amazing opportunities to study two iconic species on the opposing sides of the globe, Tibetan antelope on the Tibetan Plateau and gray wolves in Washington state. I want to thank him for encouraging me to become an independent, motivated and multi-skilled researcher over the past few years.

I would also like to thank my committee members Noah Snyder-Mackler, Richard Olmstead, Trevor Branch and Caroline Strömberg for their valuable and insightful suggestions for my dissertation. I am very grateful to Dick and Trevor for being willing to become my committee members in the last minute when I had difficulties scheduling my defense date in the summer of 2019. Dick is very old-fashioned in terms of providing feedback. He would print out my chapters and mark on it with red pen. He is so detailed-oriented that he found errors that nobody else could find. Noah is an amazing mentor and always responsive to my questions. I really appreciate his comments on my chapter 2 & 3. I thank Noah and his lab members for their advices on library prep and MiSeq sequencing.

I want to thank my collaborators at Northwest Institute of Plateau Biology, China for making my research projects possible. To begin with, I owe a huge thank you to professor Dr. Jianping Su, who has played many roles in my PhD study. He was with me in every single field trip from 2013 to 2018. He helped me facilitate all the field work, provided me with his lab environment/equipment for sample processing, and offered helpful suggestions for manuscripts. He is an amazing mentor and has taught me many life lessons. His enthusiasm for natural history, positive attitude towards life and curiosity about the nature truly inspired me.

Unfortunately, he passed away on June 27th, 2018. I would like to dedicate my first two chapters to him and his mentorship. I like to thank members in Su lab for their help with sampling collection and lab work. I thank Kekexili Natural Nature Reserve Administration for assistance in the fieldwork.

I would like to thank the previous and current Wasser lab members for their friendship, support and assistance during my time here. I would like to thank Rebecca Booth for lab work advice. I thank all the conservation canines and dog handlers who conducted sample collection for my chapter three. Special thanks to Hyeon Jeong Kim! I want to thank her for everything she has done for me. She is a great friend and peer mentor. I feel privileged to have had the opportunity to work with her. I am deeply touched and inspired by her kindness and compassion. She has made my experience at graduate school much more enjoyable. I feel very fortunate to have her as my academic sister.

I would like to thank my friends in Seattle. My seven years in Seattle have been so much fun because of their friendship. I also want to thank my family in China for believing in me and letting me live my life in my own way.

Last but not least, great thanks to all the fellowships and awards I have received, including China Scholarship Council (CSC) Graduate Research Fellowship, Fritz/Boeing International Research Fellowship, WRF Hall Fellowship, Wingfield-Ramenofsky Award and Riddiford-Truman Award.

Table of Contents

Chapter One

Genetic resilience of a once endangered species, Tibetan antelope (*Pantholops hodgsonii*)

Yue Shi[1, §, *], Jiarui Chen[2, §], Jianping Su[3, †], Tongzuo Zhang[3, *], Samuel K. Wasser[1]

[1] Department of Biology, University of Washington, Box 351800, Seattle, WA 98195, USA

[2] College of Eco-Environmental Engineering, Qinghai University, Xining, Qinghai, 810016, China

[3] Qinghai Key Laboratory of Animal Ecological Genomics, Northwest Institute of Plateau Biology, Chinese Academy of Sciences, No. 23 Xinning Road, Xining, Qinghai 810008, China

[§]: contributed equally to this work

[*]Correspondence: Yue Shi (yueshi@uw.edu) and Tongzuo Zhang (zhangtz@nwipb.cas.cn)

[†]: Deceased on 27 June 2018

Abstract

Population decline is assumed to reduce the population's genetic diversity and its ability to adapt to environmental changes. If life history traits can buffer against such impacts, conservation efforts should aim to maintain those traits in vulnerable species. Tibetan antelope *(Pantholops hodgsonii*) have experienced population decline by 95% due to illegal poaching in the 20th century. We hypothesize that opportunities for gene flow provided by their female-specific migration buffer their genetic diversity from the poaching impacts. We measured the mtDNA (control region or CR) and nuDNA (microsatellites or STR) diversity and population differentiation and tested for a genetic bottleneck. Our results showed that Tibetan antelope maintained considerable genetic diversity in both mtDNA CR and STR markers (H_d = 0.997; H_{obs} = 0.845). Post-poaching populations showed no evidence of a genetic bottleneck and no clear population structure. Pairwise F_{st} values using CR haplotype frequencies were higher than those using STR allele frequencies, suggesting different degrees of gene flow mediated by females and males. This study suggests that the movement conducted by either female or male Tibetan antelope may have buffered their loss of genetic diversity in the face of severe demographic decline. It is important to ensure the migration routes of Tibetan antelope remain unobstructed by growing human disturbances while continuing to enforce anti-poaching law enforcement efforts.

Keywords resilience, genetic diversity, gene flow, Tibetan antelope, conservation

Introduction

Biodiversity is one of the most important priorities in conservation biology, where genetic diversity is an essential pillar. The need to conserve genetic diversity within populations is based on two arguments: (1) the necessity of genetic diversity for evolution in response to changing environments (Lacy, 1987; Morris, Austin, & Belov, 2012); (2) the expected correlation between genetic diversity and population fitness (Reed & Frankham, 2003) and links to the "extinction vortex" from inbreeding depression among fragmented populations (Frankham, 2005; Keller & Waller, 2002). Many natural populations have experienced severe demographic reduction due to rapid human population growth, overexploitation, environmental change, and habitat fragmentation. While it is generally assumed that population decline can drive the loss of genetic diversity, some species are able to maintain high genetic diversity even after a significant population crash (Busch, Waser, & DeWoody, 2007; Gonzalez-Suarez, 2010; Hailer et al., 2006; Kuo & Janzen, 2004; Lippé, Dumont, & Bernatchez, 2006; O' Donnell, Richter, Dool, Monks, & Kerth, 2015). In such cases, life-history traits appear to buffer against the loss of genetic diversity (Hailer et al., 2006; Kuo & Janzen, 2004; Lippé et al., 2006). The life history of many migratory species offers great opportunities for gene flow via migration, introducing new alleles to the existing genetic diversity that might otherwise be lost from genetic drift (Busch et al., 2007; Frankham, 2015; Jangjoo, Matter, Roland, & Keyghobadi, 2016; Sremba, Hancock-Hanser, Branch, LeDuc, & Baker, 2012).

About one million Tibetan antelope (*Pantholops hodgsonii*) ranged across the Tibetan Plateau in the early 20th century (Buzzard, Wong, & Zhang, 2012). At the end of the 20th century, Tibetan antelope populations were reduced to the brink of extinction by illegal poaching for their

underfur, which was used to made Shahtoosh shawls. Its population size reached a low of 50,000 individuals in 2003, declining by 95% relative to its size in 1950 (Leclerc, Bellard, Luque, & Courchamp, 2015). International conservation efforts successfully curbed poaching activities through law enforcement and habitat protection, and by 2011, the number of Tibetan antelope individuals was estimated to have increased to 200,000 (Leclerc et al., 2015). The severe population reduction due to illegal poaching raised concerns regarding the genetic viability of Tibetan antelope populations and how it would affect their recovery.

Previous studies suggested that Tibetan antelope populations maintained high genetic variation with no signs of population structure (Ahmad et al., 2016; Du et al., 2016; Zhou, Li, Zhang, Yang, & Liu, 2007), although the genetic effects of the population crash on Tibetan antelope remain unclear. We hypothesize that the unique life history of Tibetan antelope may have buffered them against the loss of genetic diversity. Every summer, female Tibetan antelope from different wintering grounds migrate to the common calving ground to give birth, leave shortly after parturition and migrate back to their original wintering grounds with their newborn calves. However, not all females migrate back to their original wintering grounds (Buho et al., 2011). Male movements may also promote gene flow since there are no obvious geographic barriers on the Tibetan Plateau, although the movement of males remains unknown (Schaller, 1998). We assessed the genetic diversity, population differentiation, population structure and effective population size of Tibetan antelope with maternal mtDNA (control region or CR) and bi-parental genetic markers (microsatellites or STRs). We predict that due to sex-specific movement, 1) there will be no obvious population structure; 2) differences in sex-specific movement could be reflected by population differentiation values using maternal markers vs. bi-parental marker; 3)

Tibetan antelope populations are able to maintain high genetic diversity and show no signs of a genetic bottleneck despite an obvious population census bottleneck.

Materials and Methods

Ethics Statement

Tibetan antelope is listed in the Category I of the National Key Protected Wild Animal Species under the China's Wild Animal Protection Law. In September 2016, Tibetan antelope was reclassified on the International Union for Conservation of Nature (IUCN) Red List from Endangered to Near Threatened due to their increased population size. Sample collection and field studies adhered to the Wild Animals Protection Law of the People's Republic of China. Fresh scat samples were collected under IACUC protocol #2850-12. Dry skin samples and placenta samples were acquired with approval from the Forestry Department of Qinghai Province, China.

Study Area and Sampling

The unique female migration pattern repeats itself for all the common calving grounds across the Tibetan Plateau (Schaller, 1998). The local-scale study described here focused on Zhuonai Lake in Kekexili Nature Reserve park (KKXL), Qinghai, China, which is the largest common calving ground for Tibetan antelope. Females from nearby wintering grounds migrate to Zhuonai Lake to give birth. Animals were observed with binoculars from a recommended viewing distance of ~ 300m (Lian, Li, Zhou, & Yan, 2012) until they defecated and left the area. A total of 383 fresh scat samples were collected along with the date and GPS coordinates in ten different wintering grounds in KKXL (KKXL1 - KKXL10) and around the calving ground Zhuonai Lake

(KKXL_ZNH). Samples were kept frozen until lab analyses. The large-scale study focused on three geographic populations of Tibetan antelope on the Tibetan Plateau, including the KKXL, examined above, along with Aerjin (AEJ) and Qiang Tang (QT) populations, using dry skin samples and placenta samples. The total sample size for the large-scale study was 141 (KKXL, N=69; AEJ, N=20; QT, N=52). See Figure 1 for sampling locations and Supplemental Table 1 for detailed sampling information.

DNA Extraction and Amplification

Fecal DNA was extracted and processed using the swabbing method (Wasser, Keim, Taper, & Lele, 2011). DNA in dry skins and placenta samples was extracted using the standard Phenol/Chloroform method (Strauss, 2001). The mtDNA control region (CR) was amplified and sequenced in all samples using the forward primer DF (5' ACCAGAGAAGGAGAACTCACTAACCT 3') and the reverse primer DR (5' AAGGCTGGGACCAAACCTAT 3'). PCR was conducted using the Qiagen Multiplex PCR kit (Qiagen Inc.,) with 0.5 µl 500 µg/mL of bovine serum albumin (BSA). We followed the recommended thermocycling conditions of the kit with an annealing temperature of 51° C.

Different sets of nuclear microsatellite loci (STR) were used for local-scale and large-scale studies. The local-scale study used six STR loci denoted BM1824, MCM38, ILSTS005, MB066, BM1225, and BM4107 (see Supplemental Table 2A) with the 5' end of forward primers fluorescently labeled with dyes 6-FAM or HEX. Annealing temperatures for PCR reactions for each locus were shown in Supplemental Table 2A. Fragment analysis was conducted on the ABI 3730 xl DNA Analyzer (Applied Biosystems). Alleles were scored with GeneMarker software (SoftGenetics, LLC.), and checked manually. We used duplicate fecal extracts and each extract

underwent at least two independent PCR reactions to confirm allele profiles and guard against allelic dropout. Genotypes were classified as heterozygotes if both alleles were observed at least twice with no other alleles present, and homozygotes if only a single fragment was observed at least three times with no other alleles present. The large-scale study used seven STR loci denoted L01, L03, L04, ILSTS005, TGLA68, MCM38, and BM1341 (see Supplemental Table 2B). Amplification of these seven loci used the same protocol described in the local-scale study, but with a single extract amplified once per sample due to higher DNA yield.

Mitochondrial CR Sequence Analyses

mtDNA CR sequences from both the local-scale and large-scale studies were pooled together. All sequences were aligned using the software CLC Main Workbench (Qiagen, Inc). DnaSP v5.10.01 (Librado & Rozas, 2009) was used to determine the number of CR haplotypes (H), the number of segregating sites (S), haplotype diversity (H_d) (Nei, 1978) and H_d standard deviation, nucleotide diversity (π) (Nei, 1978) and π standard deviation. We performed network analyses by constructing median-joining networks (Bandelt, Forster, & Rohl, 1999) on the control region haplotypes using the software PopART 1.7 (http://popart.otago.ac.nz).

Nuclear STR Analyses

Expected heterozygosity (H_{exp}) observed heterozygosity (H_{obs}), polymorphic information content (PIC) and estimated null allele frequency (F_{null}) and combined probability of identity (PI, the probability of two independent samples having the save identical genotype by chance) were calculated using CERVUS v3.0.3 (Kalinowski, Taper, & Marshall, 2007). R packages *pegas* (Paradis, 2010) and *poppr* (Kamvar, Tabima, & Grünwald, 2014) were used to perform the

exact test for Hardy-Weinberg equilibrium (HWE) and Linkage Equilibrium, respectively, using the Monte Carlo test with 1,000 iterations. Significance level was adjusted with sequential Bonferroni correction for multiple comparisons. Duplicate samples from the same genotypes were identified and excluded with the software CERVUS v3.0.3 (Kalinowski et al., 2007).

We evaluated population structure using Bayesian inference with the software STRUCTURE v2.2.3 considering an admixture model with correlated allele frequency (Pritchard, Stephens, & Donnelly, 2000). The individuals were assigned to possible genetic groups, K, varying from one to ten without a priori definition of populations. Twenty independent MCMC runs were carried out with 500,000 iterations following a burn-in period of 500,000 iterations for each value of the number of clusters (K). The best estimate of K was determined from both the likelihood of K and the ad hoc statistic delta K (Evanno, Regnaut, & Goudet, 2005). Genetic structure was also accessed through a discriminant analysis on principal components (DAPC) (Jombart, Devillard, & Balloux, 2010) implemented in the *adegenet* R package (Jombart, 2008).

Population Differentiation Estimate

Pairwise F_{st} was assessed with 20,000 permutations in Arlequin v3.5.2 (Excoffier & Lischer, 2010) for mtDNA CR and STR data respectively. We performed an analysis of molecular variance (AMOVA) (Excoffier, Smouse, & Quattro, 1992) using Arlequin v3.5.2 to understand how genetic variation is partitioned. The significance of the proportion of variation at each category was obtained by MCMC test with 20,000 permutations. Isolation-by-distance (IBD) between Euclidean geographical distances and genetic distances (F_{st}) were assessed using the Mantel test (Mantel 1967) with the *hierfstat* R package (Goudet, 2005) and 20,000 permutations.

Significance values were adjusted for multiple comparisons using the Bonferroni correction (Rice, 1989).

Effective Population Size (N_e) Estimation

We estimated historical (pre-poaching) and contemporary (post-poaching) effective population sizes of Tibetan antelope with the large-scale dataset. The historical effective population size N_{ef} of the mitochondrial genome was calculated from the CR region using the estimate of the female-specific theta ($\theta_f = 2N_{ef}\mu$). θ_f estimate was derived from LAMARC (Kuhner, 2006) using Bayesian inference with 25 randomly selected samples, 10 initial search chains of 10,000 steps and 2 final chains of 1,000,000 iterations. A range of substitution rates (3.60×10^{-10} to 1.80×10^{-8} substitutions/site/gen) (Guo et al., 2006; Pesole, Gissi, De Chirico, & Saccone, 1999) in the CR region was used to reflect uncertainty in μ. The historical effective population size N_e was calculated based on the parameter theta $\theta = 4N_e\mu$ from LAMARC as with the estimate of θ_f. N_e was estimated with 25 random samples using a range of STR mutation rates from 6.0×10^{-5} *to* 1.0×10^{-3} mutations/locus/generation (Crawford & Cuthbertson, 1996; Waples & Do, 2008) and the same running configuration as mtDNA CR sequences. The contemporary N_e was estimated using the linkage disequilibrium (LD) method in the software Ne Estimator v.2 (Do et al., 2014) with P_{crit} =0.01.

Detection of Genetic Bottleneck

We used four approaches to determine whether the overall Tibetan antelope population experienced a genetic bottleneck. First, we tested for allele frequency mode-shifts using BOTTLENECK v. 1.2.02 (Piry, Luikart, & Cornuet, 1999). Secondly, we tested for the presence

of heterozygosity excess by using the one-tailed Wilcoxon signed rank test (Busch et al., 2007; Cornuet & Luikart, 1996) implemented in BOTTLENECK v. 1.2.02. Heterozygote excess was tested under all three STR mutation models: infinite alleles model (IAM), step-wise mutation model (SMM) and two-phase model (TPM). For TPM, we set p_s=0.9 (the frequency of single-step mutations) and the variance of those mutations as 12 (Busch et al., 2007). Third, we calculated the M-ratio, the mean ratio of the number of alleles to the range in allele size, using the software M_P_VAL (Garza & Williamson, 2001). Critical values (M_c) set at the lower 5% tail of the distribution were determined using the program CRITICAL_M. If the observed ratio is below M_c, it can be assumed that the population has experienced a bottleneck (Garza & Williamson, 2001). To calculate M_c, we estimated three TPM parameters: p_s, Δ_g (the mean size of single-step changes) and pre-bottleneck $\theta = 4N_e\mu$. We set p_s = 0.9, and Δ_g = 3.5. We varied θ from 0.01 to 500, encompassing a wide range of biologically plausible values. To ensure this range of θ values was relevant, we estimated θ using a common STR mutation rate μ (5.0×10^{-4} mutations/generation/locus) (Garza & Williamson, 2001) and N_e estimates from LAMARC. Lastly, we employed coalescent simulations with the Approximate Bayesian Computation (ABC) approach to infer past demographic history, as implemented in DIYABC v2.1.0 (Cornuet et al., 2014; Cornuet, Ravigne, & Estoup, 2010). Simulations were conducted with STR and mtDNA CR data separately. Only samples in the large-scale study were included. We compared two competing scenarios, scenario 1 with constant N_e, and scenario 2 with population bottleneck (Supplemental Figure 2). The parameter settings and priors were shown in the Supplemental Table 3A & 3B and Supplemental method.

Results

Mitochondrial CR Sequence Analyses

The final alignment included 524 CR sequences of 1029 bp excluding insertions-deletions (indels). In total, we found 381 different haplotypes. All three geographical populations (KKXL, AEJ, QT) had high haplotype diversity (0.989 - 1.000) and nucleotide diversity (0.020 - 0.024). The AEJ population had the largest standard deviation of haplotype diversity and nucleotide diversity, probably due to its small sample size (18 haplotypes in 20 sequences) (Table 1). The local-scale analysis of samples from 10 wintering locations in KKXL (KKXL1-KKXL10) revealed an overall pattern of haplotypes containing samples from multiple regions and no clusters with geographical affiliation (Supplemental Figure 1). In total, there were 17 haplotypes shared among 10 sampling locations from KKXL. The large-scale analysis of samples from KKXL, AEJ, and QT had a similar pattern (Supplemental Figure 1). There were two haplotypes shared between AEJ and QT, one haplotype shared between AEJ and KKXL, and one haplotype shared between QT and KKXL.

Nuclear STR Analyses

The set of STRs used in both local-scale and large-scale studies revealed high power and accuracy. Combined probability of identity (PI) and sib identity (P_{sib}) using all STRs in either study was shown in Supplemental Table 4. In the local-scale study, the number of STR alleles per locus was 8-14, with an average of 11.167 (Table 2). All loci had high H_{exp} (0.704 - 0.875) and PIC (0.655 - 0.859), with mean H_{exp} of 0.777 and PIC of 0.745. Most loci were in Hardy-Weinberg equilibrium (HWE) and Linkage Equilibrium across all populations after Bonferroni Correction. BM1824 violated HWE in KKXL10 population and MB066 violated HWE across all populations. BM1824 and MB066 showed signs of an excess of observed homozygote genotypes

as suggested by relatively large positive F_{null} values (0.041 and 0.072, respectively) (Table 2). It is difficult to identify a null allele with certainty in the absence of a known parent-offspring relationship. Therefore, all loci were kept for further analyses. In the large-scale study, the number of STR alleles per locus was 7-24, with an average of 14.714 (Table 2). All loci had high H_{obs} except TGLA68 (0.314), and high PIC (0.679-0.921), with mean H_{exp} of 0.845 and PIC of 0.824. Most loci were in HWE across all populations after Bonferroni Correction. L03 violated HWE only in AEJ population and TGLA68 violated HWE across all populations. All loci were in Linkage Equilibrium except the pair of L04 and TGLA68, and L03 and L04. TGLA68 had a very high F_{null} value of 0.445 (Table 2). TGLA68 was excluded from further analyses. STRUCTURE analysis showed that the true K was equal to 1 for local-scale and large-scale studies. DAPC analyses showed that there was no clear separation of 10 wintering locations within KKXL, and a high degree of overlap among the three geographical populations, KKXL, AEJ and QT (Figure 2).

Population Differentiation Estimate

Population differentiation among geographic populations KKXL, AEJ and QT was low (Table 3), and only the F_{st} value calculated between AEJ and QT was significantly different from zero (Table 3). Pairwise F_{st} values were higher using the CR haplotype frequencies than the STR allele frequencies. Most genetic variation was attributed within populations instead of among populations (p values from AMOVA tests were 0.231 and 0.386 for CR haplotype frequency and STR allele frequency respectively). No significant correlation was detected between linearized genetic distances and geographic distance among KKXL, AEJ, and QT (p values from Mantel tests were 0.827 and 0.486 for CR haplotype frequency and STR allele frequency respectively).

Effective Population Size

The most probable estimate of θ_f from LAMARC was 0.084 (95% CI 0.054 - 0.135) and the most probable estimate of θ from LAMARC was 9.990 (95% CI 9.850 - 10.015). The long-term estimate of N_{ef} was in the range of 1.53×10^6 - 1.79×10^8, and the long-term estimate of N_e was in the range of 4.93×10^3 - 4.17×10^4. The contemporary N_e estimate was 368.90 (95% CI of 249.30 - 660.60).

Genetic Bottleneck Analyses

The mode-shift test did not detect any evidence of a genetic bottleneck (Table 4). Heterozygosity excess was detected only under the IAM mutation model (Table 4). While using Δ_g=3.5, most M-ratio values were above the critical value thresholds except for the small pre-bottleneck θ values (0.01, 0.1 and 0.5) (See Table 4), which were very unlikely because historically Tibetan antelope had a large effective population size. All calculated M-ratios were above the suggested threshold value of 0.68 identified for bottlenecked populations (Garza & Williamson, 2001). ABC method also didn't support the scenario of a population bottleneck. The best-supported model was constant population size model, with a posterior probability of 0.526 (95% confidence interval CI: 0.515 - 0.537) for STR, and a posterior probability of 0.714 (95% confidence interval CI: 0.706 - 0.723) for mtDNA CR sequences (Supplemental Figure 3). Analyses to estimate confidence in scenario choice indicated that type I (false-positive) and type II (false-negative) errors for the best-supported scenario (scenario 1 with constant N_e) were high (0.438 and 0.389 for STR, 0.320 and 0.455 for mtDNA CR), suggesting low confidence in choosing the true scenario. Point estimate for N_e was 4.44×10^5 (95% CI: 2.29×10^5-

9.45×10^5) and 1.05×10^4 (95% CI: 4.80×10^3- 1.93×10^4) for mtDNA CR and STR respectively.

Discussion

This study tests the hypothesis that female-specific migration can buffer populations from the impacts of population reduction with the case of migratory Tibetan antelope populations. Our results showed that 1) Tibetan antelope maintained high genetic diversity in both mtDNA CR and STR markers after a historical population decline; 2) No population genetic bottleneck was detected; 3) There was no obvious population structure among three geographical populations, which is a sign of high gene flow among populations. Males are also likely to contribute to gene flow than females since pairwise F_{st} values were higher using the maternal CR haplotype frequencies than the biparental STR allele frequencies. This study suggests that movement conducted by either female or male Tibetan antelope might have reduced their loss of genetic diversity in the face of severe demographic decline. However, Tibetan antelope have not fully recovered from poaching in terms of effective population size, since there is a marked reduction in post-poaching effective population size 368.9 (95% CI of 249.30 - 660.60) compared to the pre-poaching average (4.93×10^3 - 4.17×10^4).

Tibetan antelope maintained high genetic diversity after a historical population decline

Overall, CR haplotype diversity (H_{d}) was 0.998 and π was 0.020. The mean H_{exp} of STR loci was 0.777 and 0.845 for the local-scale and large-scale studies respectively. Our results are consistent with previous studies (Du et al., 2016; Zhang, Jiang, Xu, Zeng, & Li, 2013). At the species level, the genetic diversity of Tibetan antelope was higher than other endangered

ungulate species, such as Saiga antelope (*Saiga tatarica*: H_d 0.785; π 0.014) (Campos et al., 2010) and Kashmir red deer (*Cervus elaphus hanglu*: H_d 0.589; π 0.008) (Mukesh, Kumar, Sharma, Shukla, & Sathyakumar, 2015). Comparing genetic diversity among species could be problematic, because the lineage-specific mutation rates, life history rates and external environmental factors can profoundly affect genetic diversity (Martinez, Willoughby, & Christie, 2018; Nabholz, Mauffrey, Bazin, Galtier, & Glemin, 2008). A comparison of related species can factor out shared traits and clarify interpretation of the results (Roe & Boyer, 2015). Tibetan antelope is usually classified with Antilopinae by morphological studies, but *P. hodgsonii* is more closely related to Caprinae (*O. aries* and *C.hircus*), rather than to Antilopinae subfamily based on molecular data (Feng et al., 2008; Xu et al., 2001). The estimated divergence time is about 2.25 million years ago between *P. hodgsonii* and *O.aries*, and about 2.22 million years between *P. hodgsonii* with *C. hircus* (Xu et al., 2001). The genetic diversity of control region in Tibetan antelope is comparable to that of the non-threatened Caprinae species on the Tibetan Plateau, such as Tibetan goat (*C.hircus*: H_d 0.983; π 0.036) (Zhao et al., 2011) and Tibetan sheep (*O. aries*: H_d 0.990; π 0.020) (Liu et al., 2018).

No population genetic bottleneck was detected

Neither the mode-shift, heterozygosity excess, M-ratio nor ABC method revealed strong evidence of a population genetic bottleneck. The mode-shift test did not detect any evidence of a bottleneck. Heterozygosity excess was detected only under the IAM model. IAM is prone to incorrectly detect heterozygosity excess in non-bottlenecked populations. Therefore, to be statistically conservative, one should use the SMM or TPM when analyzing STR data to test for recent bottlenecks (Luikart & Cornuet, 1998). The M-ratio approach detected bottleneck

signatures, but only under extreme conditions (very small θ values), suggesting a weak signal, if any. The model with constant population size has higher support over the model with population bottleneck based on ABC method, though it has high Type I and II errors.

No obvious population structure was detected among three geographical populations

Despite large-scale sampling efforts, phylogenetic analysis with Bayesian inference, haplotype network analysis of the CR region, STRUCURE and DAPC analyses of STR loci revealed no obvious geographic structure for Tibetan antelope in AEJ, QT, and KKXL populations. The Mantel test detected no IBD pattern with neither mtDNA CR nor STR loci. This finding suggests historically high gene flow, which is consistent with results of previous studies (Zhang et al., 2013; Zhou et al., 2007). Tibetan antelope can ascent high hills, penetrate mountain ranges, and cross passes to neighboring valleys at elevations of 3,700 - 5,500 m and there are no obvious geographic barriers blocking population exchange on the Plateau (Ruan, He, Zhang, Wan, & Fang, 2005). During the course of female Tibetan antelope migration, it is possible that a number of females from one population translocate to another. This would promote gene exchange between populations of different localities, which is reflected in the shared haplotypes among different populations (Supplemental Figure 1). However, males are likely to play a bigger role in gene flow since pairwise F_{st} values were higher using the maternal CR haplotype frequencies than the biparental STR allele frequencies. Tibetan antelope have a harem polygyny mating system, in which a male generally mates with most or all of the females in his harem (5-10 females) during the breeding season. Mate competition is an important driver explaining the spatial movement of males among populations during the breeding season. Breeding dispersal is not restricted to young males. It also occurs among prime-aged individuals and even among

harem holders (Jarnemo, 2011; Richard, White, & Côté, 2014).

Tibetan antelope has not fully recovered from poaching yet in terms of effective population size

In 2003, the estimation of Tibetan antelope population size reached the lowest number of 50,000 individuals. Since then, the Tibetan antelope population has begun to recover, with about 200,000 individuals currently (Leclerc et al., 2015). Their protection status has been changed from "endangered" to "near-threatened" by IUCN. However, our effective population size comparison analyses suggest that Tibetan antelope has not yet fully recovered. Their contemporary N_e estimate is 368.90 (95% CI of 249.30 - 660.60), which is markedly lower than their long-term N_e average (4.93×10^3 - 4.17×10^4). Long-term N_e estimate with ABC method using STR loci is 1.05×10^4 (95% CI: 4.80×10^3- 1.93×10^4), which mostly agrees with the estimate with LAMARC method. N_e is defined as the size of an ideal population that experiences genetic change at the same rate as the population under consideration (Waples, 1991). It determines the rate of loss of genetic diversity. The magnitude of the difference is much greater for the effective population size than for measures of genetic diversity (Roe & Boyer, 2015). This might be why there was a relatively large change in N_e whereas the genetic diversity remained consistently high over time.

The contemporary N_e estimate has a wide confidence interval (95% CI of 249.30 - 660.60). In the LD method implemented in Ne Estimator v.2, CI of N_e is an increasing function of N_e (Posada & Crandall, 2001; Waples & Do, 2010). Like all the other genetic methods for estimating contemporary N_e, LD method is most powerful with small populations and has difficulty distinguishing large populations from infinite ones. However, it should provide a useful lower

bound for N_e, which can be important in conservation biology where a major concern is avoidance and early detection of population bottlenecks (Bandelt et al., 1999; Waples & Do, 2010).

Surprisingly, the mtDNA CR-based estimate of N_{ef} (1.53×10^6 - 1.79×10^8) was larger than the STR-based estimate N_e (4.93×10^3 - 4.17×10^4). Long-term N_e estimate with ABC method using mtDNA CR sequences is 4.44×10^5 (95% CI: 2.29×10^5- 9.45×10^5), which is lower than the estimate with LAMARC, but still larger than the STR-based estimate. In theory, the mitochondrial genome has an effective population size one quarter that of an average nuclear locus because of the different inheritance modes of nuclear and mtDNA, as well as the haploid nature of the mitochondrial genome. The observed disparity between mtDNA and STR-based estimates could result from the Tibetan antelope's mating system, historical demography, mutation or all three combined. Tibetan antelope have a harem polygyny mating system, as mentioned above. Non-independent mating paring has a large effect when there is intense male-male competition for reproduction in a harem social system and reduces N_e for wholly or paternally inherited components of genome (Evans & Charlesworth, 2013; Nunney, 1996). Historical events may also explain the apparent discord between mtDNA and STR-based of long-term population size. For instance, if the historical source populations that contributed to the origin of the contemporary population were isolated from each other but with male-biased dispersal, then the populations would more rapidly diverge at mtDNA loci than nuclear loci because mtDNA is matrilineally inherited. A secondary contact of these isolates would merge a relatively homogenous pool of nuclear genes, but mtDNA lineages would remain differentiated. This evolutionary scenario is supported by our pairwise F_{st} results (Table 3) that Pairwise F_{st} values were higher using the CR haplotype frequencies than the STR allele frequencies. N_{ef} may

reflect the collective genetic diversity of all source populations, which would possibly contribute to the reversal in expected sizes for N_e and N_{ef}. Another possibility is that size homoplasy of STRs might have obscured the signal on the historical origin of the study population. Some STR alleles can be identical in size but may not identical by descent due to convergent mutations. Size homoplasy is especially problematic in large populations (Estoup, Jarne, & Cornuet, 2002), such as Tibetan antelope population. Thus, STR-derived N_e estimates may not reflect the composite origin of these populations as well as N_{ef}. Regardless of the ultimate cause of the discord between N_e and N_{ef}, all estimators indicate that the historical population size of Tibetan antelope is very large.

How did Tibetan antelope maintain such high genetic diversity despite a massive population decline?

We expected the Tibetan antelope to have suffered a serious population bottleneck from the near 95% decline in the original population due to poaching. However, we found no evidence of such an event by any of the methods used in the study. Tibetan antelope still maintains high genetic diversity. The high genetic variability in Tibetan antelope population after a population crash likely reflects the effect of gene flow. A few immigrants entering a population each generation can counteract the effects of genetic drift and obscure any genetic signature of this population's decline. The great potential for gene flow can profoundly increases a species' ability to maintain genetic diversity. For example, populations of outcrossing species tend to be more genetically diverse and less genetically differentiated (Hamrick & Godt, 1996). Anadromous Atlantic salmon populations have significantly higher level of genetic diversity and population differentiation than their freshwater Atlantic salmon counterparts (Tonteri, Veselov, Titov,

Lumme, & Primmer, 2007). Increasing human activities on the Tibetan Plateau is now threatening this once-paradise for wildlife. Habitat fragmentation, such as fencing and road construction, might affect gene flow among populations, impeding Tibetan antelope population's recovery (Su et al., 2015). Here, we call for the conservation management efforts to maintain the historical patterns of between-population gene flow in Tibetan antelope.

Additionally, other factors might also be important in maintaining high genetic diversity, such as historically large population size and recent population bottleneck. The contemporary N_e of Tibetan antelope estimate was 368.90, with a wide 95% confidence interval of 249.30 - 660.60, which could be large enough to preclude losses of neutral genetic diversity. Small populations caused by massive population reduction are at risk of extinction vortex due to demographic stochasticity and random genetic drift. An N_e of 500-1000 and census population size of 5000 - 12,500 are required for endangered species to retain their evolutionary potential (Franklin & Frankham, 1998). The lower limit of the required N_e, 500, falls into the wide 95% confidence interval of the contemporary N_e estimate of Tibetan antelope (249.30 - 660.60) and their estimated census population size is around 200,000 (Leclerc et al., 2015). It is also possible that insufficient time has been elapsed since the start of population reduction to markedly reduce Tibetan antelope genetic diversity. It is hard to detect a recent population genetic bottleneck, as reflected by the high type I and II error in DIYABC analyses. According to the coalescent theory (Crow & Kimura, 1970), H_t/H_o (the ratio between heterozygosity at generation t vs. generation 0) depends on $(1 - 1/2\mathrm{N})^t$. For populations with fluctuating population size from generation to generation, one should replace N with harmonic mean of the generation-specific effective sizes $N_e{}^*$ If we assume that the year 1950 is time 0 and $N_e{}^*$ = 249 (we chose the lower bound of contemporary effective population size as $N_e{}^*$ to be conservative), by 2016 H_t/H_o would be

0.957 (assuming generation time is 6 years). Thus, we would not expect to see a significant loss of genetic diversity by genetic drift. We postulate that our data are not adequate to detect a recent genetic bottleneck event and we would not be able observe a significant loss of genetic diversity by genetic drift.

Future Research Recommendations

We acknowledge that the few loci used in this study provide limited resolution and considerable uncertainty for demographic inference. Each locus on the genome only provides a genealogy regarding this particular locus. The only way to reduce the uncertainty of the demographic model is to sample throughout the entire genome, which will contain a wealth of information for demographic inference.

It is essential to establish a baseline for genetic diversity representing the pre-disturbing conditions when assessing the genetic changes of endangered species(Matocq & Villablanca, 2001). The use of archival (e.g., museum samples) specimens may allow for a powerful test of loss in genetic diversity over time. If archival reference samples represent genetic variation found in a population prior to the events leading to endangered status (e.g. samples from the pre-poaching era), such samples would provide the most appropriate reference to track temporal changes in genetic diversity (Dures et al., 2019; Feng et al., 2019).

Acknowledgements

We thank Hyeon Jeong Kim, Adam Leaché, Chad Klumb for valuable comments that greatly improved this manuscript. We thank Rebecca Booth for lab work advice. We are thankful to Lei Wang, Jundong Yang and Jie Yang for the help with sample collection and lab work. We thank

Kekexili Natural Nature Reserve Administration for assistance in the fieldwork. The study was funded by 1) Biodiversity Study in Kekexili, Department of Housing and Urban-Rural Development of Qinghai Province, China; 2) Construction Fund for Qinghai Key Laboratories (2017-ZJ-Y23); 3) The Strategic Priority Research Program of the Chinese Academy of Sciences (XDA23060602, XDA2002030302); 4) Wingfield-Ramenofsky Award, University of Washington. Yue Shi was funded by China Scholarship Council (CSC) Graduate Research Fellowship, Fritz/Boeing International Research Fellowship and WRF Hall Fellowship from the University of Washington.

Data Accessibility

After peer review and prior to final publication, mtDNA sequences will be deposited in GenBank and microsatellite genotype dataset will be archived at Dryad.

Author Contributions

Y.S., S.K.W., and J.P.S. designed the project. J.R.C., Y.S., T.Z.Z. and J.P.S. conducted sample collection in the field. Y.S. and J.R.C. performed the lab experiment. J.P.S. oversaw the study and offered insight into data analysis and interpretation. Y.S. wrote the manuscript, and all other authors provided comments and approved the manuscript. All authors declare no conflict of interests.

References

Ahmad, K., Kumar, V. P., Joshi, B. D., Raza, M., Nigam, P., Khan, A. A., & Goyal, S. P. (2016). Genetic diversity of the Tibetan antelope (*Pantholops hodgsonii*) population of Ladakh,

India, its relationship with other populations and conservation implications. *BMC Research Notes*, 1–10. http://doi.org/10.1186/s13104-016-2271-4

Bandelt, H.-J., Forster, P., & Rohl, A. (1999). Median-Joining Networks for Inferring Intraspecific Phylogenies. *Molecular Biolgoy and Evolution*, *16*(1), 37–48.

Buho, H., Jiang, Z., Liu, C., Yoshida, T., Mahamut, H., Kaneko, M., et al. (2011). Preliminary study on migration pattern of the Tibetan antelope (*Pantholops hodgsonii*) based on satellite tracking. *Advances in Space Research*, *48*(1), 43–48. http://doi.org/10.1016/j.asr.2011.02.015

Busch, J. D., Waser, P. M., & DeWoody, J. A. (2007). Recent demographic bottlenecks are not accompanied by a genetic signature in banner-tailed kangaroo rats (*Dipodomys spectabilis*). *Molecular Ecology*, *16*(12), 2450–2462.

Buzzard, P. J., Wong, H. M., & Zhang, H. (2012). Population increase at a calving ground of the Endangered Tibetan antelope *Pantholops hodgsonii* in Xinjiang, China. *Oryx*, *46*(02), 266–268. http://doi.org/10.1017/S0030605311001657

Campos, P. F., Kristensen, T., Orlando, L., Sher, A., Kholodova, M. V., Götherström, A., et al. (2010). Ancient DNA sequences point to a large loss of mitochondrial genetic diversity in the saiga antelope (*Saiga tatarica*) since the Pleistocene. *Molecular Ecology*, *19*(22), 4863–4875. http://doi.org/10.1111/j.1365-294X.2010.04826.x

Cornuet, J. M., & Luikart, G. (1996). Description and power analysis of two tests for detecting recent population bottlenecks from allele frequency data. *Genetics*, *144*(4), 2001–2014.

Cornuet, J. M., Pudlo, P., Veyssier, J., Dehne-Garcia, A., Gautier, M., Leblois, R., et al. (2014). DIYABC v2.0: a software to make approximate Bayesian computation inferences about population history using single nucleotide polymorphism, DNA sequence and microsatellite data. *Bioinformatics*, *30*, 1187–1189. http://doi.org/10.1093/bioinformatics/btt763/-/DC1

Cornuet, J. M., Ravigne, V., & Estoup, A. (2010). Inference on population history and model checking using DNA sequence and microsatellite data with the software DIYABC (v1.0). *BMC Bioinformatics*, *11*(401).

Crawford, A. M., & Cuthbertson, R. P. (1996). Mutations in sheep microsatellites. *Genome Research*, *6*(9), 876–879.

Crow, J. F., & Kimura, M. (1970). An Introduction to Population Genetics Theory.

Do, C., Waples, R. S., Peel, D., Macbeth, G. M., Tillett, B. J., & Ovenden, J. R. (2014). NeEstimator v2: re-implementation of software for the estimation of contemporary effective population size (Ne) from genetic data. *Molecular Ecology Resources*, *14*(1), 209–214. http://doi.org/10.1111/1755-0998.12157

Du, Y., Zou, X., Xu, Y., Guo, X., Li, S., Zhang, X., et al. (2016). Microsatellite Loci Analysis Reveals Post-bottleneck Recovery of Genetic Diversity in the Tibetan Antelope. *Scientific Reports*, 1–7. http://doi.org/10.1038/srep35501

Dures, S. G., Carbone, C., Loveridge, A. J., Maude, G., Midlane, N., Aschenborn, O., & Gottelli, D. (2019). A century of decline: Loss of genetic diversity in a southern African lion-conservation stronghold. *Diversity and Distributions*, *25*(6), 870–879. http://doi.org/10.1111/ddi.12905

Estoup, A., Jarne, P., & Cornuet, J. M. (2002). Homoplasy and mutation model at microsatellite loci and their consequences for population genetics analysis. *Molecular Ecology*, *11*(9), 1591–1604. http://doi.org/10.1046/j.1365-294X.2002.01576.x

Evanno, G., Regnaut, S., & Goudet, J. (2005). Detecting the number of clusters of individuals using the software structure: a simulation study. *Molecular Ecology*, *14*(8), 2611–2620. http://doi.org/10.1111/j.1365-294X.2005.02553.x

Evans, B. J., & Charlesworth, B. (2013). The Effect of Nonindependent Mate Pairing on the Effective Population Size. *Genetics*, *193*, 545–556. http://doi.org/10.1534/genetics.112.146258/-/DC1

Excoffier, L., & Lischer, H. E. L. (2010). Arlequin suite ver 3.5: a new series of programs to perform population genetics analyses under Linux and Windows. *Molecular Ecology Resources*, *10*(3), 564–567. http://doi.org/10.1111/j.1755-0998.2010.02847.x

Excoffier, L., Smouse, P. E., & Quattro, J. M. (1992). Analysis of molecular variance inferred from metric distances among DNA haplotypes: application to human mitochondrial DNA restriction data. *Genetics*, *131*(2), 479–491.

Feng, S. H., Fang, Q., Barnett, R., Li, C., Han, S., Kuhlwilm, M., et al. (2019). The Genomic Footprints of the Fall and Recovery of the Crested Ibis. *Current Biology*, *29*(2), 340–349.e7. http://doi.org/10.1016/j.cub.2018.12.008

Feng, Z., Fan, B., Li, K., Zhang, Q. D., Yang, Q. S., & Liu, B. (2008). Molecular characteristics of Tibetan antelope (*Pantholops hodgsonii*) mitochondrial DNA control region and phylogenetic inferences with related species. *Small Ruminant Research*, *75*(2-3), 236–242. http://doi.org/10.1016/j.smallrumres.2007.06.011

Frankham, R. (2005). Genetics and extinction. *Biological Conservation*, *126*(2), 131–140. http://doi.org/10.1016/j.biocon.2005.05.002

Frankham, R. (2015). Genetic rescue of small inbred populations: meta-analysis reveals large and consistent benefits of gene flow. *Molecular Ecology*, *24*(11), 2610–2618. http://doi.org/10.1111/mec.13139

Franklin, I. R., & Frankham, R. F. (1998). How large must populations be to retain evolutionary potential? *Animal Conservation*, 69–73.

Garza, J. C., & Williamson, E. G. (2001). Detection of reduction in population size using data from microsatellite loci. *Molecular Ecology*, *10*(2), 305–318.

Gonzalez-Suarez, M. (2010). Past exploitation of California sea lions did not lead to a genetic bottleneck in the Gulf of California. *Ciencias Marinas*, *36*(2), 199–211. http://doi.org/10.7773/cm.v36i2.1672

Goudet, J. (2005). HIERFSTAT, a package for R to compute and test hierarchical F-statistics. *Molecular Ecology Notes*, *5*, 184–186. http://doi.org/10.1111/j.1471-8278

Guo, S., Savolainen, P., Su, J., Zhang, Q., Qi, D., Zhou, J., et al. (2006). Origin of mitochondrial DNA diversity of domestic yaks. *BMC Evolutionary Biology*, *6*, 73. http://doi.org/10.1186/1471-2148-6-73

Hailer, F., Helander, B., Folkestad, A. O., Ganusevich, S. A., Garstad, S., Hauff, P., et al. (2006). Bottlenecked but long-lived: high genetic diversity retained in white-tailed eagles upon recovery from population decline. *Biology Letters*, *2*(2), 316–319. http://doi.org/10.1098/rsbl.2006.0453

Hamrick, J. L., & Godt, M. J. W. (1996). Effects of life history traits on genetic diversity in plant species. *Philosophical Transactions of the Royal Society B: Biological Sciences*, *351*, 1291–1298.

Jangjoo, M., Matter, S. F., Roland, J., & Keyghobadi, N. (2016). Connectivity rescues genetic diversity after a demographic bottleneck in a butterfly population network. *Proceedings of*

the National Academy of Sciences of the United States of America, *113*(39), 10914–10919. http://doi.org/10.1073/pnas.1600865113
Jarnemo, A. (2011). Male red deer (*Cervus elaphus*) dispersal during the breeding season. *Journal of Ethology*, *29*(2), 329–336. http://doi.org/10.1007/s10164-010-0262-9
Jombart, T. (2008). *adegenet*: a R package for the multivariate analysis of genetic markers. *Bioinformatics*, *24*(11), 1403–1405. http://doi.org/10.1093/bioinformatics/btn129
Jombart, T., Devillard, S., & Balloux, F. (2010). Discriminant analysis of principal components: a new method for the analysis of genetically structured populations. *BMC Genetics*, *11*, 94. http://doi.org/10.1186/1471-2156-11-94
Kalinowski, S. T., Taper, M. L., & Marshall, T. C. (2007). Revising how the computer program CERVUS accommodates genotyping error increases success in paternity assignment. *Molecular Ecology*, *16*(5), 1099–1106. http://doi.org/10.1111/j.1365-294X.2007.03089.x
Kamvar, Z. N., Tabima, J. F., & Grünwald, N. J. (2014). *Poppr*: an R package for genetic analysis of populations with clonal, partially clonal, and/or sexual reproduction. *PeerJ*, *2*, e281–14. http://doi.org/10.7717/peerj.281
Keller, L. F., & Waller, D. M. (2002). Inbreeding effects in wild populations. *Trends in Ecology & Evolution*, *17*, 230–241.
Kuhner, M. K. (2006). LAMARC 2.0: maximum likelihood and Bayesian estimation of population parameters. *Bioinformatics*, *22*(6), 768–770. http://doi.org/10.1093/bioinformatics/btk051
Kuo, C.-H., & Janzen, F. J. (2004). Genetic Effects of a Persistent Bottleneck on a Natural Population of Ornate Box Turtles (*Terrapene ornata*). *Conservation Genetics*, *5*(4), 425–437. http://doi.org/10.1023/B:COGE.0000041020.54140.45
Lacy, R. C. (1987). Loss of Genetic Diversity from Managed Populations: Interacting Effects of Drift, Mutation, Immigration, Selection, and Population Subdivision. *Conservation Biology*, *1*, 143–158.
Leclerc, C., Bellard, C., Luque, G. M., & Courchamp, F. (2015). Overcoming extinction: understanding processes of recovery of the Tibetan antelope. *Ecosphere*, *6*(9), art171–art171. http://doi.org/10.1890/ES15-00049.1.sm
Lian, X., Li, X., Zhou, D., & Yan, P. (2012). Avoidance distance from Qinghai-Tibet Highway in sympatric Tibetan antelope and gazelle. *Transportation Research Part D: Transport and Environment*, *17*(8), 585–587. http://doi.org/10.1016/j.trd.2012.06.009
Librado, P., & Rozas, J. (2009). DnaSP v5: a software for comprehensive analysis of DNA polymorphism data., *25*(11), 1451–1452. http://doi.org/10.1093/bioinformatics/btp187
Lippé, C., Dumont, P., & Bernatchez, L. (2006). High genetic diversity and no inbreeding in the endangered copper redhorse, *Moxostoma hubbsi* (Catostomidae, Pisces): the positive sides of a long generation time. *Molecular Ecology*, *15*(7), 1769–1780. http://doi.org/10.1111/j.1365-294X.2006.02902.x
Liu, J., Ding, X., Zeng, Y., Guo, X., Sun, X., & Yuan, C. (2018). Phylogenetic Evolution and Phylogeography of Tibetan Sheep Based on mtDNA D-Loop Sequences. In *Mitochondrial DNA - New Insights* (pp. 135–152). InTech. http://doi.org/10.5772/intechopen.76583
Luikart, G., & Cornuet, J. M. (1998). Empirical Evaluation of a Test for Identifying Recently Bottlenecked Populations from Allele Frequency Data. *Conservation Biology*, *12*(1), 228–237. http://doi.org/10.2307/2387479?ref=search-gateway:45cb0b6176d70ed0cd739aab44db6389

Martinez, A. S., Willoughby, J. R., & Christie, M. R. (2018). Genetic diversity in fishes is influenced by habitat type and life-history variation. *Ecology and Evolution*, *8*(23), 12022–12031. http://doi.org/10.1002/ece3.4661

Matocq, M. D., & Villablanca, F. X. (2001). Low genetic diversity in an endangered species: recent or historic pattern? *Biological Conservation*, *98*(1), 61–68. http://doi.org/10.1016/S0006-3207(00)00142-7

Morris, K., Austin, J. J., & Belov, K. (2012). Low major histocompatibility complex diversity in the Tasmanian devil predates European settlement and may explain susceptibility to disease epidemics. *Biology Letters*, *9*(1), 20120900–20120900. http://doi.org/10.1098/rsbl.2012.0900

Mukesh, Kumar, V. P., Sharma, L. K., Shukla, M., & Sathyakumar, S. (2015). Pragmatic Perspective on Conservation Genetics and Demographic History of the Last Surviving Population of Kashmir Red Deer (*Cervus elaphus hanglu*) in India. *PLoS ONE*, *10*(2), e0117069. http://doi.org/10.1371/journal.pone.0117069.s006

Nabholz, B., Mauffrey, J.-F., Bazin, E., Galtier, N., & Glemin, S. (2008). Determination of mitochondrial genetic diversity in mammals. *Genetics*, *178*(1), 351–361. http://doi.org/10.1534/genetics.107.073346

Nei, M. (1978). Estimation of average heterozygosity and genetic distance from a small number of individuals. *Genetics*, *89*(3), 583–590.

Nunney, L. (1996). The influence of variation in female fecundity on effective population size. *Biological Journal of the Linnean Society*, *59*(4), 411–425. http://doi.org/10.1006/bijl.1996.0072

O' Donnell, C. F. J., Richter, S., Dool, S., Monks, J. M., & Kerth, G. (2015). Genetic diversity is maintained in the endangered New Zealand long-tailed bat (*Chalinolobus tuberculatus*) despite a closed social structure and regular population crashes. *Conservation Genetics*, *17*(1), 91–102. http://doi.org/10.1007/s10592-015-0763-8

Paradis, E. (2010). pegas: an R package for population genetics with an integrated-modular approach. *Bioinformatics*, *26*(3), 419–420. http://doi.org/10.1093/bioinformatics/btp696

Pesole, G., Gissi, C., De Chirico, A., & Saccone, C. (1999). Nucleotide substitution rate of mammalian mitochondrial genomes. *Journal of Molecular Evolution*, *48*(4), 427–434.

Piry, S., Luikart, G., & Cornuet, J. M. (1999). Computer note. BOTTLENECK: a computer program for detecting recent reductions in the effective size using allele frequency data.

Posada, D., & Crandall, K. (2001). Intraspecific gene genealogies: trees grafting into networks. *Trends in Ecology & Evolution*, *16*(1), 37–45.

Pritchard, J. K., Stephens, M., & Donnelly, P. (2000). Inference of population structure using multilocus genotype data. *Genetics*, *155*(2), 945–959.

Reed, D. H., & Frankham, R. (2003). Correlation between Fitness and Genetic Diversity. *Conservation Biology*, *17*(1), 230–237. http://doi.org/10.2307/3095289?ref=search-gateway:560ab92dafa5a1244957f0514072eba0

Rice, W. R. (1989). Analyzing Tables of Statistical Tests. *Evolution*, *43*, 223–225.

Richard, J. H., White, K. S., & Côté, S. D. (2014). Mating effort and space use of an alpine ungulate during the rut. *Behavioral Ecology and Sociobiology*, *68*(10), 1639–1648. http://doi.org/10.1007/s00265-014-1772-1

Roe, K. J., & Boyer, S. L. (2015). A comparison of genetic diversity between sympatric populations of the endangered Winged-Mapleleaf (*Quadrula fragosa*) and the Pimpleback

(*Amphinaias pustulosa*) in the St. Croix River, U.S.A. *American Malacological Bulletin*, *33*(1), 1–9.
Ruan, X.-D., He, P.-J., Zhang, J.-L., Wan, Q.-H., & Fang, S.-G. (2005). Evolutionary History and Current Population Relationships of the Chiru (*Pantholops Hodgsonii*) Inferred from mtDNA Variation. *Journal of Mammalogy*, *86*(5), 881–886. http://doi.org/10.2307/4094432?ref=search-gateway:4087f63799f4e0ab5a1359b0d118b441
Schaller, G. B. (1998). Wildlife of the Tibetan Steppe. University of Chicago Press.
Sremba, A. L., Hancock-Hanser, B., Branch, T. A., LeDuc, R. L., & Baker, C. S. (2012). Circumpolar Diversity and Geographic Differentiation of mtDNA in the Critically Endangered Antarctic Blue Whale (*Balaenoptera musculus intermedia*). *PLoS ONE*, *7*(3), e32579–13. http://doi.org/10.1371/journal.pone.0032579
Strauss, W. M. (2001). Preparation of genomic DNA from mammalian tissue. *Current Protocols in Immunology*, *Chapter 10*(Unit 10.2). http://doi.org/10.1002/0471142735.im1002s08
Su, X., Liu, S., Dong, S., Zhang, Y., Wu, X., Zhao, H., et al. (2015). Effects of potential mining activities on migration corridors of Chiru (*Pantholops hodgsonii*) in the Altun National Nature Reserve, China. *Journal for Nature Conservation*, *28*(C), 119–126. http://doi.org/10.1016/j.jnc.2015.09.008
Tonteri, A., Veselov, A. J., Titov, S., Lumme, J., & Primmer, C. R. (2007). The effect of migratory behaviour on genetic diversity and population divergence: a comparison of anadromous and freshwater Atlantic salmon *Salmo salar*. *Journal of Fish Biology*, *70*(sc), 381–398. http://doi.org/10.1111/j.1095-8649.2007.01519.x
Waples, R. S. (1991). Genetic Methods for Estimating the Effective Size of Cetacean Populations. *Report - International Whaling Commission*, (13), 280–300.
Waples, R. S., & Do, C. (2008). LDNE: a program for estimating effective population size from data on linkage disequilibrium. *Molecular Ecology Resources*, *8*(4), 753–756. http://doi.org/10.1111/j.1755-0998.2007.02061.x
Waples, R. S., & Do, C. (2010). Linkage disequilibrium estimates of contemporary Neusing highly variable genetic markers: a largely untapped resource for applied conservation and evolution. *Evolutionary Applications*, *3*(3), 244–262. http://doi.org/10.1111/j.1752-4571.2009.00104.x
Wasser, S. K., Keim, J. L., Taper, M. L., & Lele, S. R. (2011). The influences of wolf predation, habitat loss, and human activity on caribou and moose in the Alberta oil sands. *Frontiers in Ecology and the Environment*, *9*(10), 546–551. http://doi.org/10.2307/41479958?ref=no-x-route:addb7ca5ae392d054664081ba69a3ef7
Xu, S. Q., Yang, Y.-Z., Zhou, J., Jin, G.-E., Chen, Y.-T., Wang, J., et al. (2001). A Mitochondrial Genome Sequence of the Tibetan Antelope (*Pantholops hodgsonii*). *Genomics Proteomics & Bioinformatics*, *3*, 5–17.
Zhang, F., Jiang, Z., Xu, A., Zeng, Y., & Li, C. (2013). Recent Geological Events and Intrinsic Behavior Influence the Population Genetic Structure of the Chiru and Tibetan Gazelle on the Tibetan Plateau. *PLoS ONE*, *8*(4), e60712–13. http://doi.org/10.1371/journal.pone.0060712
Zhao, Y., Zhang, J., Zhao, E., Zhang, X., Liu, X., & Zhang, N. (2011). Mitochondrial DNA diversity and origins of domestic goats in Southwest China (excluding Tibet). *Small Ruminant Research*, *95*(1), 40–47. http://doi.org/10.1016/j.smallrumres.2010.09.004
Zhou, H., Li, D., Zhang, Y., Yang, T., & Liu, Y. (2007). Genetic Diversity of Microsatellite DNA Loci of Tibetan Antelope (Chiru, *Pantholops hodgsonii*) in Hoh Xil National Nature Reserve, Qinghai, China. *Journal of Genetics and Genomics*, *34*(7), 600–607.

Table 1 Genetic diversity of Control Region according to geographical regions based on alignment of 524 sequences excluding indels (1029bp). Note: S = number of segregating sites (excluding sites with gaps/missing data); H_d = haplotype diversity; H_dSD= standard deviation of H_d; π = nucleotide diversity; πSD = standard deviation of π.

Region	n	S	Haplotypes	H_d	H_dSD	π	πSD
KKXL (local-scale)	383	147	274	0.996	0.001	0.021	0.0004
KKXL	69	119	68	1.000	0.003	0.020	0.0011
AEJ	20	82	18	0.989	0.019	0.024	0.0018
QT	52	95	48	0.997	0.004	0.020	0.0011
Total	524	180	381	0.997	0.000	0.020	0.0003

Table 2 Genetic diversity and summary statistics of STR loci used in the study. A = number of alleles per locus; H_{obs} = observed heterozygosity; H_{exp} = expected heterozygosity; PIC = polymorphism information content; F_{null} = estimated frequency of null alleles (note: * $p<0.05$).

Study	Loci	A	H_{obs}	H_{exp}	PIC	F_{null}
Local-scale study	BM1824	8	0.717	0.779	0.747	0.041
	MCM38	9	0.739	0.704	0.655	-0.031
	ILSTS005	12	0.875	0.875	0.859	-0.001
	MB066	14	0.637	0.739	0.705	0.072
	BM1225	12	0.768	0.785	0.762	0.010
	BM4107	12	0.737	0.778	0.743	0.027
Large-scale study	L01	12	0.707	0.772	0.743	0.051
	L03	24	0.887	0.928	0.921	0.020
	L04	23	0.900	0.928	0.919	0.014
	BM1341	15	0.858	0.885	0.872	0.015
	ILSTS005	13	0.871	0.866	0.848	-0.004
	TGLA68	7	0.314	0.815	0.788	0.445
	MCM38	9	0.702	0.716	0.679	0.013

Table 3 Pairwise F_{st} among populations KKXL, AEJ and QT calculated using control region haplotype frequencies (lower diagonal) and 6 microsatellite loci frequencies (six loci used in the large-scale study) (upper diagonal) with 20,000 permutations.

	AEJ	KKXL	QT
AEJ		0.004	0.008*
KKXL	0.013		0.005
QT	0.016**	0.009	

Table 4 Summary of the parameters and results for the M-ratio and BOTTLENECK analyses used to detect genetic bottleneck. NS=non-significant.

	M-ratio		BOTTLENECK		
θ	Mean M-ratio	M_c (Δ_g=3.5)	Mode shift	Mutation model	Heterozygote excess
0.01	0.754	0.817			
0.1	0.754	0.817			
0.5	0.754	0.780			
1	0.754	0.749		IAM	p=0.008*
5	0.754	0.712	NS	TPM	NS
10	0.754	0.710		SMM	NS
50	0.754	0.715			
100	0.754	0.705			
500	0.754	0.640			

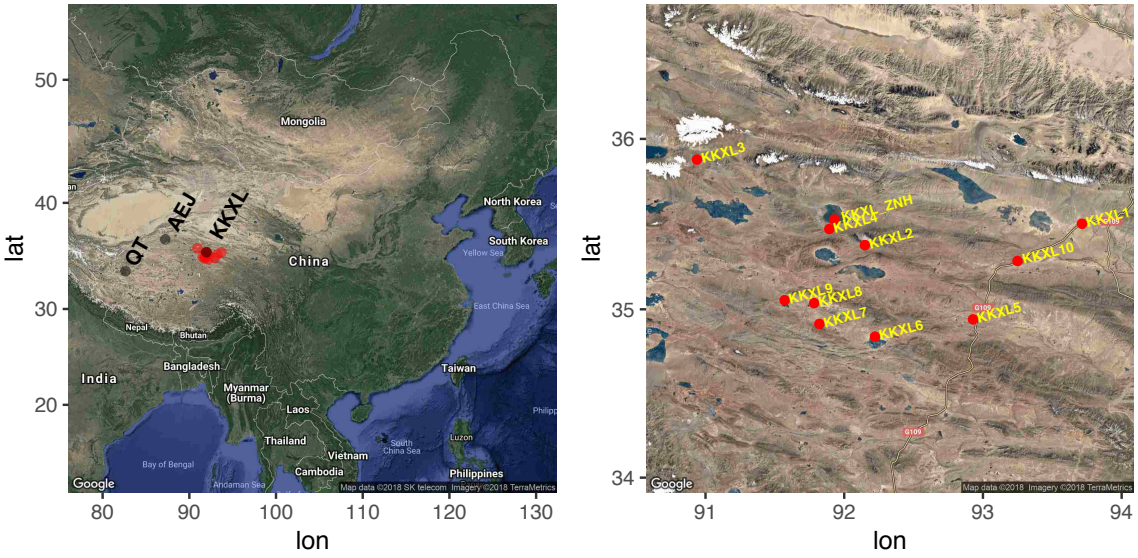

Figure 1 Sampling locations used for the large-scale study (left) and the local-scale study (right). Note: In the local-scale study, fresh scat samples were collected in ten different wintering grounds in KKXL (KKXL1 - KKXL10) and around the calving ground Zhuonai Lake (KKXL_ZNH). The large-scale study focused on three geographic populations of Chiru on the Tibetan Plateau, including the KKXL, examined above, along with Aerjin (AEJ) and Qiang Tang (QT) populations.

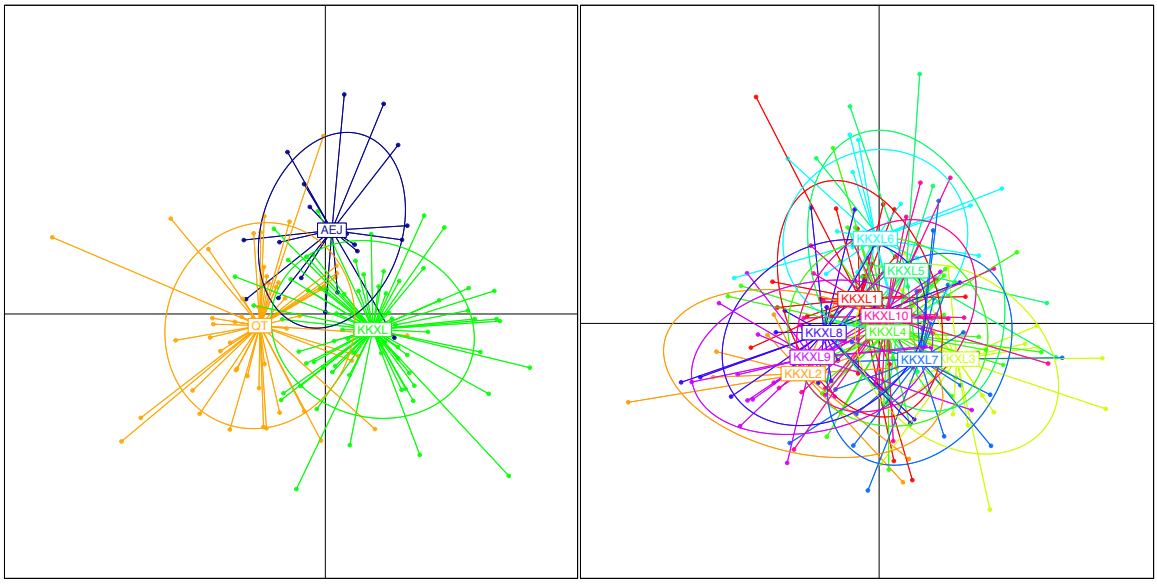

Figure 2 DAPC analyses with three geographical populations KKXL, AEJ and QT (left panel) and 10 sampling locations within KKXL (KKXL1-KKXL10, excluding KKXL_ZHN) (right panel) with discriminant function 1 on the x-axis and discriminant 2 on the y-axis.

Supplemental Table 1 Sampling location Information

Study	Sampling Site ID	Latitude	Longitude	Sample Type	Sampling Time	Sample Size
Local-scale	KKXL1	35.504	93.714	Feces	May, 2015/ April, 2016	24
	KKXL 2	35.378	92.149	Feces	May, 2015	10
	KKXL 3	35.880	90.939	Feces	May, 2015	23
	KKXL 4	35.472	91.893	Feces	May, 2015	44
	KKXL 5	34.941	92.928	Feces	Apr, 2016	15
	KKXL 6	34.838	92.222	Feces	Apr, 2016	20
	KKXL 7	34.914	91.821	Feces	Apr, 2016	22
	KKXL 8	35.036	91.783	Feces	Apr, 2016	20
	KKXL 9	35.054	91.570	Feces	Apr, 2016	20
	KKXL 10	35.285	93.249	Feces	May, 2015/ Apr, 2016	36
	KKXL_ZNH	35.529	91.930	Feces	Jul, 2015	149
Large-scale	QT	33.696	82.639	Dry skin	Sep, 2013	52
	AEJ	36.702	87.224	Placenta	Jul, 2014	20
	KKXL	35.498	91.977	Placenta	Jul, 2014	69

Supplemental Table 2A Six polymorphic microsatellite loci selected for fecal samples in the local-scale study

Loci	Primer (5'-3')	Ta (℃)	Multiplex Set	Reference
BM1824	F: GAGCAAGGTGTTTTTCCAATC R: CATTCTCCAACTGCTTCCTTG	58	1	(Bishop et al., 1994)
MCM38	F: TGGTGAATGGTGCTCTCATACCAG R: CAGCCAGCAGCCTCTAAAGGAC	58*	2	(H. Zhou, Li, Zhang, Yang, & Liu, 2007)
ILSTS005	F: GGAAGCAATGAAATCTATAGCC R: TGTTCTGTGAGTTTGTAAGC	55	3	(Brezinsky, Kemp, & Teale, 1993)
MB066	F: ATCTGCCTGAAGCCAGTCAC R: GGTTTCCTGCACCTGCATGA	56	4	(H. Zhou et al., 2007)
BM1225	F: TTTCTCAACAGAGGTGTCCAC R: ACCCCTATCACCATGCTCTG	56	4	(Bishop et al., 1994)
BM4107	F: AGCCCCTGCTATTGTGTGAG R: ATAGGCTTTGCATTGTTCAGG	56	5	(Bishop et al., 1994)

Note: All loci except for MCM38 were amplified as following: 95 ℃ (15 min), then 40 cycles at 94℃ (30s) / Ta℃ (90s) / 72℃ (60s), and a final extension at 60℃ for 30 min. MB066 and BM1225 were amplified in a duplex PCR. *: MCM38 was amplified in a touchdown PCR. 95 ℃ (15 min), then 12 cycles at 94℃ (30s) / 70℃ (90s) (with decrement of 1℃ per cycle) / 72℃ (60s), 28 cycles at 94℃ (30s) / 58℃ (90s)/ 72℃ (60s) and a final extension at 60℃ for 30 min.

Supplemental Table 2B Seven polymorphic microsatellite loci selected for dry skin and placenta samples in the large-scale study

Loci	Primer (5'-3')	Ta (℃)	Reference
L01	F:TCTTGTGATCTCTTCCAGTAGAG R:CGTCAGGCAATGAAGGTAG	54	(Zhou et al., 2014)
L03	F:CTGACTTCTTTCTCCCTACGA R:CAACCACTTTTGGATTCACAG	54	(Zhou et al., 2014)
L04	F:CAAGGGATCATTTCAATGCT R:TGTTCTGTGAGTTTGTAAGC	58.5	(Zhou et al., 2014)
ILSTS005	F:GGAAGCAATGAAATCTATAGCC R:TGTTCTGTGAGTTTGTAAGC	58	(Brezinsky et al., 1993)
TGLA68	F:ATCTTACTTACCTTCTCAGCGCT R:GGGACAAAATTTTACATATACACTT	59	(H. Zhou et al., 2007)
MCM38	F:TGGTGAATGGTGCTCTCATACCAG R:CAGCCAGCAGCCTCTAAAGGAC	58	(H. Zhou et al., 2007)
BM1341	F:CCTACCTACTGCACAGTTTTGC R:CTCCCATATAAGTTACCCACCC	60	(H. Zhou et al., 2007)

Note: All loci were amplified as following: as following: 95 ℃ (15 min), then 40 cycles at 94℃ (30s) / Ta℃ (90s) / 72℃ (60s), and a final extension at 60℃ for 30 min in singlex PCR.

Supplemental Table 3A Demographic parameters used for the Approximate Bayesian Computation (ABC) models of constant population size, population bottleneck with local-scale microsatellite dataset. N – Effective population size; Na – Ancestral population size; Nc – Contemporary population size; t: time of population bottleneck.

Parameter	Prior (uniform distribution)
Na	10-20,000
Nb	10-20,000
Nc (Nc<=Na)	10-20,000
Tb (in generations)	0-100

Supplemental Table 3B Demographic parameters used for the Approximate Bayesian Computation (ABC) models of constant population size, population bottleneck with mtDNA CR sequences. N – Effective population size; Na – Ancestral population size; Nc – Contemporary population size; t: time of population bottleneck.

Parameter	Prior (uniform distribution)
Na	10-1,000,000
Nb	10-1,000,000
Nc (Nc<=Na)	10-1,000,000
Tb (in generations)	0-100,000

Supplemental Table 4 Combined non-exclusion probability for STR loci used in studies. PI: combined non-exclusion probability for identity; P_{sib}: combined non-exclusion probability for sib identity.

Study	PI	P_{sib}
Local-scale study	5.28×10^{-11}	2.90×-7
Large-scale study	5.10×10^{-4}	3.40×10^{-3}

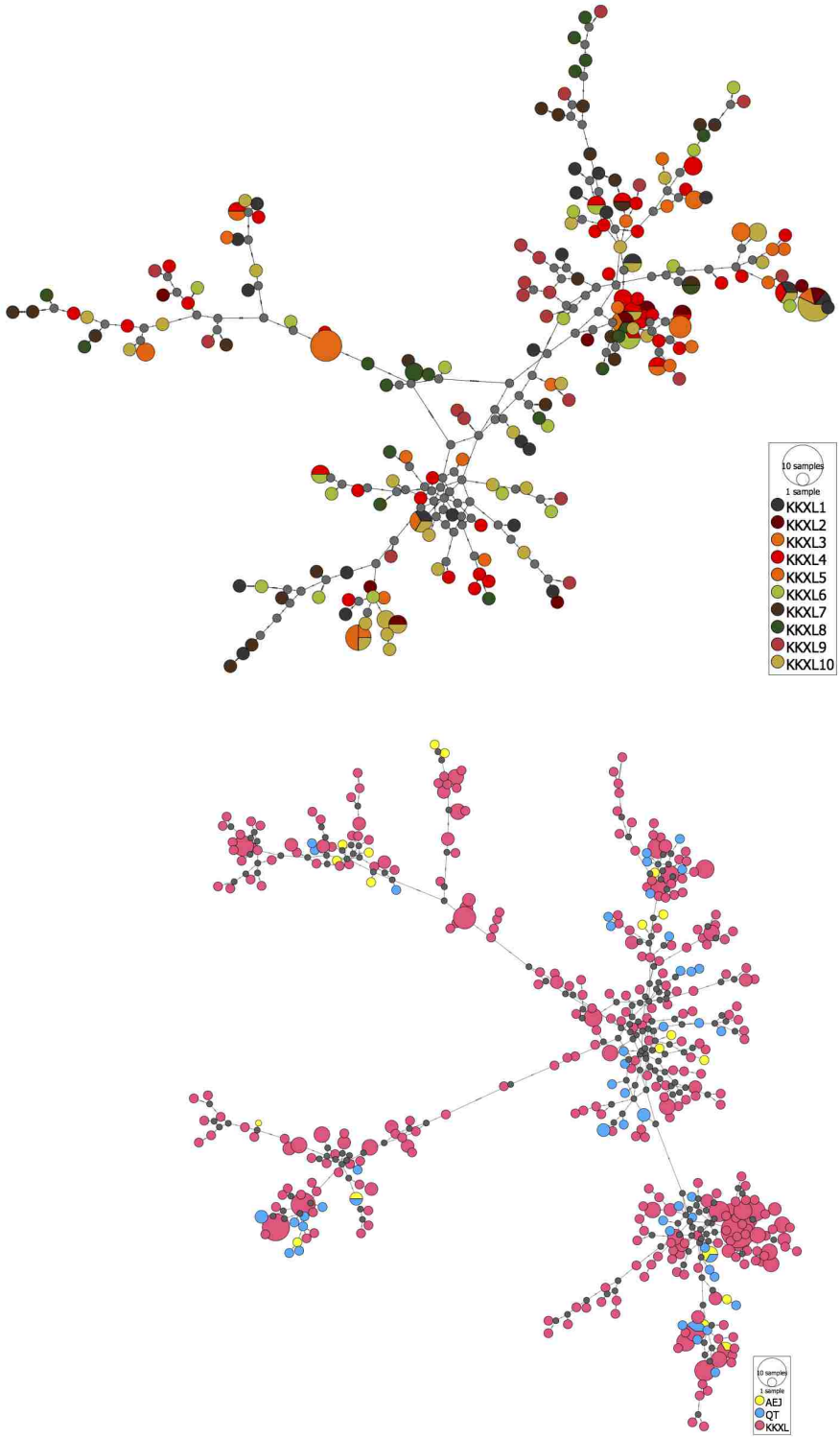

Supplemental Figure 1 Median-joining network analysis based on 1029 bp control region haplotypes (excluding indels). Top panel shows 190 haplotypes from 10 wintering locations within KKXL (excluding KKXL_ZHN). Bottom panel shows 381 haplotypes from three geographical populations AEJ, QT, and KKXL.

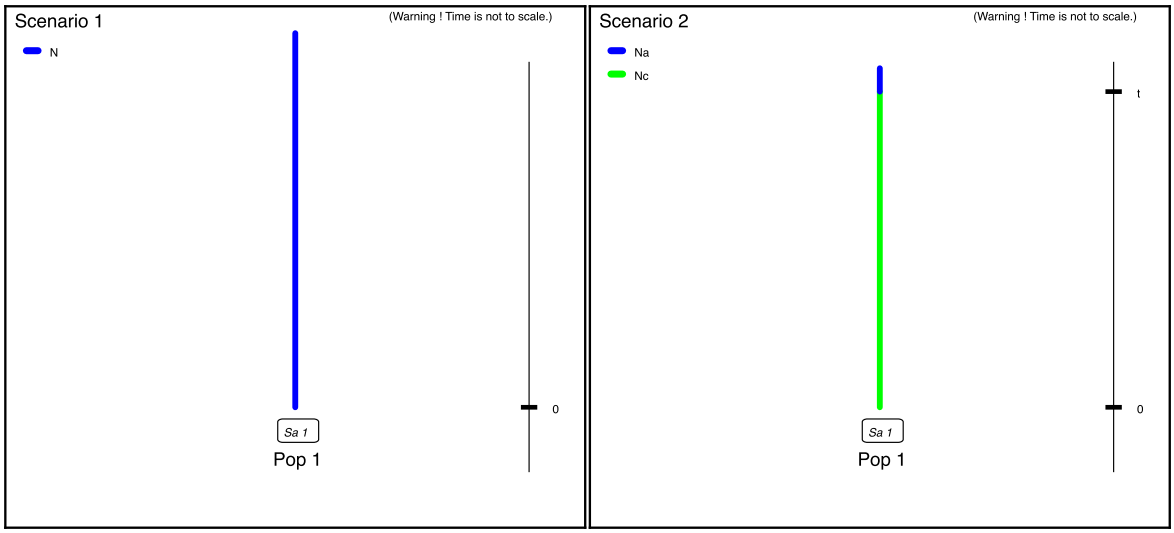

Supplemental Figure 2 Demographic scenarios for comparison used for ABC simulations. Scenario 1 is for constant population size and Scenario 2 is for population bottleneck.

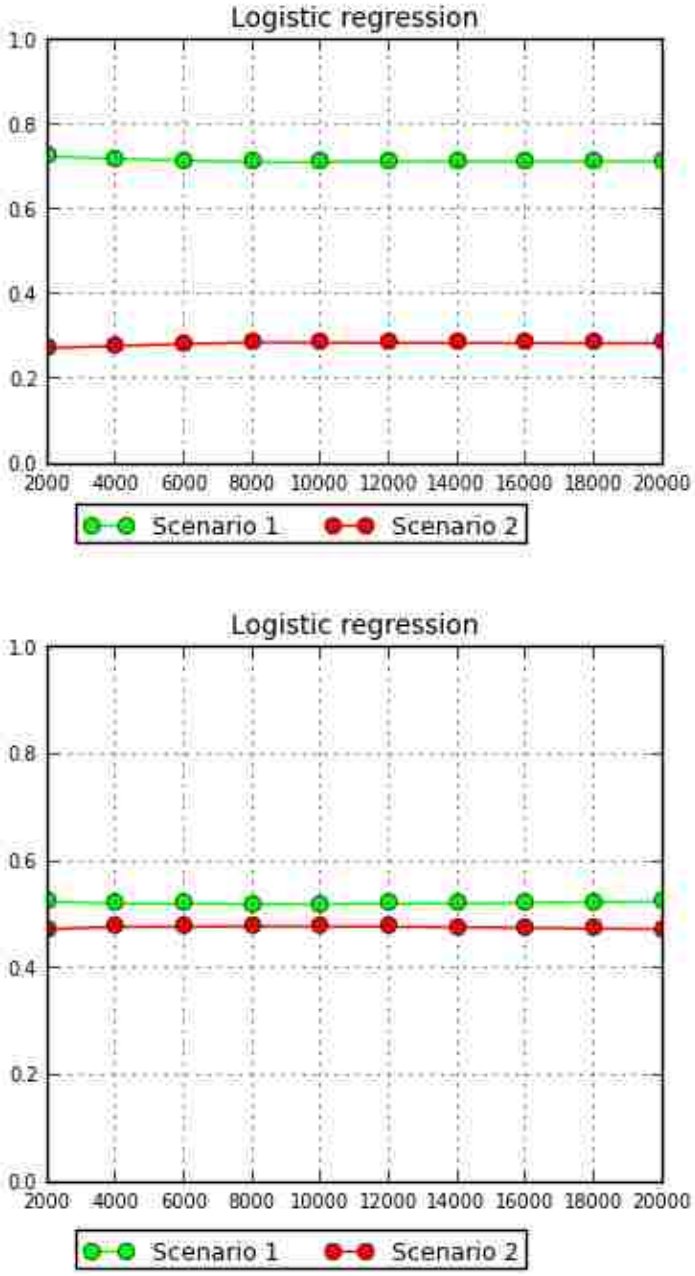

Supplemental Figure 3 Posterior probability of models in comparison with logistic regression implemented in DIYABC. Note: Scenario 1 is for constant population size and Scenario 2 is for population bottleneck. Top panel was based on simulation with mtDNA CR sequences and bottle panel was based on simulation with STR loci.

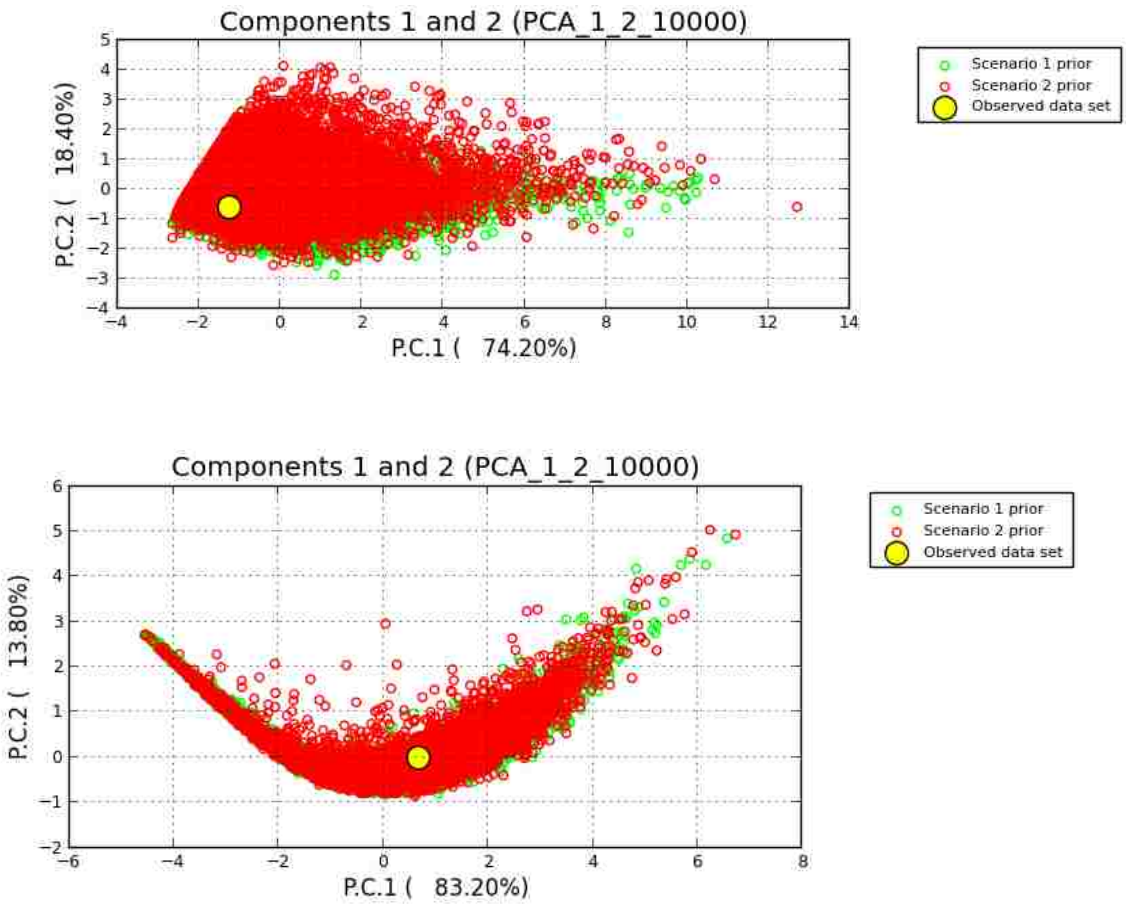

Supplemental Figure 4 Pre-evaluation of scenario-prior combination suitability with PCA analyses implemented in DIYABC. Observed dataset was placed within the 1% of simulated data sets. This suggests that the selected summary statistics and priors were suited for the models. Note: Scenario 1 is for constant population size and Scenario 2 is for population bottleneck. Top panel was based on simulation with mtDNA CR sequences and bottle panel was based on simulation with STR loci.

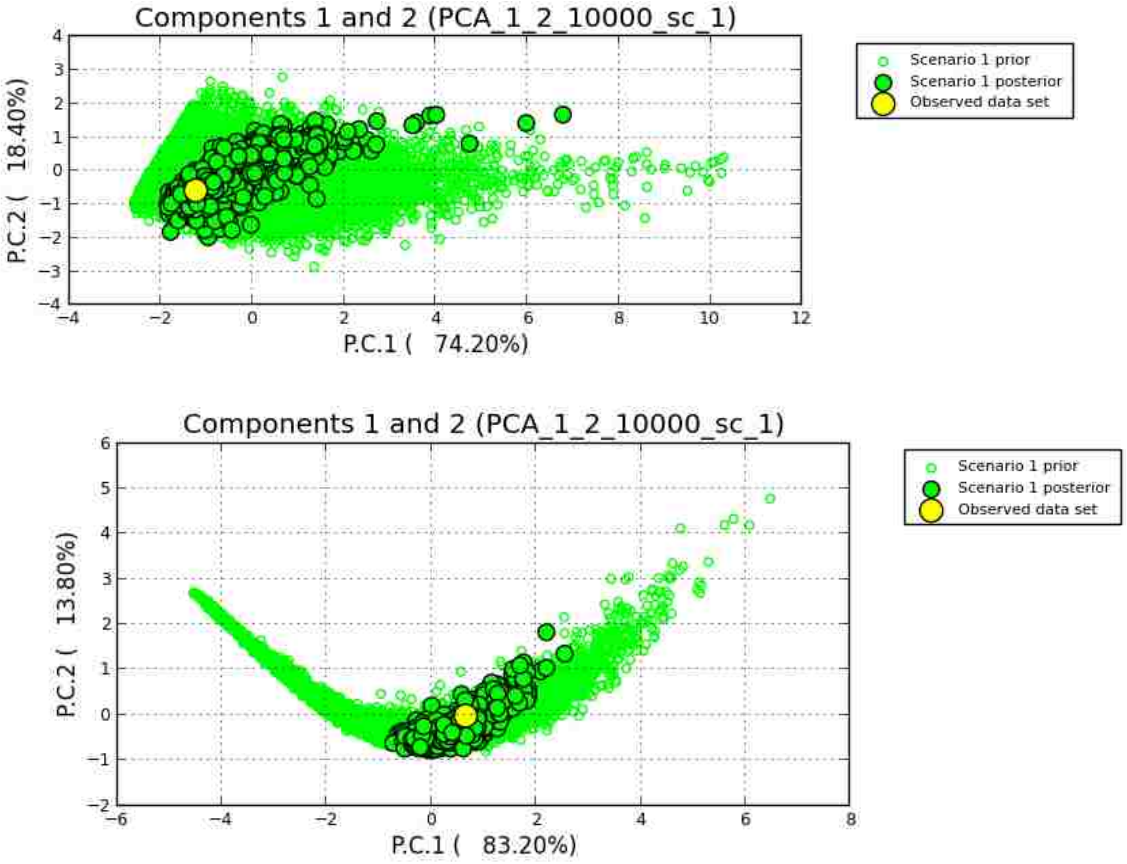

Supplemental Figure 5 Model checking to assess the goodness-of-fit for the best-supported scenario (Scenario 1 with constant population size) implemented in DIYABC. Model checking showed a large cluster of simulated data from the prior and a small cluster of data from the posterior predictive distribution with the observed data set placed within both, suggesting the model/posterior for scenario 1 provided a good fit to the observed data. Note: Top panel was based on simulation with mtDNA CR sequences and bottle panel was based on simulation with STR loci.

Supplemental method --- DIYABC methods

Larger demographic and temporal prior ranges were given for mtDNA CR sequences due to their larger N_e estimates from initials tests. Because no genetic structure was found in Chiru populations, both scenarios were simulated under the framework of a single population. We used a Generalized Stepwise Mutation (GSM) model with a mean STR mutation rate of 10^{-5} to 10^{-3} drawn from a uniform distribution. We set the shape to 0 so all individual loci took the same values (=mean). The prior for the mutation rate in mtDNA CR sequence was set to draw from a gamma distribution with mean 2.109×10^{-7} with mutation model as Hasegawa-Kishino-Yano or HKY (1985). All other default settings remained in place. We chose the following as summary statistics: 1) for mtDNA CR sequences: number of segregating sites, mean of pairwise differences, variance of pairwise differences and Tajima's D; 2) for STRs: mean number of alleles. Mean genic diversity and mean size variance. A total of 2×10^6 data sets were simulated and summary statistics per scenario were calculated on each simulation, with roughly equal representation of each scenario in the reference table. We used Principal Component Analysis (PCA) in the "pre-evaluate" option to initially evaluate scenario-prior combinations. To compare scenarios, we computed the posterior probability of each of them by performing a logistic regression based on 1% of the simulated data closest to observed data. The scenario with the higher posterior probability was selected as the best. For the best-supported scenario, we performed the option "model check" to assess the goodness-of-fit. A good fitting model should produce a cloud of data points simulated from the priors, on top of which lies the observed data within a smaller cloud of datasets from the posterior predictions. To assess confidence in scenario choice, we calculated type I and II error rates from 20,000 pseudo-observed datasets (PODs) for the "logistic approach. We measured the proportion of times that the best-fit scenario had the highest posterior probability compared the competing scenario out of 1000 requested PODs. Point estimates for demographic and temporal parameters were obtained by local linear regression on the 1% of simulated data sets closest to the observed dataset for the best-supported scenarios.

Chapter Two

Shift of maternal gut microbiome of Tibetan antelope (*Pantholops hodgsonii*) during the perinatal period

Yue Shi[1] *, Ziyan Miao[2], Jianping Su[2†], Samuel K. Wasser[1]

[1] Department of Biology, University of Washington, Box 351800, Seattle, WA 98195, USA

[2] Qinghai Key Laboratory of Animal Ecological Genomics, Northwest Institute of Plateau Biology, Chinese Academy of Sciences, No. 23 Xinning Road, Xining, Qinghai 810008, China

[*]Correspondence: Yue Shi (yueshi@uw.edu)

[†:] Deceased on 27 June 2018

Abstract

Maternal gut microbiome can influence and be affected by the substantial physiological changes taking place during the perinatal period. However, little information is known about the changes of the maternal gut microbiome during this period. Tibetan antelope (*Pantholops hodgsonii*) provide a unique system to address this issue because their summer migration cycle is synchronized with the perinatal period. We used 16S rRNA gene sequencing to generate gut microbiome profiles using fecal samples collected from female migratory Tibetan antelope. We then correlated microbiome diversity with fecal hormone metabolite concentrations of glucocorticoids (GCs) and triiodothyronine (T3) extracted from the same fecal samples. The maternal gut microbiome of Tibetan antelope was dominated by Firmicutes and Bacteroidetes. There was a clear separation in gut microbial composition by female reproductive states based on both hierarchical clustering and PCoA analyses. The shift in the maternal gut microbiome likely reflects the metabolic and immune system dynamics during the perinatal period. Overall, the microbiome diversity was higher in the late pregnancy compared to the postpartum period. The negative association between T3 and microbiome diversity may be moderated by the shift of reproductive states, since the correlations disappeared when considering each reproductive state separately. Integrating microbiome dimension, migration pattern and reproduction may have direct conservation implications as by establishing a base line of the physiological changes during the migration/perinatal period, we can have a better understanding on the impacts of increasing human activities on the Tibetan Plateau on the reproductive health of Tibetan antelope.

Keywords maternal gut microbiome, perinatal period, hormone, Tibetan antelope, reproductive heath

Introduction

The transition from pregnancy to lactation during the perinatal period is among the most important determinants of maternal-offspring health outcomes (Blaser & Domínguez-Bello, 2016; Dunlop et al., 2015; Prince et al., 2015). Substantial physiological changes occur during this transition, including changes in hormones, immune system modulation, and metabolism to shift resource allocation from energy storage to milk synthesis and preserve the health of both the mother and her offspring (Lain & Catalano, 2007; Zeng, Liu, & Li, 2017). Both late pregnancy and lactation are the two most energetic demanding female reproductive periods, with even more pronounced energy demands during lactation (Butte & King, 2005). Hormones serve as mediators in the process, directing nutrients and energy to the highly specialized maternal reproductive tissues and the developing fetus (Picciano, 2003). Two important metabolic hormones are involved in this transition, including glucocorticoids (GCs) and thyroid hormones (THs). GCs are released from the adrenal glands in vertebrates and regulated by the hypothalamic-pituitary-adrenal (HPA) axis. GCs can rapidly mobilize glucose in response to physiological and psychological stress (Palme, Rettenbacher, Touma, EL-Bahr, & Mostl, 2006). GC levels are elevated during pregnancy, allowing for greater substrate availability for fetal growth (Lain & Catalano, 2007; Zeng et al., 2017). THs are released by the thyroid gland and regulated by hypothalamus-pituitary-thyroid gland axis. THs function as a metabolic thermostat, continuously monitoring energy intake, and regulating metabolism accordingly (Douyon & Schteingart, 2002). Thyroid activity increases throughout the pregnancy. During the transition from pregnancy to

lactation, metabolic adjustments of thyroid hormones are essential in establishing metabolic priority for the lactating mammary gland (Capuco, Connor, & Wood, 2008).

Maternal gut microbiome is likely to influence and be affected by the physiological changes during the perinatal period and it is critical for the establishment and development of the neonatal microbiome (Prince et al., 2015). Pregnancy is associated with a profound alteration of maternal gut microbiota (Koren et al., 2012). However, little research has been conducted to assess whether maternal gut microbiota changes during the transitionary perinatal period. Two studies focused on human microbiome but had inconsistent results: one study found that human maternal gut microbiota remained stable over the perinatal period (Jost, Lacroix, Braegger, & Chassard, 2013) and the other study concluded that there was a change in microbial community structure and reduced microbiome diversity from pregnancy to postpartum in humans (Crusell et al., 2018). A third study, conducted on dairy cows, revealed distinct microbiome profiles between pre- and postpartum females, and argued that these changes resulted from the shifts in diet regime (Lima et al., 2015). More information is needed to document the shift in the microbiota composition during this critical transition period, which has profound impacts on the health outcomes of both females and offspring.

Gut microbiome studies have been conducted predominantly on humans and nonhuman primates (West et al., 2019). Comprehensive surveys of the microbiome composition in non-model species remain relatively rare, with primary focuses on the species of economic importance, such as cattle and horse (O’ Donnell, Harris, Ross, & O'Toole, 2017). The phyla Firmicutes and Bacteroidetes have been identified as the predominant phyla in the gut

microbiome of a variety of mammals, including carnivores, herbivores (ruminant and hindgut fermenters) and omnivores (Ley et al., 2008). Microbiome research in wildlife tend to focus on the impacts of land use change, climate change, captive breeding, non-native species invasion, antibiotics, infectious disease and environmental contamination on the microbiome diversity and community structure (Redford, Segre, Salafsky, del Rio, & McAloose, 2012; Trevelline, Fontaine, Hartup, & Kohl, 2019). We found no research integrating the microbiome dimension into wildlife reproduction.

Tibetan antelope (*Pantholops hodgsonii*) provide a unique system to study changes in microbiome during the perinatal period. Every summer, female Tibetan antelope depart from the wintering sites to the calving sites in May - June and return with their newborns in late July - early August (Schaller, 1998). Their summer migration cycle is synchronized with the perinatal period (Buho et al., 2011) with considerable energy demand (Butte & King, 2005) when both the females and offspring are most vulnerable. Tibetan antelope were reduced to the brink of extinction at the end of the 20th century by illegal poaching for their underfur. International conservation efforts successfully curbed the poaching through law enforcement and habitat protection. Their population size has recovered since 2011 (Leclerc, Bellard, Luque, & Courchamp, 2015). Integrating microbiome dimension, migration pattern and reproduction may have direct conservation implications as by establishing a baseline of the physiological changes during the migration/perinatal period, we can have a better understanding on the impacts of increasing human activities on the Tibetan Plateau on the reproductive health of Tibetan antelope.

The aim of this study was to characterize the changes in the maternal gut microbiome of Tibetan antelope during the perinatal period. We predicted that 1) the maternal gut microbiome of Tibetan antelope is dominated by Firmicutes and Bacteroidetes as with other mammals (Ley et al., 2008); 2) there is a shift in microbiome community composition in the perinatal period in response to the metabolic adjustments during the same time period. To control for the potential confounding impact of dietary changes during the sampling period on the maternal gut microbiome composition, we also included the sampling time into our linear models. We also explored the relationships between the changes in metabolic hormones and the gut microbiome diversity. We used 16S rRNA gene sequencing to generate gut microbiota profile in the perinatal period using fecal samples and correlated the microbiome diversity with fecal hormone metabolite concentrations of GC and triiodothyronine (T3). T3 is the most biologically active form of THs. Fecal samples are often used as a proxy for the gut microbiome due to their accessibility and non-invasive nature (Yasuda et al., 2015), though fecal samples are not completely representative of the entire gut microbiome (Ingala et al., 2018). This study sheds light on how the microbiome composition shifts during this transition period and emphasizes the importance of incorporating the maternal gut microbiome into the conservation management efforts to support animal reproductive health and overall recovery success of Tibetan antelope.

Materials and Methods

Ethics Statement

Tibetan antelope is listed in the Category I of the National Key Protected Wild Animal Species under China's Wild Animal Protection Law. In September 2016, Tibetan antelope were reclassified from Endangered to Near Threatened by the International Union for Conservation of Nature (IUCN) Red List due to the recovery of their population size. Sample collection and field studies adhered to the Wild Animals Protection Law of the People's Republic of China. Fresh scat samples were collected under IACUC protocol #2850-12 and local regulations to minimize disturbance.

Sample Collection

Qinghai-Tibet Railway bisects the migration route of Tibetan antelope approximately 40 km from their summer calving area at Zhuonai Lake. Female Tibetan antelope almost exclusively use the Wubei Bridge underpass (35°15'2.71"N, 93° 9'45.12"E), a 198m long, 30m wide structure (Xia, Yang, Li, Wu, & Feng, 2007). We collected fecal samples at the Wubei Bridge underpass when females migrated to and returned from the calving ground in 2017. Females are in the late pregnancy stage when migrating to the calving ground, and in the postpartum period when on their return to the wintering ground. Animals were observed with binoculars from a recommended viewing distance of ~ 300 m (Lian, Zhang, Cao, Su, & Thirgood, 2007) until they defecated and left the area. To minimize the chance of collecting multiple fecal samples from the same individual, three field assistants were involved in sample collection in three different directions. We excluded fecal samples of small size to avoid collecting fecal samples from the young and newborns. Adult males do not conduct the seasonal migration. A total of 65 fresh scat samples were collected and placed into individual zip-loc bags along with records of the date and GPS coordinates. Fifty

samples were collected during the late pregnancy stage and 15 samples collected during the postpartum period. Samples were kept frozen at – 20 °C until lab analyses.

DNA Extraction and Species Identification

To minimize environmental contamination, we extracted DNA from the well-preserved core of one fecal pellet per sample (Menke, Meier, & Sommer, 2015) using the E.Z.N.A.® DNA isolation kit (Omega Biotek, Norcross, GA, U.S.). The DNA concentration and quality were evaluated using Nanodrop™ 2000 Spectrophotometer (Nanodrop, Wilmington, DE, USA), and visualized with 1% agarose gel electrophoresis. A short fragment (196 bp) of mtDNA cytochrome c oxidase subunit I gene was amplified and sequenced using the forward primer (5' GCCCCTGATATAGCATTCCC 3') and the reverse primer (5' CTGCCAGGTGTAGGGAGAAG 3'). PCR was conducted using EasyTaq PCR SuperMix (Transgen Biotech, Inc.) with 4 ul DNA template. 2.5 ul 10 mg/ml of bovine serum albumin was added to the PCR mix to improve amplification success. We followed the recommended thermo protocol in the kit with an annealing temperature of 51° C. Sequences were checked against the NCBI database using BLAST for species confirmation.

Library Preparation

The V3-V4 region of the 16S rRNA gene was amplified using the forward primer 338F (5'-ACTCCTACGGGAGGCAGCAG-3') and the reverse primer 806R (5'-GGACTACHVGGGTWTCTAAT-3') (Mori et al., 2014). Each primer was designed to contain: 1) the appropriate Illumina adapter sequence allowing amplicons to bind to the flow cell; 2) an 8bp index sequence; and 3) gene-specific primer sequences as described above. PCR

reactions were conducted using the TransStart® FastPfu DNA Polymerase kit (TransBionova Co., Ltd, Beijing, China) with 20 μL reaction solution in total including 10 ng template DNA, 4 μL 5×FastPfu buffer, 2 μL 2.5 mM dNTPs, 0.8 μL of each primer (5 μM), 0.4 μL FastPfu Polymerase and 0.2 μL 20 ng/ μL of bovine serum albumin. The PCR cycling conditions were as follows: 95 ℃ for 3 min, followed by 27 cycles of 95 ℃ for 30 s, 55 ℃ for 30 s, and 72 ℃ for 45 s and a final extension of 72 ℃ for 10 min. All PCR products were visualized on agarose gels (2% in TAE buffer) and purified with AxyPrep DNA Gel Extraction Kit (Axygen Biosciences, Union City, CA, USA). Before sequencing, DNA samples were quantified using QuantiFluor™-ST (Promega, USA). Paired-end amplicon libraries were constructed, and sequencing was performed using the Illumina MiSeq PE300 platform at Majorbio BioPharm Technology Co., Ltd., Shanghai, China.

Bioinformatics Analyses

Sequencing reads were analyzed using the *DADA2* pipeline (Callahan et al., 2016) with the following steps: 1) Initial quality filtering was performed using the *filterAndTrim* command with default parameters. Forward and reverse reads were truncated at 290 bp and 210 bp respectively; 2) Amplicon sequence variants (ASVs) were inferred using the core DADA2 sample inference algorithm, *dada*, after error rate model generation and sequence dereplication; 3) Forward and reverse reads were merged together to obtain the full denoised sequences using the *mergePairs* command; 4) Chimeric sequences were identified and removed using the *removeBimeraDenovo* command; 5) Taxonomy classification was assigned to each ASV using the *assignTaxonomy* command using the Silva reference database (version 132/16s_bacteria) (Quast et al., 2012). 16S rRNA gene analysis is limited

for species-level classification because closely related bacterial species may have near identical 16S rRNA gene sequences (Plummer & Twin, 2015). Therefore, each ASV was assigned only down to the genus level. Finally, ASVs with less than 10 copies in the resulting ASV table were removed.

Fecal Hormone Metabolite Analyses

Fecal samples were freeze-dried to remove water content. Fecal GC and T3 metabolites were then extracted from freeze-dried fecal samples following previously described protocols (Wasser et al., 2010; 2004; 2000). Briefly, each freeze-dried fecal sample was thoroughly homogenized before suspending ~0.1 g of fecal powder in 15 ml of 70% ethanol, followed by 30 min continuous agitation. After centrifugation (1800 g; 20 min), the supernatant was poured into a new vessel. An additional 15 ml of 70% ethanol was added to the remaining fecal power for a second extraction. This mixture was agitated for 30 min and centrifuged at 1800 g for 20 min. Supernatants from both extractions were combined and stored at -20 °C.

Since most native hormones are excreted as metabolites in feces (Palme, Fischer, Schildorfer, & Ismail, 1996), it is essential to select an appropriate assay system that includes a group-specific antibody, which is capable of detecting the predominant fecal metabolites of the parent hormone in the species investigated (Palme et al., 1996; Touma & Palme, 2006; Wasser et al., 2000). Fecal GC metabolites were diluted with assay buffer at the ratio of 1:30 and analyzed using DetectX® Corticosterone Immunoassay kit (Arbor Assays). This assay kit was chosen because a previous study has shown that corticosterone antibody has the highest affinity for the major cortisol metabolites (Wasser et al., 2000).

Fecal T3 metabolites were diluted at the ratio of 1:60 and analyzed using DetectX® Triiodothyronine (T3) Immunoassay kit (Arbor Assays), because T3 metabolite maintains its pure form in many mammalian species (Wasser et al., 2010). Both hormone assays were validated using serially diluted fecal extracts pooled from 10 random samples. The displacement curves were parallel to those of standard hormone preparations, indicating that hormone concentrations were reliably measured across their ranges of concentrations. In addition, the recovery rate of the GC and T3 standards was 127.8% and 127.6% respectively, indicating limited amount of interference in hormone binding from the substances in the fecal extracts of Tibetan antelope.

Statistical Analyses

Rarefaction curves were plotted for each sample using the *rarecurve* function in the *vegan* R package to assess the adequacy of sequencing depth. Variations in sequencing depth among samples were normalized using the variance stabilizing transformation (VST) implemented in the *DESeq2* R package (McMurdie & Holmes, 2014). Hierarchical clustering and principal coordinate analyses (PCoA) based on the Euclidean distance matrix of VST data were performed to visualize microbial composition differences as a function of reproductive states (late pregnancy vs. postpartum period). Analysis of Similarity (ANOSIM) test was used to assess significant differences in microbial community composition as a function of reproductive states, while controlling for the time of the year using *strata*. We filtered out phyla, classes and orders with relative abundance less than 0.1% and familiae and genera with a relative abundance less than 1%. Changes in the relative abundance of taxa between reproductive states were analyzed through Wilcoxon

signed-rank tests and *p* values were adjusted with the Benjamini-Hochberg method to control for false discovery rate. We used the *Phyloseq* R package to compute alpha diversity including richness measurements (Observed number of ASVs, Chao 1 richness estimator, Abundance-Based Coverage Estimator or ACE) and diversity indices (Shannon diversity index, Inverse of the Simpson diversity estimator or InvSimpson, Fisher's index). T-tests were conducted to compare microbial alpha diversity between reproductive states. Fecal hormone metabolite concentrations were natural log-transformed to meet the assumption of normality. We used Wilcoxon signed-rank tests to compare fecal hormone metabolite concentrations between reproductive states since the assumption of homogeneity of variance was not met. We constructed linear models of microbial alpha diversity as a function of fecal hormone metabolite concentrations (natural-log transformed), reproductive states and interactions between main effects. We used analysis of covariance (ANCOVA) to compute the analysis of covariance tables for fitted models.

Results

Maternal gut microbiota is dominated by Firmicutes and Bacteroidetes

After quality filtering, denoising, read merging and singleton/chimera removal, 1,415,743 high quality sequence reads were retained with an average of 21,781 reads per sample (from 15,129 to 32,148) and a median sequence length of 406 bp. In total, there were 6,026 ASVs identified. The rarefaction curves on the number of ASVs reached a plateau, suggesting that the sequencing depth was adequate, and the microbial community was well surveyed (Supplementary Figure 1). Taxonomic assignments revealed 8 bacterial phyla

with relative abundance above 0.1% (Figure 1). Dominant phyla were Firmicutes (67.97%), Bacteroidetes (26.30%), Verrucomicrobia (2.94%) and Actinobacteria (1.12%). There were 11 classes with relative abundance above 0.1% with dominant classes including Clostridia (phylum: Firmicutes; 66.92%), Bacteroidia (phylum: Bacteroidetes; 26.30%), Verrucomicrobiae (phylum: Verrucomicrobia; 2.94%) and Actinobacteria (phylum: Actinobacteria; 1.03%) (Supplementary Figure 2). All sequence reads were assigned at the levels of phylum and class, suggesting there was few sequencing artifacts in the dataset. At the order level, we found 11 orders with the relative abundance above 0.1%, with dominant orders including Clostridiales (phylum: Firmicutes; 66.89%), Bacteroidales (phylum: Bacteroidetes; 26.06%), Verrucomicrobiales (phylum: Verrucomicrobia; 2.93%) and Micrococcales (phylum: Actinobacteria; 1.03%) (Supplementary Figure 3). Ten families with relative abundance greater than 1% were found (Figure 2). Dominant families included *Ruminococcaceae* (phylum: Firmicutes; 46.79%), *Lachnospiraceae* (phylum: Firmicutes; 12.17%), *Bacteroidaceae* (phylum: Bacteroidetes; 9.21%), *Rikenellaceae* (phylum: Bacteroidetes; 8.42%) and *Christensenellaceae* (phylum: Firmicutes; 5.79%), *Akkermansiaceae* (phylum: Verrucomicrobia; 2.93%), *Prevotellaceae* (phylum: Bacteroidetes; 2.80%), *Muribaculaceae* (phylum: Bacteroidetes; 1.21%) and *Micrococcaceae* (phylum: Actinobacteria; 1.03%). About 4.41% of sequence reads could not be assigned at the family level. The taxonomic classification at the genus level is ambiguous as about 21.58% of sequence reads could not be assigned at the genus level (Supplementary Figure 4).

The composition of maternal gut microbiota shifts in the perinatal period

There was a clear separation in maternal gut microbial composition by female reproductive states based on the results of both hierarchical clustering (Figure 3) and PCoA analyses (Supplementary Figure 5). The differences in the microbial composition remained significant after controlling for the time of the year ($p = 0.001$). The core set of maternal gut microbiome (including the dominant phylum Firmicutes, Bacteroidetes and Verrucomicrobia) remained stable in the transition from the late pregnancy to the postpartum period (Figure 1). However, there was significant enrichment in Actinobacteria (+1.44%; adjusted $p < 0.05$), Tenericutes (+0.42%; adjusted $p < 0.01$), Cyanobacteria (+0.48%; adjusted $p < 0.001$) and Proteobacteria (+0.15%; adjusted $p < 0.05$) during late pregnancy compared to the postpartum period (Figure 1). At the family level, *Christensenellaceae* were more abundant (+3.31%; adjusted $p < 0.001$) during late pregnancy, while *Muribaculaceae* were more abundant during the postpartum period (+1.6%; adjusted $p < 0.001$). At the genus level, *Christensenellaceae_R-7_ group* (+3.33%; adjusted $p < 0.001$), *Ruminococcaceae_UCG-010* (+2.46%; adjusted $p < 0.01$) and *Ruminococcaceae_UCG-014* (+0.95%; adjusted $p < 0.01$) were significantly enriched during the late pregnancy, whereas *Ruminococcaceae_UCG-005* (+9.04%; adjusted $p < 0.001$), *Alistipes* (1.87%; adjusted $p < 0.001$) and *Lachnospiraceae_NK4A136_ group* (+1.08%; adjusted $p < 0.01$) were significantly enriched during the postpartum period.

Impacts of hormonal changes on gut microbiome diversity

Overall, alpha diversity in the gut microbiota of female Tibetan antelope was significantly higher in the late pregnancy period compared to those in postpartum period across all alpha diversity indices we tested (observed number of ASVs: $p < 0.0001$; Chao1: $p < 0.0001$; ACE: $p < 0.0001$;

Shannon: $p < 0.001$; InvSimpson: $p < 0.0001$; Fisher: $p < 0.0001$) (Figure 4). Fecal GC metabolite concentrations did not significantly differ between reproductive states ($p = 0.06$; Figure 5, left). However, T3 concentrations were significantly higher in the postpartum period compared to late pregnancy ($p < 0.0001$; Figure 6, right). There was significant negative correlation between T3 and alpha diversity measurement (Observed, Chao1, ACE and Fisher) during the transition from late pregnancy to the postpartum period ($p<0.05$; Supplementary Figure 6), however this relationship became insignificant when only considering each reproductive state separately (Figure 6). There was no significant correlation between GC and any microbiome alpha diversity measurement (Figure 6 and Supplementary Figure 6). T3 only explained 5.70% of the total variance in microbiome alpha diversity among samples (*adj* R^2 = 0.057). When we included both T3 and the reproductive states in the linear model, the fit of the model increased with *adj* R^2 as 0.306.

Discussion

In this study, we characterized the maternal gut microbiota of Tibetan antelope and revealed a significant shift in the microbiome community composition and reduced microbiome diversity in the transition from late pregnancy to the postpartum period. We also found that there was significant negative correlation between T3 and microbiome diversity (Observed, Chao1, ACE and Fisher) during this transition, however this relationship became insignificant when considering each reproductive state separately.

The maternal gut microbiota of Tibetan antelope is dominated by Firmicutes and Bacteroidetes (Figure 1). This finding is consistent with the microbiome composition in other mammals (Lau et al., 2018; Ley et al., 2008). In herbivores, these two dominant phyla

accounted for 79% - 86% of the total microbiome community (O' Donnell et al., 2017). Microbiome composition responds to the *in vivo* oxygen level. The animal gut is deeply anaerobic and thus dominated by strict anaerobes, such as Firmicutes and Bacteroidetes (Friedman et al., 2018). Facultative anaerobes, such as Proteobacteria and Actinobacteria, are typically 100-fold lower in abundance compared to strict anaerobes (Nagpal et al., 2017). One of the vital roles played by the symbiont gut microbiome is nutrient uptake (Krajmalnik-Brown, Ilhan, Kang, & DiBaise, 2012). Animals are capable of digesting proteins, lipids, and simple sugars through enzymatic breakdown. However, these enzymes are not able to digest the complex structural polysaccharides of plants (Dearing & Kohl, 2017). Microbes can break down these structural polysaccharides into volatile fatty acids, allowing them to be absorbed and assimilated to provide energy for the host (Dearing & Kohl, 2017). The average ratio between Firmicutes and Bacteroidetes in Tibetan antelope is 2.52:1, which corresponds to the trade-offs between carbohydrate and protein fermentation. Plant-based diets increase the relative abundance of Firmicutes that metabolize dietary plant polysaccharides while decreasing the relative abundance of Bacteroidetes that is closely associated with protein-based diets (David et al., 2013; Lima et al., 2015). Verrucomicrobia is the third most abundant phylum (2.94%) in the gut microbiome of Tibetan antelope (Figure 1) and is reportedly important for hydrolyzing multiple polysaccharides, including laminarin, xylan and chondroitin sulfate (Cardman et al., 2014). The majority of Verrucomicrobia-associated sequences were classified to the genus *Akkermansia*, which are biomarkers for a healthy mucus layer in the animal gut and brings a competitive advantage during nutrient deprivation (Belzer & de Vos, 2012). In total, these three phyla had a combined relative abundance of 97.21%. This core set of

maternal gut microbiome represents a significant benefit for Tibetan antelope in terms of energy and nutrition acquisition from food. We also found the presence of Cyanobacteria in the gut microbiome community of Tibetan antelope, though its prevalence was only 0.472% (Figure 1). Cyanobacteria have only been recently recognized in the gut microbiome, and is specifically common in the guts of herbivores (Di Rienzi et al., 2013). Recently, these Cyanobacteria-related gut bacteria have been assigned to a new phylum, Melainabacteria. In addition to helping with the digestion of plant fibers, Melainabacteria can also synthesize several B and K vitamins (Di Rienzi et al., 2013).

There was a significant reduction in the microbiome alpha diversity from late pregnancy to the postpartum period (Figure 4), consistent with a previous study (Crusell et al., 2018). We also found distinct microbiome profiles during late pregnancy and the postpartum period (Figure 3). This finding is not surprising, considering the postpartum period plays a vital role in "resetting" maternal changes accumulated during pregnancy (Stuebe & Rich-Edwards, 2008). Visceral fat accumulates and insulin resistance level increase throughout gestation (Lain & Catalano, 2007; Nelson, Matthews, & Poston, 2010). The accumulated fat stores are mobilized post-partum to support lactation, shifting resource allocation from energy storage to milk synthesis. Lactation results in improved insulin sensitivity, drop in inflammation and reduced adiposity. Microbiome might play a crucial role in this transition, ensuring continuous energy supply to support the growth and development of the fetus and lactation. We found increased abundance of members of Actinobacteria and Proteobacteria during late pregnancy, as previously reported (Koren et al., 2012). Actinobacteria are positively related to the plasma glucose level (Crusell et al., 2018) and may increase insulin insensitivity during pregnancy (Koren et al., 2012). Proteobacteria are

known to include multiple pathogens and to drive proinflammatory change, alter the gut microbiota in favor of dysbiosis, and ultimately lead to inflammation such as gastrointestinal disease (Mukhopadhya, Hansen, El-Omar, & Hold, 2012; Shin, Whon, & Bae, 2015). Normal healthy pregnancy is characterized with controlled mild maternal systemic inflammatory response, with increased leukocytes (CD11b, CD14 and CD64) and increase intracellular reactive oxygen species (Sacks, Studena, Sargent, & Redman, 1998). When the fetus has completed its development during the third trimester, the maternal proinflammatory environment promotes the contraction of uterus, expulsion of the baby and rejection of the placenta (Mor, Cardenas, Abrahams, & Guller, 2011). But heightened maternal inflammation during pregnancy can have adverse impacts on the offspring, including increased risk of brain development problems (Rudolph et al., 2018). *Ruminococcaceae_UCG-005* was significantly enriched during postpartum period and they are positively related with elevated concentration of acetate, butyrate and total SCFA (Gao et al., 2019). Taken collectively, these changes in microbiome composition represent reflect the metabolic and immune changes in the critical transition period from late pregnancy to the postpartum period. However, unexpectedly, we found *Christensenellaceae* were more abundant during late pregnancy. Members of *Christensenellaceae* are reportedly associated with lean host phenotype (Goodrich et al., 2014), however, pregnancy is characterized with excess adiposity and weight gain. We only started to decipher the functions of gut microbiome in the perinatal period and many unknowns remain to be explored. For example, the family *Muribaculaceae* is recently classified (Lagkouvardos et al., 2019) and we are not sure about their precise roles in the transition from late pregnancy to postpartum period. The same applies to other taxa, such as *Christensenellaceae_R-7_ group*,

Ruminococcaceae_UCG-010, *Ruminococcaceae_UCG-014*, *Alistipes* and *Lachnospiraceae_NK4A136_ group*. Additional in-depth genetic analysis and functional studies will be required to understand the roles of these important taxa in this transition period.

We found higher T3 levels in the postpartum period (Figure 5). T3 declines in response to persistent nutritional stress, slowing down metabolism to guard against the body using up its remaining reserves (Douyon & Schteingart, 2002). Majority studies have shown similar basal metabolic rate in the lactating and pregnancy state (Butte & King, 2005) and relatively constant T3 level in this transition period (Hendrick, Altshuler, & Suri, 2011). Study in wild Amazon river dolphin showed that lactating and non-pregnant adult females had significantly higher total T3 concentrations than pregnant females, and this difference was primarily driven by the drop in the total T3 concentrations during the late pregnancy, likely due to competition for circulating iodine from the fast-growing fetus (Robeck et al., 2019). The observed increased T3 level in the postpartum period in our study might also suggest an increase in energy intake and/or increase in energetic demands in migratory lactating female Tibetan antelope. In fact, their return trip takes twice as long as the trip migrating to the calving grounds (Buho et al., 2011). We did not observe a reduction in GC level in the postpartum period (Figure 5), unexpectedly. In humans, maternal plasma GC level increases throughout pregnancy, reaching a peak near term (Concannon, Butler, Hansel, Knight, & Hamilton, 1978). The GC level declines towards pre-pregnancy level after delivery as the HPA axis gradually recovers from its activated state during pregnancy (Hendrick et al., 2011; Mastorakos & Ilias, 2003). However, the rate of HPA normalization period varies from a couple of days to a couple of months in humans (Abou-Saleh, Ghubash, Karim, Krymski, & Bhai, 1998; Glynn, Davis, & Sandman, 2013; Jung et al., 2011; Mastorakos & Ilias, 2003).

Sampling time may have also been a factor in our study. It takes Tibetan antelope about 8 days to reach the calving ground from our sampling location at Wubei Bridge. The animals usually stay at the calving ground for 8-20 days, and the return trip takes about 14-16 days (Buho et al., 2011). Since we did not collect samples immediately prior to parturition, we may have missed the samples with the peak GC level. By the time we collected the postpartum samples, the GC level could have dropped to the degree that is comparable to the level in the pregnant samples we collected.

We did not find a significant correlation between hormonal changes (T3 or GC) and the microbiome diversity when considering each reproductive state separately (Figure 6). T3 only explained 5.70% of the total variance in microbiome alpha diversity among samples ($adj\ R^2 = 0.057$). When we included both T3 and the reproductive states in the linear model, the fit of the model increased to 30.6%. Therefore, the observed change in the microbiome diversity was mainly and significantly driven by the reproductive transition in the linear models. However, our results do not rule out the impacts of metabolic hormones on microbiome diversity, because there was a small but significant negative correlation between T3 and alpha diversity measurement (Observed, Chao1, ACE and Fisher) during the transition from late pregnancy to the postpartum period (Supplementary Figure 6). We only focused on the perinatal period, which was a relative short period (about 45 days). The lack of correlation between T3 and microbiome diversity right before and after parturition should not be generalized to the whole gestation and lactation period. There might be other hormones worth investigating in the future studies, such as insulin, insulin-like growth factor, C-peptide, glucagon, gastrointestinal polypeptide, ghrelin, leptin, and resistin (Gomez-Arango et al., 2016). However, these hormones are peptide hormones and

can only be measured with serum samples. The immune system can also have profound effects on the gut microbiota (Koren et al., 2012), which was not investigated in this study. Future studies should also look at metabolomics, as hormones might affect metabolic activities of microbiome as well.

One assumption we made throughout this study is that fecal samples collected in May - June were collected from pregnant females (during westward migration to the calving ground), and the samples collected in July - August (during eastward migration back to the wintering ground) were from postpartum females. Since only female Tibetan antelope conduct seasonal long-distance migration (Schaller, 1998), we were confident that there were no adult male samples in our collection. We acknowledge that not all migratory females are pregnant and a proportion of migratory individuals are non-pregnant yearlings (Schaller, 1998). In the postpartum period, the ratio of adult to young females is about 2:1 based on field observations (Schaller, 1998; Xia et al., 2007). We avoided collecting fecal samples from the young and newborns by ignoring smaller sized fecal pellets. Future studies could include progesterone in the suit of fecal hormonal metabolite assays to filter out nonpregnant migratory females. However, there are no fecal endocrine measures that can identify lactating females (Hodges & Heistermann, 2011).

The gut microbiome can respond rapidly to dietary change (David et al., 2013) and thus seasonal dietary change could be a confounding factor in this study. However, the differences in the microbial composition remained significant after controlling for the time of the year (p = 0.001). We collected fecal samples at the same location when female Tibetan antelope cross the Wubei Bridge during the late pregnancy and postpartum period,

so the vegetation composition in their diets were relatively consistent. Their migration period overlaps with the short plant-growing season on the Tibetan Plateau (Mo et al., 2018). The forage quality is relatively consistent throughout the migratory period, and only drops after September (Leslie & Schaller, 2008). Therefore, the impacts of dietary changes on microbiome during the migration period were likely minimal compared to the shift in reproductive states.

In conclusion, we characterized the maternal gut microbiota of wild Tibetan antelope and demonstrated its shift during the transition from late pregnancy to the postpartum period. These changes appear to support energetic demands of these two reproductive states. Microbiome diversity was significantly reduced in the postpartum period. Neither GC nor T3 significantly affected microbiome diversity when only considering each reproductive state separately. Further investigations on other metabolic hormones or immune system are needed in order to clarify underlying reasons for community shift and reduced diversity of maternal gut microbiome during the perinatal period. Our study is the first case to integrate microbiome analysis into wildlife reproduction research. More information needs to be gathered about how the microbiota composition shifts during the perinatal period in order to optimize the reproductive health and overall recovery success for priority species.

Acknowledgements

We thank Rebecca Booth for the advice on hormonal assays. We thank Kekexili Natural Nature Reserve Administration for assistance in the fieldwork. We thank Richard G.

Olmstead and Noah Synder-Mackler for feedback that greatly improved the manuscript. The study was funded by the China Scholarship Council (CSC) Graduate Research Fellowship, Fritz/Boeing International Research Fellowship and WRF Hall Fellowship.

Data Accessibility

After peer review and prior to final publication, the raw sequence data will be deposited in NCBI under the SRA accession number #########. The following data will be deposited in Dryad: (i) filtered ASV sequences (*fastq* format); (ii) filtered ASV abundance table with taxonomic affiliations (*csv* file); (iii) sample metadata information (*csv* file).

Author Contributions

YS, JPS, and SKW conceived the project. YS designed the experiments. YS and ZYM conducted the experiments. YS conducted the analyses and wrote the manuscript. SKW edited the manuscript. All authors declare no conflict of interests.

References

Abou-Saleh, M. T., Ghubash, R., Karim, L., Krymski, M., & Bhai, I. (1998). Hormonal Aspects of Postpartum Depression. *Psychoneuroendocrinology*, *23*, 465–475.

Belzer, C., & de Vos, W. M. (2012). Microbes inside - from diversity to function: the case of *Akkermansia*. *The ISME Journal*, *6*(8), 1449–1458. http://doi.org/10.1038/ismej.2012.6

Blaser, M. J., & Domínguez-Bello, M. G. (2016). The Human Microbiome before Birth. *Cell Host and Microbe*, *20*(5), 558–560. http://doi.org/10.1016/j.chom.2016.10.014

Buho, H., Jiang, Z., Liu, C., Yoshida, T., Mahamut, H., Kaneko, M., et al. (2011). Preliminary study on migration pattern of the Tibetan antelope (*Pantholops hodgsonii*) based on satellite tracking. *Advances in Space Research*, *48*(1), 43–48. http://doi.org/10.1016/j.asr.2011.02.015

Butte, N. F., & King, J. C. (2005). Energy requirements during pregnancy and lactation. *Public Health Nutrition*, *8*(7a), 1010–1027. http://doi.org/10.1079/PHN2005793

Callahan, B. J., McMurdie, P. J., Rosen, M. J., Han, A. W., Johnson, A. J. A., & Holmes, S. P. (2016). DADA2: High-resolution sample inference from Illumina amplicon data. *Nature Methods*, *13*(7), 581–583. http://doi.org/10.1038/nmeth.3869

Capuco, A. V., Connor, E. E., & Wood, D. L. (2008). Regulation of mammary gland sensitivity to thyroid hormones during the transition from pregnancy to lactation. *Experimental Biology and Medicine*, *233*(10), 1309–1314. http://doi.org/10.3181/0803-RM-85

Cardman, Z., Arnosti, C., Durbin, A., Ziervogel, K., Cox, C., Steen, A. D., & Teske, A. (2014). Verrucomicrobia are candidates for polysaccharide-degrading bacterioplankton in an arctic fjord of Svalbard. *Applied and Environmental Microbiology*, *80*(12), 3749–3756. http://doi.org/10.1128/AEM.00899-14

Concannon, P. W., Butler, W. R., Hansel, W., Knight, P. J., & Hamilton, J. M. (1978). Parturition and Lactation in the Bitch: Serum Progesterone, Cortisol and Prolactin. *Biology of Reproduction*, *19*, 1113–1118.

Crusell, M. K. W., Hansen, T. H., Nielsen, T., Allin, K. H., Rühlemann, M. C., Damm, P., et al. (2018). Gestational diabetes is associated with change in the gut microbiota composition in third trimester of pregnancy and postpartum, 1–19. http://doi.org/10.1186/s40168-018-0472-x

David, L. A., Maurice, C. F., Carmody, R. N., Gootenberg, D. B., Button, J. E., Wolfe, B. E., et al. (2013). Diet rapidly and reproducibly alters the human gut microbiome. *Nature*, *505*(7484), 559–563. http://doi.org/10.1038/nature12820

Dearing, M. D., & Kohl, K. D. (2017). Beyond Fermentation: Other Important Services Provided to Endothermic Herbivores by their Gut Microbiota. *Integrative and Comparative Biology*, *57*(4), 723–731. http://doi.org/10.1093/icb/icx020

Di Rienzi, S. C., Sharon, I., Wrighton, K. C., Koren, O., Hug, L. A., Thomas, B. C., et al. (2013). The human gut and groundwater harbor non-photosynthetic bacteria belonging to a new candidate phylum sibling to Cyanobacteria. *eLife*, *2*, 611–25. http://doi.org/10.7554/eLife.01102

Douyon, L., & Schteingart, D. E. (2002). Effect of obesity and starvation on thyroid hormone, growth hormone, and cortisol secretion. *Endocrinology and Metabolism Clinics of North America*, *31*(1), 173–189.

Dunlop, A. L., Mulle, J. G., Ferranti, E. P., Edwards, S., Dunn, A. B., & Corwin, E. J. (2015). Maternal Microbiome and Pregnancy Outcomes That Impact Infant Health. *Advances in Neonatal Care*, *15*(6), 377–385. http://doi.org/10.1097/ANC.0000000000000218

Friedman, E. S., Bittinger, K., Esipova, T. V., Hou, L., Chau, L., Jiang, J., et al. (2018). Microbes vs. chemistry in the origin of the anaerobic gut lumen. *Proceedings of the National Academy of Sciences*, *115*(16), 4170–4175. http://doi.org/10.1073/pnas.1718635115

Gao, K., Pi, Y., Mu, C. L., Farzi, A., Liu, Z., & Zhu, W. Y. (2019). Increasing carbohydrate availability in the hindgut promotes hypothalamic neurotransmitter synthesis: aromatic amino acids linking the microbiota–brain axis. *Journal of Neurochemistry*, *149*(5), 641–659. http://doi.org/10.1111/jnc.14709

Glynn, L. M., Davis, E. P., & Sandman, C. A. (2013). New insights into the role of perinatal HPA-axis dysregulation in postpartum depression. *Neuropeptides*, *47*(6), 363–370. http://doi.org/10.1016/j.npep.2013.10.007

Gomez-Arango, L. F., Barrett, H. L., McIntyre, H. D., Callaway, L. K., Morrison, M., & Dekker Nitert, M. (2016). Connections Between the Gut Microbiome and Metabolic Hormones

in Early Pregnancy in Overweight and Obese Women. *Diabetes*, *65*(8), 2214–2223. http://doi.org/10.2337/db16-0278
Goodrich, J. K., Waters, J. L., Poole, A. C., Sutter, J. L., Koren, O., Blekhman, R., et al. (2014). Human Genetics Shape the Gut Microbiome. *Cell*, *159*(4), 789–799. http://doi.org/10.1016/j.cell.2014.09.053
Hendrick, V., Altshuler, L. L., & Suri, R. (2011). Hormonal Changes in the Postpartum and Implications for Postpartum Depression. *Psychosomatics*, *39*(2), 93–101. http://doi.org/10.1016/S0033-3182(98)71355-6
Hodges, K., & Heistermann, M. (2011). Field and Laboratory Methods in Primatology. A practical guide. (J. M. Setchell & D. J. Curtis, Eds.) (pp. 353–370). Cambridge University Press.
Ingala, M. R., Simmons, N. B., Wultsch, C., Krampis, K., Speer, K. A., & Perkins, S. L. (2018). Comparing Microbiome Sampling Methods in a Wild Mammal: Fecal and Intestinal Samples Record Different Signals of Host Ecology, Evolution. *Frontiers in Microbiology*, *9*, 141–13. http://doi.org/10.3389/fmicb.2018.00803
Jost, T., Lacroix, C., Braegger, C., & Chassard, C. (2013). Stability of the Maternal Gut Microbiota During Late Pregnancy and Early Lactation. *Current Microbiology*, *68*(4), 419–427. http://doi.org/10.1007/s00284-013-0491-6
Jung, C., Ho, J. T., Torpy, D. J., Rogers, A., Doogue, M., Lewis, J. G., et al. (2011). A Longitudinal Study of Plasma and Urinary Cortisol in Pregnancy and Postpartum. *Journal of Clinical Endocrinology & Metabolism*, *96*(5), 1533–1540. http://doi.org/10.1210/jc.2010-2395
Koren, O., Goodrich, J. K., Cullender, T. C., Spor, A., Laitinen, K., Backhead, H. K., et al. (2012). Host Remodeling of the Gut Microbiome and Metabolic Changes during Pregnancy. *Cell*, *150*(3), 470–480. http://doi.org/10.1016/j.cell.2012.07.008
Krajmalnik-Brown, R., Ilhan, Z.-E., Kang, D.-W., & DiBaise, J. K. (2012). Effects of Gut Microbes on Nutrient Absorption and Energy Regulation. *Nutrition in Clinical Practice*, *27*(2), 201–214. http://doi.org/10.1177/0884533611436116
Lagkouvardos, I., Lesker, T. R., Hitch, T. C. A., Gálvez, E. J. C., Smit, N., Neuhaus, K., et al. (2019). Sequence and cultivation study of *Muribaculaceae* reveals novel species, host preference, and functional potential of this yet undescribed family, *7*, 1–15. http://doi.org/10.1186/s40168-019-0637-2
Lain, K. Y., & Catalano, P. M. (2007). Metabolic changes in pregnancy. *Clinical Obstetrics and Gynecology*, *50*(4), 938–948. http://doi.org/10.1097/GRF.0b013e31815a5494
Lau, S. K. P., Teng, J. L. L., Chiu, T. H., Chan, E., Tsang, A. K. L., Panagiotou, G., et al. (2018). Differential Microbial Communities of Omnivorous and Herbivorous Cattle in Southern China. *Computational and Structural Biotechnology Journal*, *16*(C), 54–60. http://doi.org/10.1016/j.csbj.2018.02.004
Leclerc, C., Bellard, C., Luque, G. M., & Courchamp, F. (2015). Overcoming extinction: understanding processes of recovery of the Tibetan antelope. *Ecosphere*, *6*(9), art171–art171. http://doi.org/10.1890/ES15-00049.1.sm
Leslie, D. M., & Schaller, G. B. (2008). *Pantholops Hodgsonii* (Artiodactyla: Bovidae). *Mammalian Species*, *817*(1), 1. http://doi.org/10.1644/817.1
Ley, R. E., Hamady, M., Lozupone, C., Turnbaugh, P. J., Ramey, R. R., Bircher, J. S., et al. (2008). Evolution of Mammals and Their Gut Microbes. *Science*, *320*(5883), 1647–1651. http://doi.org/10.1126/science.1155390

Lian, X., Zhang, T., Cao, Y., Su, J., & Thirgood, S. (2007). Group size effects on foraging and vigilance in migratory Tibetan antelope. *Behavioural Processes*, *76*(3), 192–197. http://doi.org/10.1016/j.beproc.2007.05.001

Lima, F. S., Oikonomou, G., Lima, S. F., Bicalho, M. L. S., Ganda, E. K., de Oliveira Filho, J. C., et al. (2015). Prepartum and Postpartum Rumen Fluid Microbiomes: Characterization and Correlation with Production Traits in Dairy Cows. *Applied and Environmental Microbiology*, *81*(4), 1327–1337. http://doi.org/10.1128/AEM.03138-14

Mastorakos, G., & Ilias, I. (2003). Maternal and Fetal Hypothalamic-Pituitary-Adrenal Axes During Pregnancy and Postpartum. *Annals of the New York Academy of Sciences*, *997*(1), 136–149. http://doi.org/10.1196/annals.1290.016

McMurdie, P. J., & Holmes, S. (2014). Waste Not, Want Not: Why Rarefying Microbiome Data Is Inadmissible. *PLoS Computational Biology*, *10*(4), e1003531. http://doi.org/10.1371/journal.pcbi.1003531.s002

Menke, S., Meier, M., & Sommer, S. (2015). Shifts in the gut microbiome observed in wildlife faecal samples exposed to natural weather conditions: lessons from time-series analyses using next-generation sequencing for application in field studies. *Methods in Ecology and Evolution*, *6*(9), 1080–1087. http://doi.org/10.1007/978-0-387-87458-6

Mo, L., Luo, P., Mou, C., Yang, H., Wang, J., Wang, Z., et al. (2018). Winter plant phenology in the alpine meadow on the eastern Qinghai–Tibetan Plateau. *Annals of Botany*, *122*(6), 1033–1045. http://doi.org/10.1093/aob/mcy112

Mor, G., Cardenas, I., Abrahams, V., & Guller, S. (2011). Inflammation and pregnancy: the role of the immune system at the implantation site. *Annals of the New York Academy of Sciences*, *1221*(1), 80–87. http://doi.org/10.1111/j.1749-6632.2010.05938.x

Mori, H., Maruyama, F., Kato, H., Toyoda, A., Dozono, A., Ohtsubo, Y., et al. (2014). Design and Experimental Application of a Novel Non-Degenerate Universal Primer Set that Amplifies Prokaryotic 16S rRNA Genes with a Low Possibility to Amplify Eukaryotic rRNA Genes. *DNA Research*, *21*(2), 217–227. http://doi.org/10.1093/dnares/dst052

Mukhopadhya, I., Hansen, R., El-Omar, E. M., & Hold, G. L. (2012). IBD—what role do Proteobacteria play? *Nature Reviews Gastroenterology & Hepatology*, *9*(4), 219–230. http://doi.org/10.1038/nrgastro.2012.14

Nagpal, R., Tsuji, H., Takahashi, T., Nomoto, K., Kawashima, K., Nagata, S., & Yamashiro, Y. (2017). Ontogenesis of the Gut Microbiota Composition in Healthy, Full-Term, Vaginally Born and Breast-Fed Infants over the First 3 Years of Life: A Quantitative Bird's-Eye View. *Frontiers in Microbiology*, *8*, 583–9. http://doi.org/10.3389/fmicb.2017.01388

Nelson, S. M., Matthews, P., & Poston, L. (2010). Maternal metabolism and obesity: modifiable determinants of pregnancy outcome. *Human Reproduction Update*, *16*(3), 255–275. http://doi.org/10.1093/humupd/dmp050

O' Donnell, M. M., Harris, H. M. B., Ross, R. P., & O'Toole, P. W. (2017). Core fecal microbiota of domesticated herbivorous ruminant, hindgut fermenters, and monogastric animals. *MicrobiologyOpen*, *6*(5), e00509–11. http://doi.org/10.1002/mbo3.509

Palme, R., Fischer, P., Schildorfer, H., & Ismail, M. N. (1996). Excretion of infused 14C-steroidhormones via faeces and urine in domestic livestock. *Animal Reproduction Science*, *43*, 43–63.

Palme, R., Rettenbacher, S., Touma, C., EL-Bahr, S. M., & Mostl, E. (2006). Stress Hormones in Mammals and Birds: Comparative Aspects Regarding Metabolism, Excretion, and

Noninvasive Measurement in Fecal Samples. *Annals of the New York Academy of Sciences*, *1040*(1), 162–171. http://doi.org/10.1196/annals.1327.021
Picciano, M. F. (2003). Pregnancy and Lactation: Physiological Adjustments, Nutritional Requirements and the Role of Dietary Supplements, *133*(6), 1997S–2002S.
Plummer, E., & Twin, J. (2015). A Comparison of Three Bioinformatics Pipelines for the Analysis of Preterm Gut Microbiota using 16S rRNA Gene Sequencing Data. *Journal of Proteomics & Bioinformatics*, *8*(12). http://doi.org/10.4172/jpb.1000381
Prince, A. L., Chu, D. M., Seferovic, M. D., Antony, K. M., Ma, J., & Aagaard, K. M. (2015). The perinatal microbiome and pregnancy: moving beyond the vaginal microbiome. *Cold Spring Harbor Perspectives in Medicine*, *5*(6), a023051–a023051. http://doi.org/10.1101/cshperspect.a023051
Quast, C., Pruesse, E., Yilmaz, P., Gerken, J., Schweer, T., Yarza, P., et al. (2012). The SILVA ribosomal RNA gene database project: improved data processing and web-based tools. *Nucleic Acids Research*, *41*(D1), D590–D596. http://doi.org/10.1093/nar/gks1219
Redford, K. H., Segre, J. A., Salafsky, N., del Rio, C. M., & McAloose, D. (2012). Conservation and the Microbiome. *Conservation Biology*, *26*(2), 195–197. http://doi.org/10.1111/j.1523-1739.2012.01829.x
Robeck, T. R., Amaral, R. S., da Silva, V. M. F., Martin, A. R., Montano, G. A., & Brown, J. L. (2019). Thyroid hormone concentrations associated with age, sex, reproductive status and apparent reproductive failure in the Amazon river dolphin (*Inia geoffrensis*). *Conservation Physiology*, *7*(1), 354–13. http://doi.org/10.1093/conphys/coz041
Rudolph, M. D., Graham, A. M., Feczko, E., Miranda-Dominguez, O., Rasmussen, J. M., Nardos, R., et al. (2018). Maternal IL-6 during pregnancy can be estimated from newborn brain connectivity and predicts future working memory in offspring. *Nature Neuroscience*, *21*, 765–772. http://doi.org/10.1038/s41593-018-0128-y
Sacks, G. P., Studena, K., Sargent, I. L., & Redman, C. W. G. (1998). Normal pregnancy and preeclampsia both produce inflammatory changes in peripheral blood leukocytes akin to those of sepsis. *American Journal of Obstetrics and Gynecology*, *179*, 80–86.
Schaller, G. B. (1998). Wildlife of the Tibetan Steppe. University of Chicago Press.
Shin, N.-R., Whon, T. W., & Bae, J.-W. (2015). *Proteobacteria*: microbial signature of dysbiosis in gut microbiota. *Trends in Biotechnology*, *33*(9), 496–503. http://doi.org/10.1016/j.tibtech.2015.06.011
Stuebe, A., & Rich-Edwards, J. (2008). The Reset Hypothesis: Lactation and Maternal Metabolism. *American Journal of Perinatology*, *26*(01), 081–088. http://doi.org/10.1055/s-0028-1103034
Touma, C., & Palme, R. (2006). Measuring Fecal Glucocorticoid Metabolites in Mammals and Birds: The Importance of Validation. *Annals of the New York Academy of Sciences*, *1046*(1), 54–74. http://doi.org/10.1196/annals.1343.006
Trevelline, B. K., Fontaine, S. S., Hartup, B. K., & Kohl, K. D. (2019). Conservation biology needs a microbial renaissance: a call for the consideration of host-associated microbiota in wildlife management practices. *Proceedings. Biological Sciences / the Royal Society*, *286*(1895), 20182448–9. http://doi.org/10.1098/rspb.2018.2448
Wasser, S. K., Azkarate, J. C., Booth, R. K., Hayward, L., Hunt, K., Ayres, K., et al. (2010). Non-invasive measurement of thyroid hormone in feces of a diverse array of avian and mammalian species. *General and Comparative Endocrinology*, *168*(1), 1–7. http://doi.org/10.1016/j.ygcen.2010.04.004

Wasser, S. K., Davenport, B., Ramage, E. R., Hunt, K. E., Parker, M., Clarke, C., & Stenhouse, G. (2004). Scat detection dogs in wildlife research and management: application to grizzly and black bears in the Yellowhead Ecosystem, Alberta, Canada. *Canadian Journal of Zoology*, *82*(3), 475–492. http://doi.org/10.1139/z04-020

Wasser, S. K., Hunt, K. E., Brown, J. L., Cooper, K., Crockett, C. M., Bechert, U., et al. (2000). A Generalized Fecal Glucocorticoid Assay for Use in a Diverse Array of Nondomestic Mammalian and Avian Species. *General and Comparative Endocrinology*, *120*(3), 260–275. http://doi.org/10.1006/gcen.2000.7557

West, A. G., Waite, D. W., Deines, P., Bourne, D. G., Digby, A., McKenzie, V. J., & Taylor, M. W. (2019). The microbiome in threatened species conservation. *Biological Conservation*, *229*, 85–98. http://doi.org/10.1016/j.biocon.2018.11.016

Xia, L., Yang, Q., Li, Z., Wu, Y., & Feng, Z. (2007). The effect of the Qinghai-Tibet railway on the migration of Tibetan antelope *Pantholops hodgsonii* in Hoh-xil National Nature Reserve, China. *Oryx*, *41*(03). http://doi.org/10.1017/S0030605307000116

Yasuda, K., Oh, K., Ren, B., Tickle, T. L., Franzosa, E. A., Wachtman, L. M., et al. (2015). Biogeography of the Intestinal Mucosal and Lumenal Microbiome in the Rhesus Macaque. *Cell Host and Microbe*, *17*(3), 385–391. http://doi.org/10.1016/j.chom.2015.01.015

Zeng, Z., Liu, F., & Li, S. (2017). Metabolic Adaptations in Pregnancy: A Review. *Annals of Nutrition and Metabolism*, *70*(1), 59–65. http://doi.org/10.1159/000459633

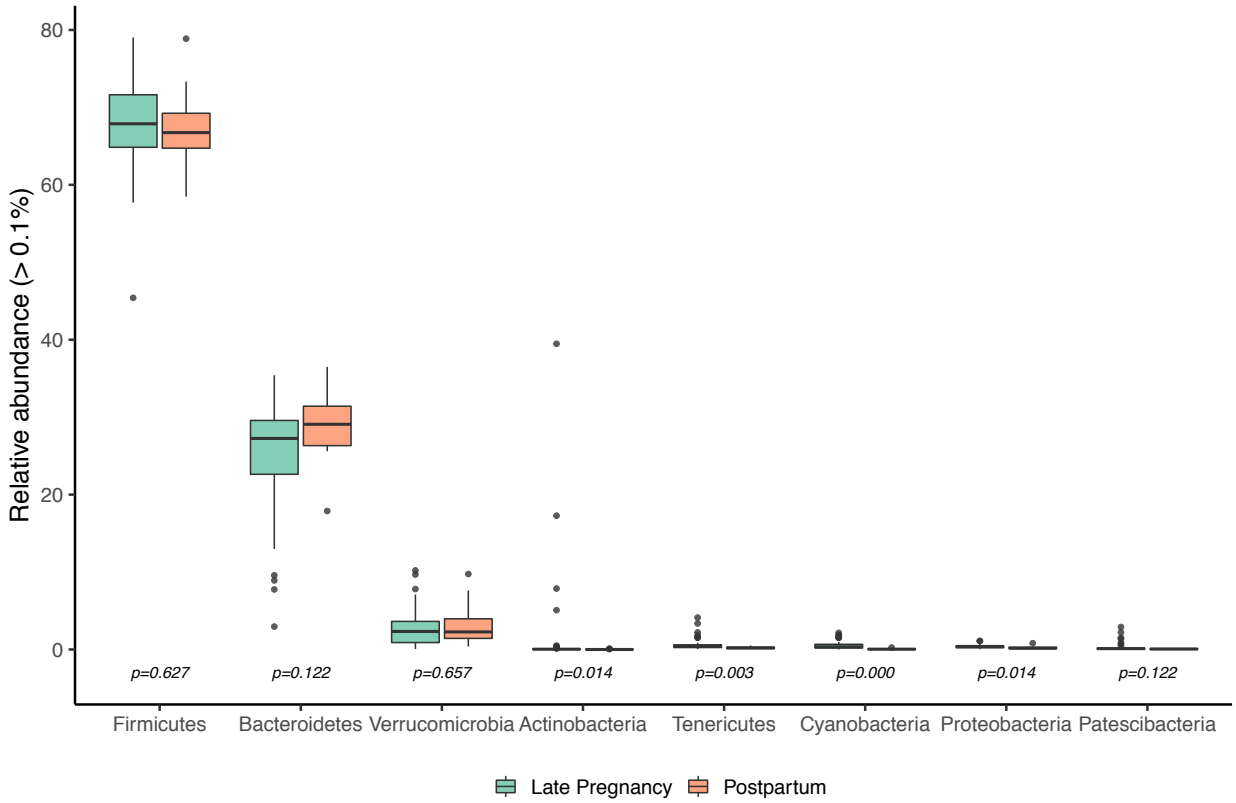

Figure 1 Phyla found in the maternal gut microbiome of Tibetan antelope with relative abundance greater than 0.1%. Changes in the relative abundance of phyla between reproductive states were analyzed through Wilcoxon signed-rank tests and p values were adjusted with the Benjamini-Hochberg method to control for false discovery rate.

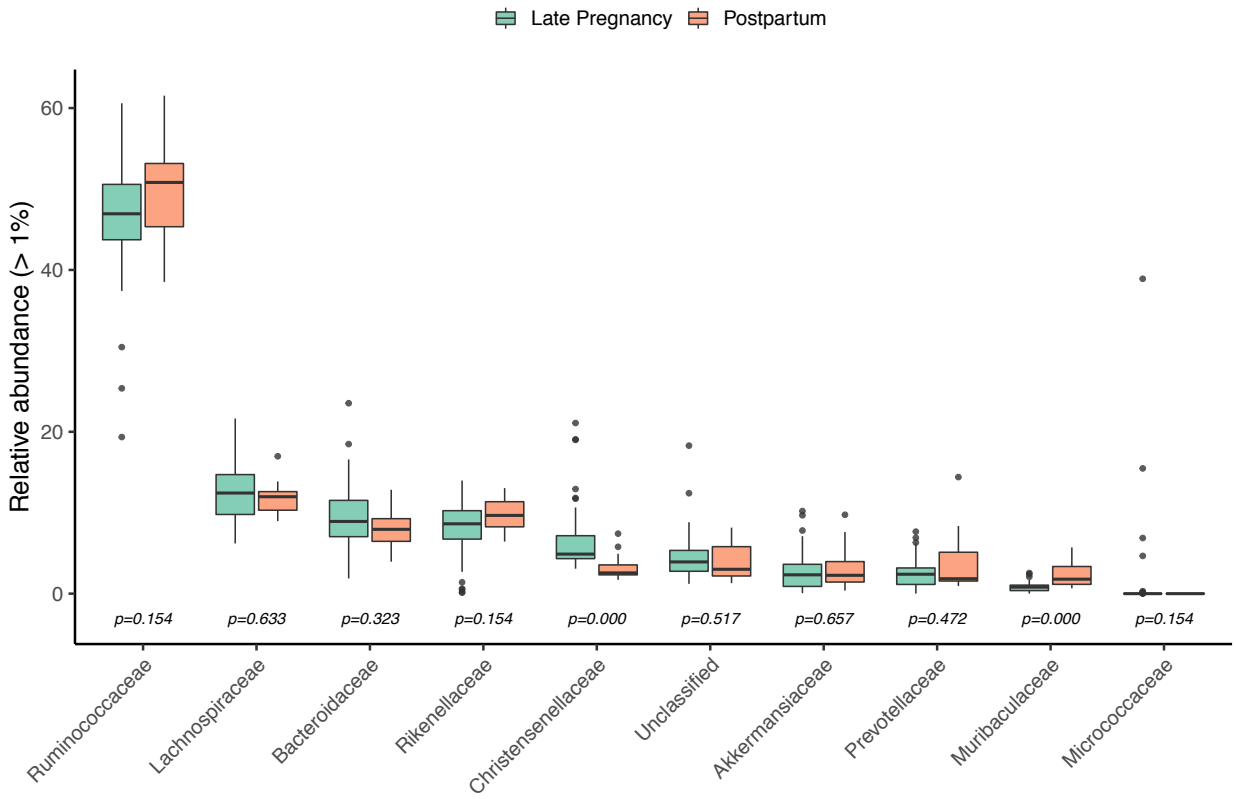

Figure 2 Families found in the maternal gut microbiome of Tibetan antelope with relative abundance greater than 1%. Changes in the relative abundance of families between reproductive states were analyzed through Wilcoxon signed-rank tests and p values were adjusted with the Benjamini-Hochberg method to control for false discovery rate.

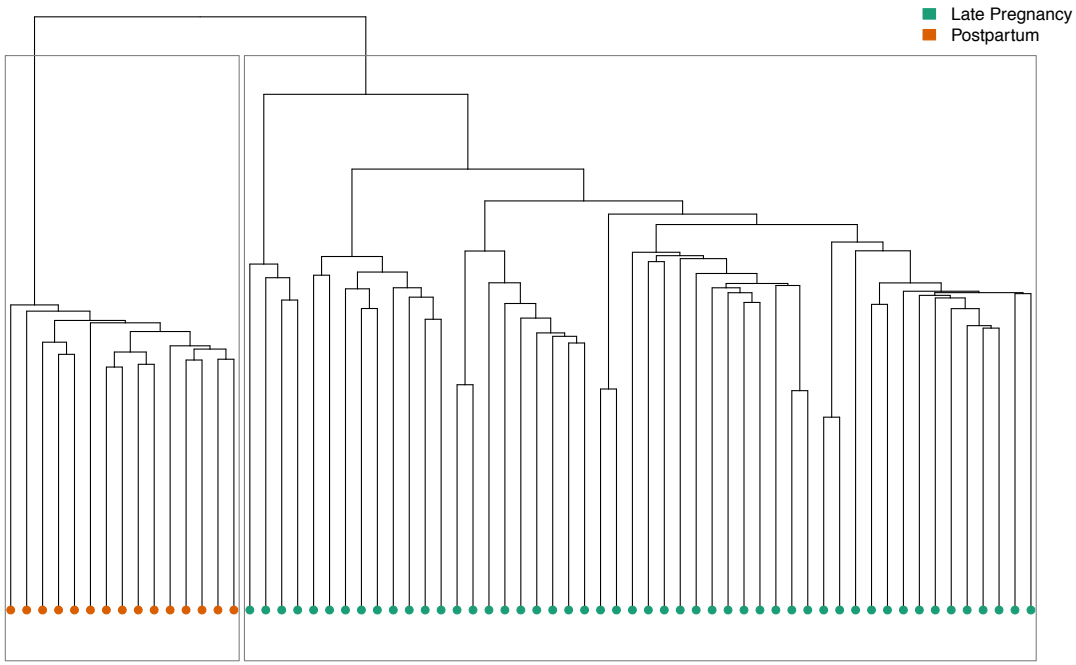

Figure 3 Hierarchical clustering analysis of maternal gut microbiota in female Tibetan antelope with Euclidean distance matrix after variance stabilizing transformation. Each leaf of the dendrogram represents one fecal sample (N=65).

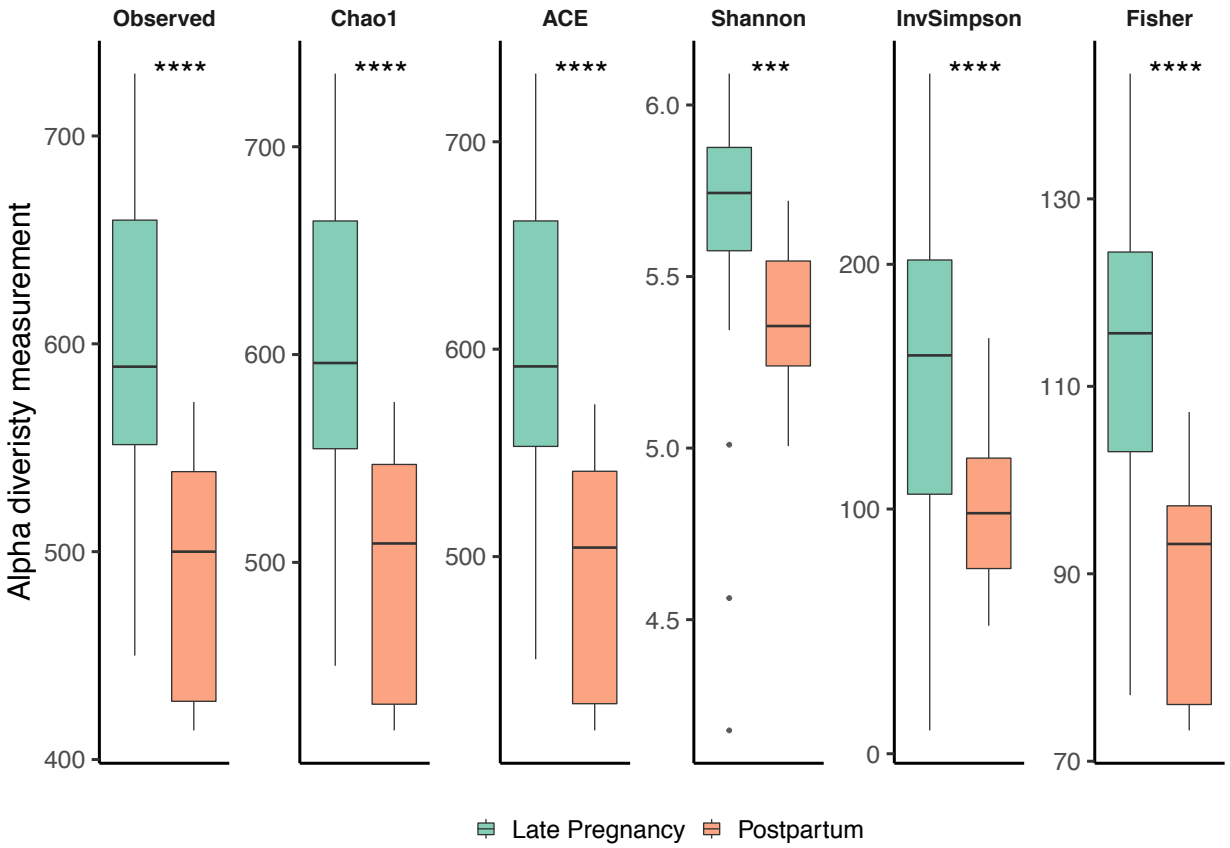

Figure 4 Changes in alpha diversity metrics of maternal gut microbiome of female Tibetan antelope in different reproductive states. Statistical significance was assessed by t-tests. Note: ***: $p < 0.001$; ****: $p < 0.0001$.

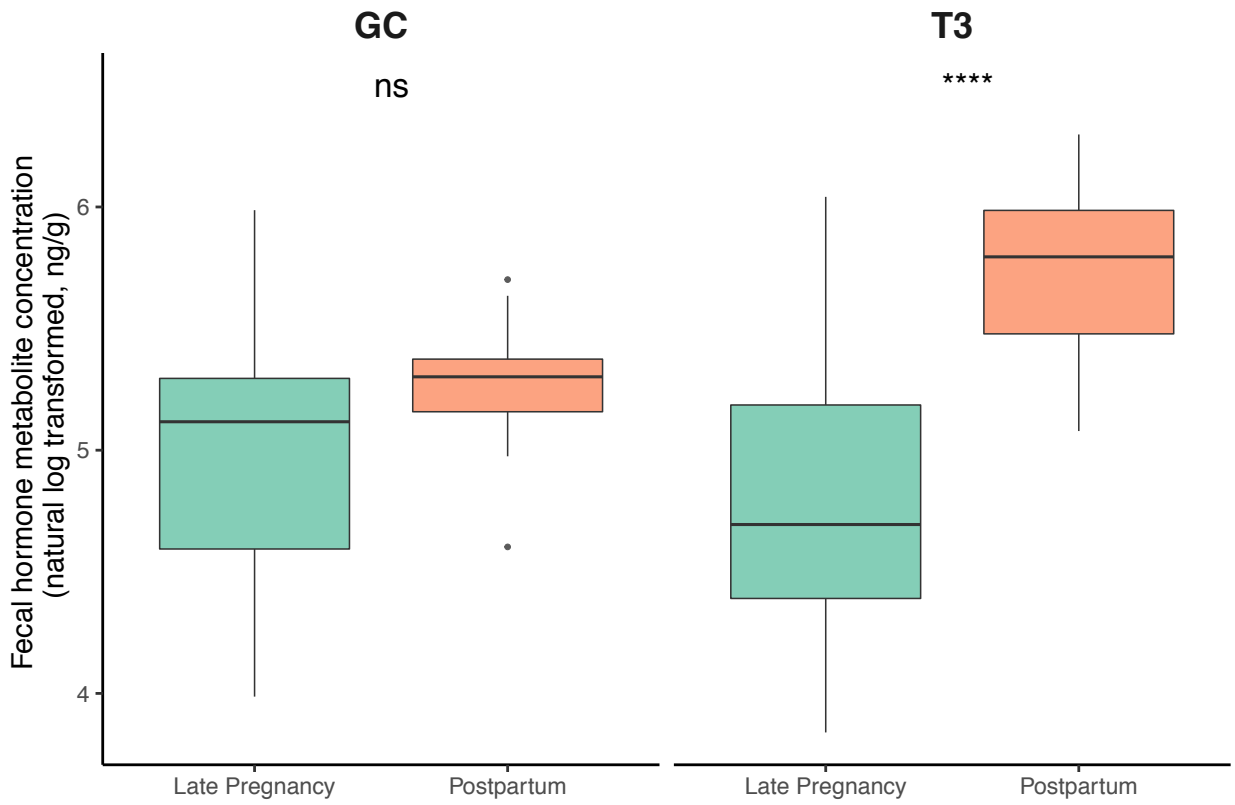

Figure 5 Changes in fecal GC and T3 metabolite concentrations (natural log-transformed) between reproductive states. Statistical significance was assessed by Wilcoxon signed-rank tests. Note: ns: not significant. ****: $p < 0.0001$.

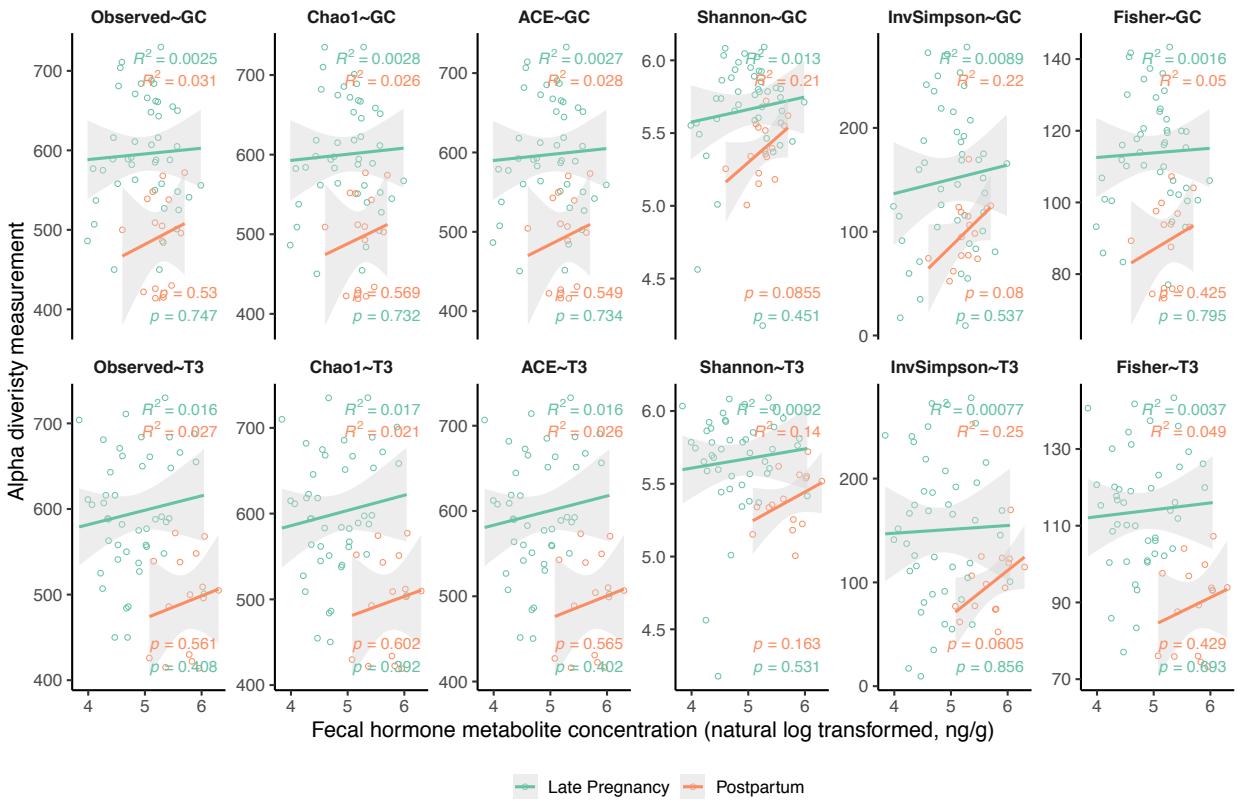

Figure 6 Relationships between fecal hormone metabolite concentrations (GC and T3) and microbiome alpha diversity measurements at different reproductive states.

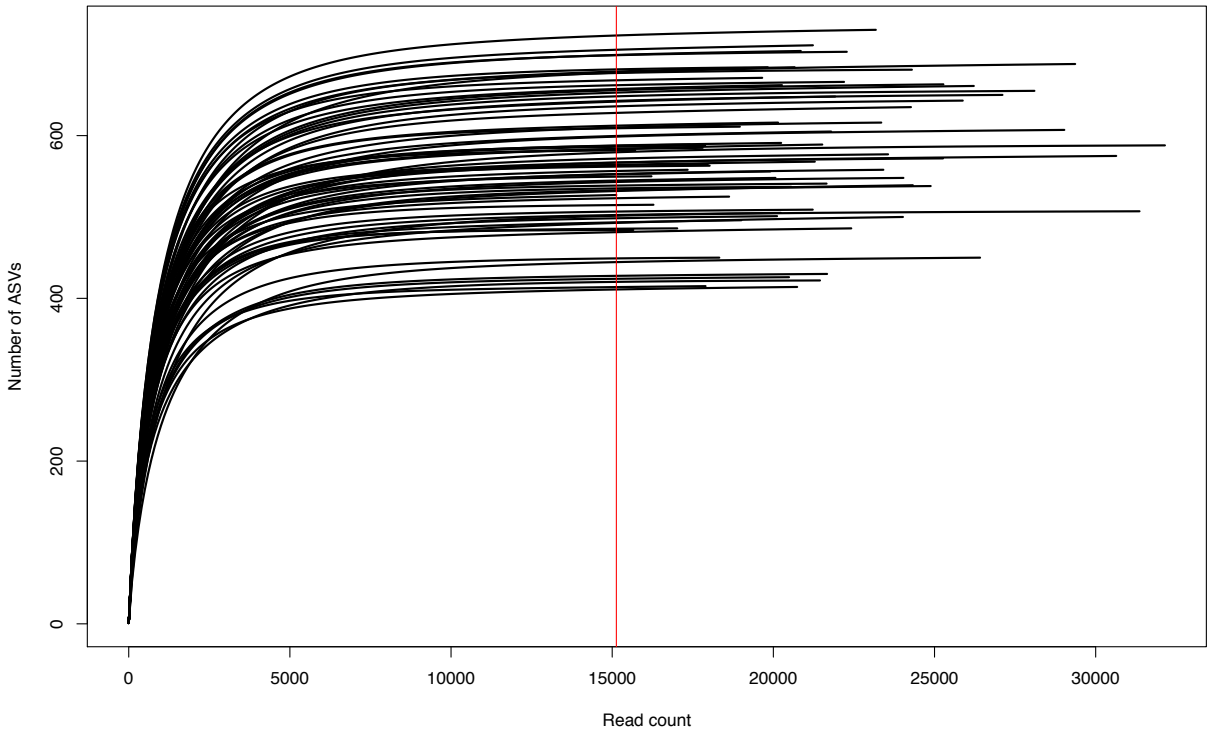

Supplementary Figure 1 Rarefaction curves calculated for the number of amplicon sequence variants (ASVs) with increasing sequencing depth. Note: each curve represents a sample and N=65. The red vertical line indicates the minimum number of reads found in the dataset after filtering, which is 15,129 reads.

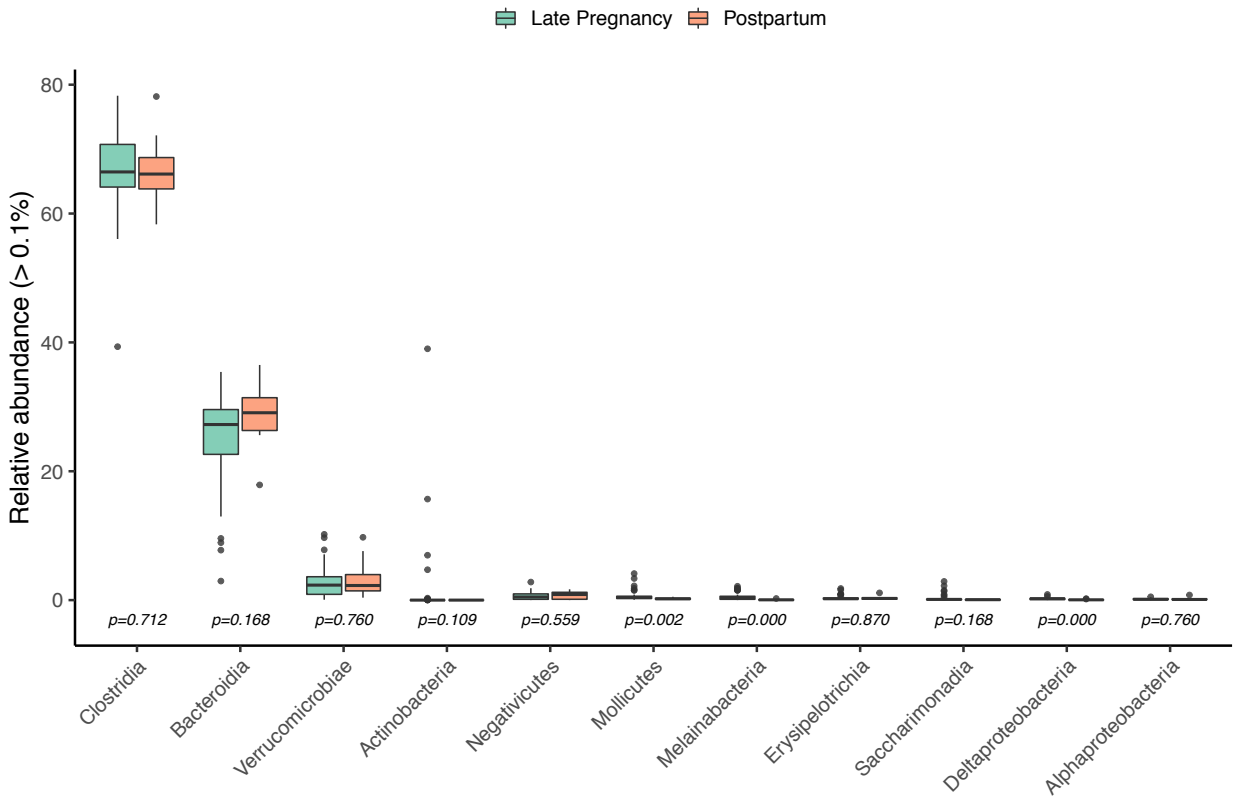

Supplementary Figure 2 Classes found in the maternal gut microbiome of Tibetan antelope with relative abundance greater than 0.1%. Changes in the relative abundance of classes between reproductive states were analyzed through Wilcoxon signed-rank tests and *p* values were adjusted with the Benjamini-Hochberg method to control for false discovery rate.

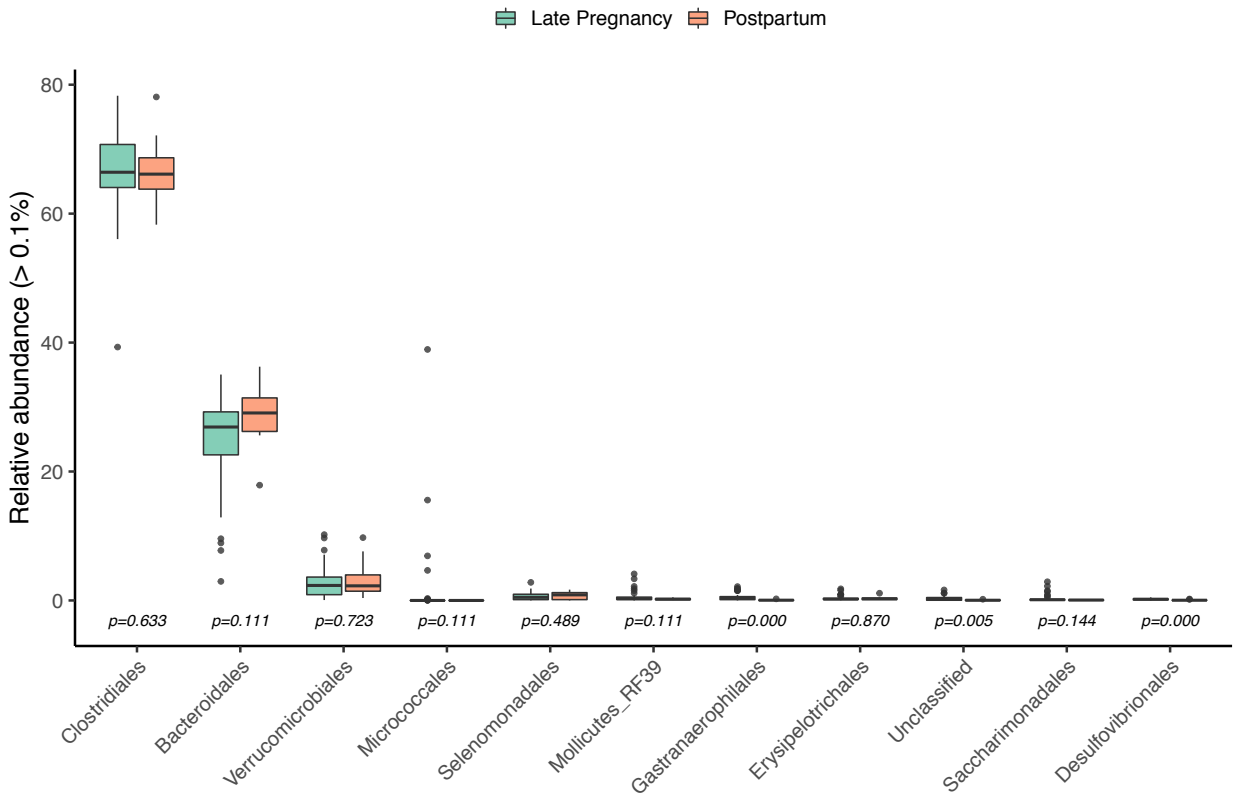

Supplementary Figure 3 Orders found in the maternal gut microbiome of Tibetan antelope with relative abundance greater than 0.1%. Changes in the relative abundance of orders between reproductive states were analyzed through Wilcoxon signed-rank tests and *p* values were adjusted with the Benjamini-Hochberg method to control for false discovery rate.

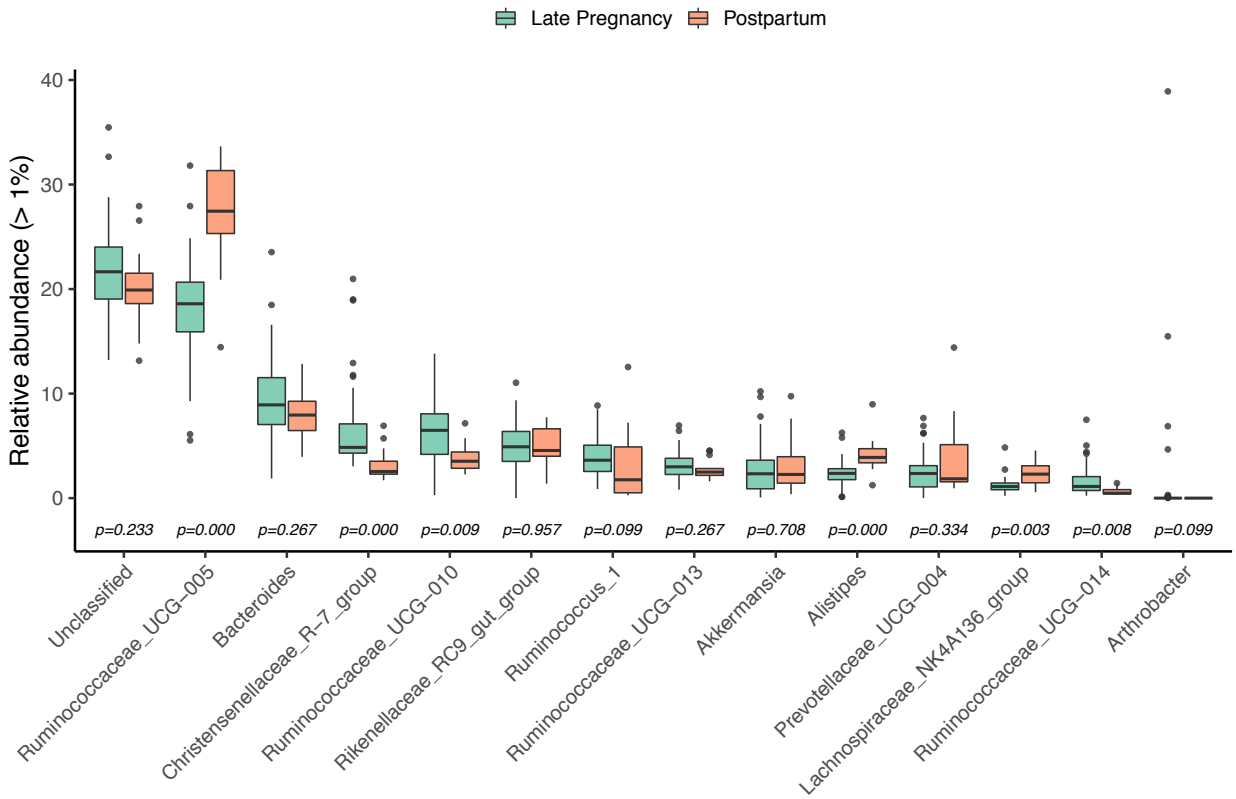

Supplementary Figure 4 Genera found in the maternal gut microbiome of Tibetan antelope with relative abundance greater than 1%. Changes in the relative abundance of genera between reproductive states were analyzed through Wilcoxon signed-rank tests and *p* values were adjusted with the Benjamini-Hochberg method to control for false discovery rate.

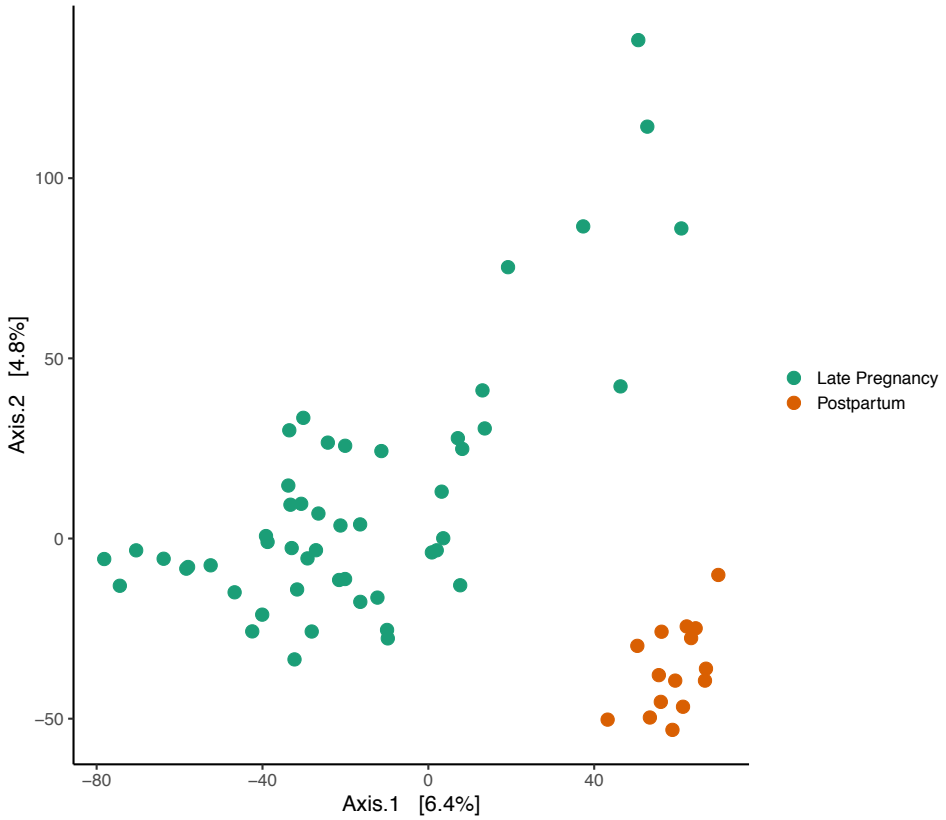

Supplementary Figure 5 Principal coordinates analysis (PCoA) for gut microbial communities as a function of reproductive state (N=65). The analysis was based on Euclidean distance after variance stabilizing transformation.

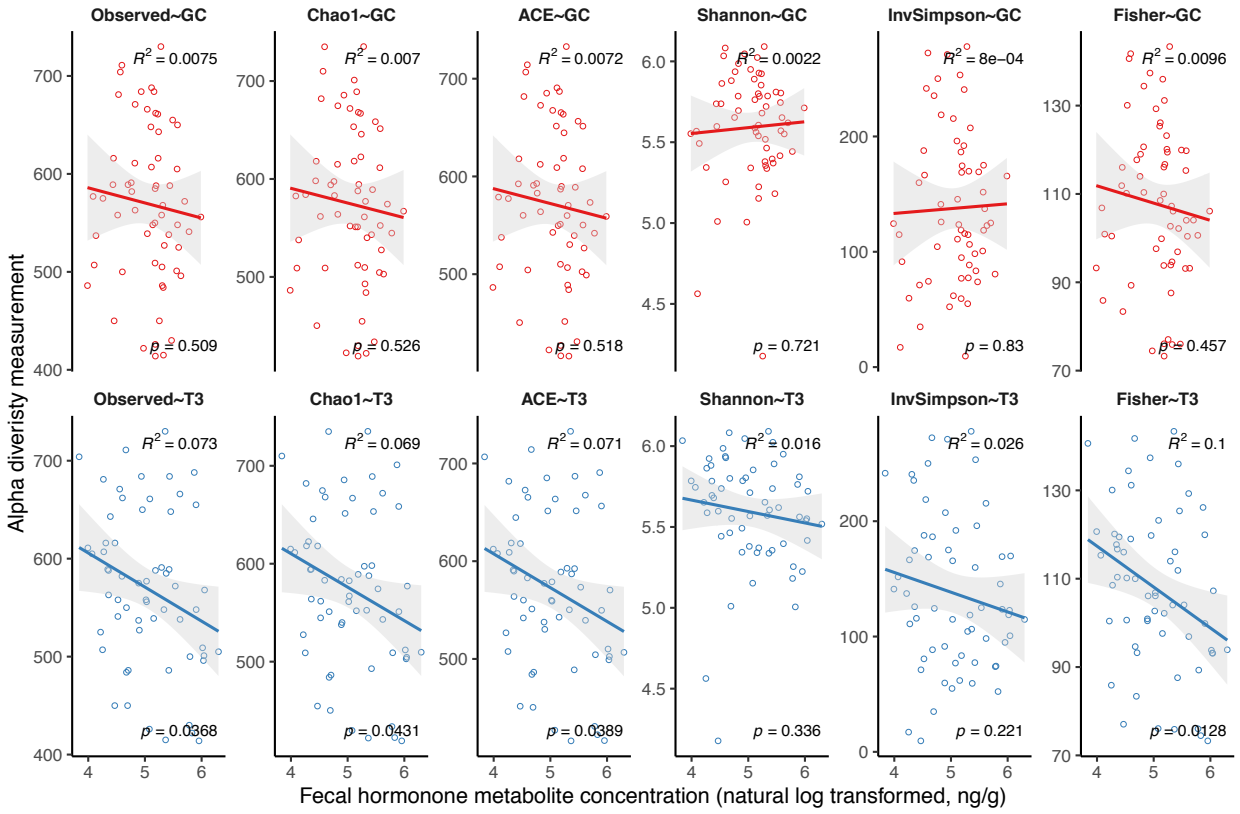

Supplementary Figure 6 Relationships between fecal hormone metabolite concentrations (GC and T3) and microbiome alpha diversity measurements regardless of reproductive states.

Chapter Three

Prey partitioning between sympatric canid species revealed by DNA metabarcoding

Yue Shi[1*], Yves Hoareau[1], Ellie Reese[2], Samuel K. Wasser[1]

[1]Department of Biology, University of Washington, Seattle, WA 98195, USA

[2] School of Environmental and Forest Sciences, University of Washington, Seattle, WA 98105, USA

*Correspondence: Yue Shi (yueshi@uw.edu)

Abstract

The recovery of apex predators relies on restoring the full suite of trophic interactions within the ecosystem. Diet analysis with DNA metabarcoding technology can help deliver insights into these trophic interactions with fine-grained resolution. The recovery of wolves in Washington state offers an excellent case to study the trophic cascade impacts of the apex predators on the ecosystem and explore prey partitioning between sympatric canid species. We used DNA metabarcoding technology on scats to characterize the diet composition and its spatiotemporal variations of wolves and coyotes and quantified the diet niche overlap between these two canid species in northeastern Washington. In total, 19 different prey taxa were detected. Frequency of occurrence data showed that wolves primarily preyed upon deer (*Odocoileus sp.*) (47.47%) and moose (*Alces alces*) (42.42%). Coyotes also consumed moose (30.10%) and deer (21.36%), but snowshoe hares (*Lepus americanus*) were the most common prey (61.17%) in their diet. There were significant spatial variations in the wolf diet composition ($p = 0.001$) with wolves in the Dirty Shirt pack range consuming more moose (71.43%). Coyotes showed significant spatial and temporal dietary variations (season: $p = 0.037$; pack: $p = 0.003$; pack:season $p = 0.043$). Our data suggested that coyotes use ungulate carrion subsidies from wolves as food resources. DNA metabarcoding with fecal DNA provides an excellent noninvasive tool to characterize diet profile at the fine-grained level and can be applied to other carnivore species to help understand the impacts of recovery of apex predators on the local ecosystems.

Keywords metabarcoding, diet, wolf, coyote, fecal DNA

Introduction

Apex predators are primarily known for their elevated position on the trophic ladder with impacts that cascade throughout their ecosystem (Wallach, Izhaki, Toms, Ripple, & Shanas, 2015). The widespread decline in apex predators due to human hunting and habitat fragmentation has been observed in many systems (Estes et al., 2011). The reestablishment of large predators and their ecological effects is fundamental for wildlife management, and relies on restoring the full suite of ecological interactions within the ecosystem, including predator-prey and predator- predator interactions (Stier et al., 2016). From a social perspective, apex predator recovery can introduce significant new conservation and legal challenges. Scientific uncertainty about the ecological interactions can hinder the progress towards resolving such challenges (Marshall, Stier, Samhouri, Kelly, & Ward, 2015). Therefore, it is essential to track changes in the predator diet to inform conservation management decisions (Marshall et al., 2015). Diet analysis with the newly developed DNA metabarcoding technology can help deliver valuable insights into these trophic interactions and the mechanism of species coexistence with the fine-grained resolution.

Conventional methods of diet analysis have relied on macro- or microscopic morphological identification of food remains in scats, such as hair (Carrera et al., 2008; Gable, Windels, Bruggink, & Barber-Meyer, 2018; Wasser, Keim, Taper, & Lele, 2011) and hard-parts (e.g. bones, hooves and teeth) (Drouilly, Nattrass, & O'Riain, 2017; Nelson, Cherry, Howze, Warren, & Mike, 2015). Such methods are very labor intensive and require reliable reference collection of prey parts as well as research expertise in identifying species from masticated, semi-digested food remains (Pompanon et al., 2011). These methods also tend

to underestimate the proportion of prey species whose remains are not found (completely digested or not consumed at all) (Deagle, Kirkwood, & Jarman, 2009). Earlier molecular attempts use a conventional genotyping methodology, involving multiplex PCR followed by fragment size determination with capillary electrophoresis and known sized allelic ladders (Morello, Braglia, Gavazzi, Gianì, & Breviario, 2019). Though very affordable, this method does not account for any sequence-based differences between fragments of the same size. DNA metabarcoding offers a promising alternative, whereby customized universal primer pairs amplify a standardized DNA region, which are sequenced and compared to a reference database for taxonomic identification (Modave, MacDonald, & Sarre, 2017; Taberlet, Coissac, Pompanon, Brochmann, & Willerslev, 2012). Coupled with next-generation sequencing (NGS), DNA metabarcoding technology can sequence many samples in a high-throughput and cost-effective fashion and reveal the entire taxonomic composition of thousands of samples simultaneously (Pompanon et al., 2011). This new molecular approach has been successfully applied for the diet analyses of various species, including carnivores (Berry et al., 2017; Smith, Thomas, Levi, Wang, & Wilmers, 2018), omnivores (De Barba et al., 2013; Robeson et al., 2017), herbivores (Kartzinel et al., 2015), small mammals (Buglione et al., 2018), lizards (Moreno-Rueda, Melero, Reguera, Zamora-Camacho, & Álvarez-Benito, 2017), birds (Sullins et al., 2018) and invertebrates (Hawlitschek, Fernández-González, Balmori-de la Puente, & Castresana, 2018; Kamenova, Bretagnolle, Plantegenest, & Canard, 2018).

Gray wolves (*Canis lupus*) were extirpated from Washington state by the 1930s as ranching and farming activities expanded (Wiles, Allen, & Hayes, 2011). Coyotes (*Canis latrans*) increased in range and abundance over the same period (Gallagher et al., 2019; Hody &

Kays, 2018). Since 2008, wolves have begun reestablishing territories in Washington through natural dispersal from adjacent states and provinces such as Idaho, Montana, Oregon, and British Columbia (Wiles et al., 2011) after being absent from the state for over 80 years. The recovery of wolves in Washington state offers an excellent case to study the trophic cascade impacts of the apex predators on the ecosystem and explore prey partitioning between sympatric canid species.

As apex predators, wolves are keenly adapted to prey on large ungulates (Gable et al., 2018; Wasser et al., 2011). Wolves are also opportunists and use small prey as seasonal food sources when abundant (Latham, Latham, Mccutchen, & Boutin, 2011). Coyotes are mesopredators and generally viewed as opportunistic generalists (Kilgo, Vukovich, Ray, Shaw, & Ruth, 2014). The majority of the coyote diet consists of small mammals, but coyotes can also prey on ungulate calves (Chitwood et al., 2015; Kilgo, Ray, Vukovich, Goode, & Ruth, 2012; Nelson et al., 2015), and vulnerable ungulate adults (Benson, Loveless, Rutledge, & Patterson, 2017; Patterson & Messier, 2000). Birds represent a nonnegligible proportion of the coyote diet (Smith et al., 2018). In addition, carrion subsidies from wolves is also a highly valued food resource for coyotes (Sivy, Pozzanghera, Colson, Mumma, & Prugh, 2017). Using traditional methods, these previous studies generally present prey species as three groups: ungulates, small mammals, and birds. All these groups encompass enormous taxonomic diversity, yet very few studies have evaluated resource partitioning of these sympatric canid species at a fine-grained taxonomic level.

In order to recover apex predators, it is critical to consider the ecological roles that these top predators play in the ecosystem, rather than focusing only on their demography (Ripple, Wirsing, Beschta, & Buskirk, 2011). Here, we use DNA metabarcoding on scats to construct high-resolution diet profiles of sympatric wolves and coyotes in northeastern Washington state, USA, with a focus on the vertebrate component of their diets. The purpose of the study is to: 1) evaluate the effectiveness of DNA metabarcoding approach for the canid diet analysis; 2) assess the necessity of applying predator-specific blocking primers to construct a full profile of prey composition. Predator DNA could swamp prey DNA during amplification because predator DNA is much more abundant. The predator-specific blocking primer was designed in a way that its 3' end was modified by replacing the 3' hydroxyl group with a spacer-C3-CPG to prevent polymerase extension (Vestheim & Jarman, 2008); 3) examine spatiotemporal variation in the diet profiles of wolves and coyotes as both pack-specific prey abundance and hunting-ability could affect prey consumption rates. We believe it is crucial to develop a holistic picture of what dietary options these sympatric canid predators exploit in different ecological contexts.

Materials and Methods

Ethics Statement

Currently, wolves in the western two-thirds of Washington are listed as endangered under federal law. Wolves in the eastern third of the state have been removed from the federal listing. However, all wolves in Washington are listed as endangered under state law (Wiles et al., 2011). Three recovery regions have been delineated in Washington: (1) Eastern Washington, (2)

Northern Cascades, and (3) Southern Cascades and Northwest Coast. Our study area is in the Eastern Washington recovery region. Coyotes are not protected under the Endangered Species Act anywhere in the contiguous United States. Fecal samples were collected using the detection dogs from the Conservation Canine Program at the University of Washington under IACUC protocol #2850-08.

Sample Collection

Fecal samples were collected in the spring season (April and May in 2015 and 2017) and fall season (October and November in 2015 and 2016) in three wolf pack ranges: Smackout, Dirty Shirt and Goodman Meadows in Pend Oreille and Stevens counties, Washington (Figure 1). Upon collection, fecal samples were stored at -20°C until DNA extraction. Samples used in this study were subsampled from a larger ongoing project (wolf: 647 fecal samples; coyote: 1893 fecal samples) (Supplementary Figure 1). Subsampling was based on relative kernel density, which was calculated using *stat_density2d* function in *ggplot2* in R (Figure 1). We selected samples from the areas with highest and lowest estimated wolf and coyote densities in each of the three wolf pack ranges.

DNA Extraction and Species Identification

Fecal DNA was extracted using the swabbing method described previously (Wasser et al., 2011) with Qiagen DNeasy 96 Blood and Tissue Kit (Qiagen Inc.,). Multiple interior surfaces of each fecal sample were swabbed and extracted in duplicate. Extraction duplicates were pooled before PCR. One extraction blank was processed along with every 45 fecal samples. Predator species identification was conducted by targeting the partial mitochondrial control region, which was

amplified in duplicate using 5'6-FAM-labeled LTPROBB13 (5'-CCACTATTAACACCCAAAGC-3') and unlabeled HSF21 (5' -GTACATGCTTATATGCATGGG-3') primers, following the instruction of Qiagen Multiplex PCR kit with annealing temperature at 60°C. Fragment analysis on a 3730 Genetic Analyzer (Applied Biosystems) was used to identify a fragment size of 170 bp unique to wolves and domestic dogs, and a fragment size of 165bp unique to coyotes. Samples identified as wolf/dog were further delineated by sequencing a 208bp cytochrome b fragment (Reese et al. 2019, in prep).

Library Preparation and Sequencing

We conducted in-silico analyses using ecoPrimer (Riaz et al., 2011) and ecoPCR (Ficetola et al., 2010) before conducting the experiments to ensure that all target species could be successfully amplified with 12S V05F/R primers (Riaz et al., 2011). We followed the two-step library preparation protocol modified from Illumina's 16S Metagenomic Sequencing Library Preparation (CT #: 15044223 Rev. B). Our protocol used customized library indices, which incorporated two distinct 10-bp index sequences on each end of the fragment. We first amplified the 12S rRNA gene V5 region using the 12SV05F/R primer pair with the addition of the overhang sequence to allow the subsequent annealing of index primers. Amplicon libraries were then amplified with index primers, which incorporated indices and Illumina sequencing adapters. We also tested the efficiency of a 10-fold excess of wolf-specific blocking oligonucleotide (via personal communication with Dr. Shehzad Wasim, University of Veterinary & Animal Sciences, Lahore, Pakistan). Since wolves and coyotes share the same sequence in the target 12S V5 region, we used the same blocking primer for both wolf and coyote samples. In total, we

conducted three PCR replicates without predator-specific blocking primer, and three PCR replicates with predator-specific blocking primer. All PCR reactions were performed using the Qiagen Multiplex PCR kit along with PCR negative controls (5 PCR negative controls per 96-well plate). Amplification products were purified with 1.8X SPRI bead solution after each PCR step (Rohland & Reich, 2012). See Supplementary File 1 for a detailed description of the library preparation protocol and primer sequences.

Libraries were quantified using the Qubit dsDNA HS (High Sensitivity) Assay Kit (Invitrogen) and checked for integrity using Agilent 2200 TapeStation High Sensitivity DNA 1000 Kit (Santa Clara, CA). Successful libraries were pooled with an equimolar concentration of 2.5 nM, and the final library pool was further diluted to 2 nM. For specific methods about library QC and pooling, see Supplementary File 2. Sequencing was performed on the MiSeq platform using MiSeq Reagent kit v3 and 150 bp pair-end read length configuration. Library pool was loaded at a loading concentration of 8 pM with 25% PhiX control V3 spike-in to improve the quality of low-diversity libraries.

Sequence Analysis and Taxonomic Assignment

MiSeq automatically separated all reads by samples during the post-run process via recognized indices. Filtering of the sequences and taxonomic inference of molecular operational taxonomic units (MOTUs) was performed using the OBITools package (Boyer et al., 2015). The following steps were performed: 1) merge paired reads with *illuminapairedend* command and filter out reads with alignment score less than 200; 2) add "sample" attribute to all reads with *obiannotate* command; 3) concatenate all reads and dereplicate globally using *obiuniq* command while keeping sample attribute; 4) remove reads that are shorter than 80 bp and less than 400 copies

with *obigrep* command; 5) remove PCR and sequencing errors with *obiclean* command; 6) assign taxonomy for each MOTU to the species or genus level using the *blastn* with e-value < 1×10^{-20} and a minimum identity of 0.98. Taxonomic assignment was restricted to the local species in Washington state, compiled from three sources of information: 1) Mammal collection at the Burke Museum, University of Washington (https://www.burkemuseum.org/research-and-collections/mammalogy/collections/mamwash/); 2) BirdWeb (http://www.birdweb.org/birdweb/); 3) Washington NatureMapping Program (http://naturemappingfoundation.org/natmap/maps/wa/).

Further filtering on the MOTU table was conducted in R using the following steps: 1) remove any MOTU whose relative frequency across the entire dataset was found to be maximum in either extraction or PCR negative controls; 2) subtract the maximum abundance in extraction or PCR negative controls of the remaining MOTUs from their abundance in each sample replicate; 3) suppress the read count of any MOTU in a sample replicate to zero when its relative abundance (abundance in a sample replicate / total abundance across the entire dataset) is below 0.03%. The sequence read count data were converted into a MOTU table with presence/absence data. The reliability of extracting quantitative information with relative read abundance (RRA) is questionable because of variations in tissue cell density, gene copy, survival rates of tissue/DNA during digestion, variance in fragment size among different food items, and, more importantly, PCR bias due to primer-template mismatches (Piñol, Mir, Gomez-Polo, & Agustí, 2014; Pompanon et al., 2011). Therefore, we only used presence/absence data for the following analyses. However, we also generated a diet profile for each predator with RRA data for the purpose of comparison. A specific prey item in a given sample was only considered as present if it was detected in at least 2 replicates.

Statistical Analyses

Frequency of occurrence (FOO) of a prey species was defined as the proportion of scats found to contain that prey item. To test if there was any significant interspecific and spatiotemporal variation in diet composition, we conducted permutational multivariate analysis of variance (perMANOVA) using the *adonis2* function in vegan package with the *jaccard* distance matrix and 999 permutations. Pairwise comparisons were conducted using the similarity percentage (SIMPER) test implemented in *vegan* R package with 999 permutations. Significance levels were adjusted with sequential Bonferroni correction for multiple comparisons. The SIMPER function also reports the contribution of each prey item to the overall diet dissimilarity and displays the most important prey item for each pair of comparison. These important species contribute at least to 70% of the differences between each pair of comparison. The rest of species are considered to have minor contributions. We used Pianka's adaptation of the niche overlap (*O* metric) (Pianka, 1973) to determine dietary overlap between wolves and coyotes in different seasons or wolf pack ranges. The *O* metric ranges from 0 (no overlap) to 1 (complete overlap).

Results

Prey Species Detected in the Study Area

We selected 99 genetically confirmed wolf scats and 103 genetically confirmed coyote scats. In total, 19 different prey species were identified, including 5 ungulate species (deer *Odocoileus sp.*, moose *Alces alces*, elk *Cervus canadensis*, domestic cow *Bos taurus*, and pig *Sus scrofa*), 10 small mammals (snowshoe hare *Lepus americanus*, deer mouse *Peromyscus*

maniculatus, meadow vole *Microtus pennsylvanicus*, red squirrel *Tamiasciurus hudsonicus*, ground squirrel *Spermophilus sp.*, red-backed vole *Myodes sp.*, flying squirrel *Glaucomys sp.*, rabbit *Oryctolagus cuniculus*, muskrat *Ondatra zibethicus*, and chipmunk *Tamias sp*.) and 4 bird species (ruffed grouse *Bonasa umbellus*, wild turkey *Meleagris gallopavo*, common starling *Sturnus vulgaris*, and spruce grouse *Dendragapus canadensis*).

Effects of Predator-Specific Blocking Primer

The use of a predator-specific blocking primer increased the proportion of prey sequences from 26.40% to 65.97% (Figure 2). However, all prey species were detected regardless of whether the predator-specific blocking primer was added. The blocking primer increased the detection of 9 prey species, while reducing the detection of chipmunk, domestic cow, muskrat, pig and snowshoe hare (Supplementary Table 1). The detection of common starling, ground squirrel, rabbit, spruce grouse and wild turkey remained the same (Supplementary Table 1). Chipmunk was not detected with addition of the blocking primer. For the subsequent analyses, we combined the data from all 6 PCR replicates of each sample. A specific prey item in a given sample was only considered present if it occurred in at least 2 out of 6 replicates.

Interspecific Differences in Diet Profiles

The diet compositions of wolves and coyotes were significantly different ($p = 0.001$) (Figure 3). Deer and moose were the two most frequent prey species (47.47% and 42.42% respectively) in the wolf diet, followed by elk (17.17%) and domestic cow (16.16%). Domestic cow was detected in 16 out of 99 wolf scats (Supplementary Table 3). By contrast, snowshoe hares were the most common prey species (61.17%) in the coyote diet,

followed by moose (30.10%) and deer (21.36%) (Figure 3). Domestic cow was only detected in 2 out of 103 coyote scats (Supplementary Table 3). Small mammals and birds were rarely detected in the wolf diet, whereas they occurred relatively more common in the coyote diet (Figure 4). In total, we found 11 prey species in the wolf diet and 18 prey species in the coyote diet. On average, there were 1.48 prey species per wolf scat, and 1.79 prey species per coyote scat. The SIMPER test showed that snowshoe hares (p = 0.001) and deer (p = 0.002) were the most influential prey species, significantly contributing to the interspecific dietary differences. Domestic cow, deer mouse, ground squirrel, meadow vole and red-backed vole also significantly contributed ($p < 0.05$) to the interspecific dietary differences, through their contributions were minor. The diet profiles of wolves and coyotes generated with RRA data was similar to those with FOO data (Supplementary Figure 2), except that each prey species had lower proportion with RRA data. For example, the average read relative abundance of domestic cow was 3.73% with RRA data, whereas the its FOO was 16.16%.

Spatiotemporal Variations in the Diet Profile of Wolves

The dietary differences among wolf pack ranges were significant (p = 0.001). As there was no significant seasonal difference in the wolf diet (p = 0.448) or significant interaction between seasons and wolf pack ranges (p = 0.095), following analyses focused only on the spatial variation in the wolf diet (Figure 5). The FOO of moose was the highest (71.43%) in the Dirty Shirt range, followed by Smackout (38.24%) and Goodman Meadows (24.32%). According to the SIMPER test, moose consumption in the Dirty Shirt range was significantly higher than that in Goodman Meadows (p = 0.001). The FOO of deer was highest in the

Smackout range (58.82%), followed by Goodman Meadows (51.35%) and Dirty Shirt (28.57%). The FOO of elk was the highest in the Goodman Meadows range (29.73%), whereas its FOO was 11.76% and 7.14% in the Smackout and Dirty Shirt ranges, respectively. Common starling was only found in the Goodman Meadows range with a FOO of 2.70%. Meadows vole and ruffed grouse were only found in the Smackout and Dirty Shirt ranges (Figure 5).

Spatiotemporal Variations in the Diet Profile of Coyotes

There were significant spatiotemporal variations in the coyote diet (season: $p = 0.037$; pack: $p = 0.003$) (Figure 6). Since there was a significant interaction between seasons and wolf pack ranges ($p = 0.043$), we investigated the spatial dietary changes in coyotes in each season separately. In the spring, the FOO of moose in the Dirty Shirt range was highest (66.67%) among three wolf pack ranges, whereas the FOO of moose in the Smackout range was the lowest (12.50%). The difference in FOO of moose between Dirty Shirt and Smackout was significant ($p = 0.001$). In the fall, deer was not detected in the coyote diet in the Goodman Meadows range, whereas its FOO was highest in Smackout (60.00%). Muskrat was only detected in the Goodman Meadows range ($p = 0.014$) and wild turkey was detected in Dirty Shirt and Smackout ranges but not in Goodman Meadows ($p = 0.015$). We also investigated the seasonal dietary changes of coyotes in each wolf pack range separately. In the Dirty Shirt range, moose consumption was higher in the spring (66.67%) than in the fall (15.38%), though the difference was not significant after correcting for multiple comparisons ($p = 0.021$, adjusted alpha=0.017). In the Goodman Meadows range, muskrat consumption was only detected in the fall ($p = 0.011$). In the Smackout range, deer

consumption was significantly higher in the fall (60.00%) than that in the spring (20.83%) (p = 0.012).

Spatiotemporal Variations in Diet Overlap between Wolves and Coyotes

There was large variation in dietary overlap (O) between wolves and coyotes, ranging from nearly no overlap (0.08) to 0.74. Dietary overlap was least in the Goodman Meadows range in the fall, at 0.08. The most substantial dietary overlap (O) between wolves and coyotes was found in the Smackout range in the fall (0.74), followed by the Dirty Shirt range in the Spring (0.70) (Table 1).

Discussion

In this study, we characterized the high-resolution diet profiles of sympatric wolves and coyotes in northeastern Washington, and also revealed their dietary spatiotemporal variations. We demonstrated that DNA metabarcoding was a successful molecular approach for diet analyses.

Prey Partitioning between Sympatric Canids in Northeastern Washington

The results with FOO data showed that wolves primarily preyed on deer (47.47%) and moose (42.42%) in northeastern Washington. This result is consistent with kill site analyses conducted by Washington Department of Fish and Wildlife (WDFW) (Kertson, 2018). Across much of the boreal forest of North America, wolves hunted moose, their historic primary prey in upland forest (Latham, Latham, Knopff, Hebblewhite, & Boutin, 2013). We couldn't determine the specific deer species with 12S V5 sequence. In

northeastern Washington, there are two deer species, mule deer (*Odocoileus hemionus*) and white-tailed deer (*Odocoileus virginianus*). White-tailed deer is the predominant deer species as there is limited mule deer habitat in the study area (Washington Department of Fish and Wildlife, 2017). Snowshoe hares (61.17%) were the most common prey in the coyote diet, which is consistent with previous studies (Latham et al., 2011; Smith et al., 2018). The high snowshoe hare consumption rate by coyotes have significant impacts on the conservation management of Canada lynx (*Lynx canadensis*). Lynx are usually considered as specialist on snowshoe hares, whereas coyotes are often considered as generalist. The roughly 10 - year population cycle of snowshoe hare is among the most well-known examples of cyclic population dynamics (Stenseth, Falck, Bjornstad, & Krebs, 1997). Coyote and lynx both mostly feed on snowshoe share except during its cyclic lows (O'Donoghue et al., 1998). In 2000, Canada lynx was listed as threatened under the US Endangered Species Act (ESA) and in 2016, Canada lynx was listed as endangered in Washington state. In the absence of wolves, coyotes may negatively affect lynx populations by increasing predation on snowshoe hares, and/or directly killing lynx (Ripple et al., 2011). The recovery of wolf populations could potentially keep the populations of coyotes and ungulates in check, leading to recovery of plant communities and eventually population growth in snowshoe hares and possibly lynx as well (Ripple et al., 2011). Coyotes also consumed a significant amount of moose (30.10%) and deer (21.36%).

High Moose Consumption by Wolf in the Dirty Shirt Pack Range

Differences in dietary composition among different wolf pack ranges may reflect prey abundance variations and pack-specific hunting behaviors. Generally, predators, such as wolves, select prey

items according to their availability and shift to consuming alternative food sources when the primary food source becomes scarce (Nordberg & Schwarzkopf, 2019; Randa, Cooper, Meserve, & Yunger, 2009). The FOO of moose was the highest (71.43%) in Dirty Shirt, followed by Smackout (38.24%) and Goodman Meadows (24.32%), which implies high moose abundance in the Dirty Shirt range. However, pack-specific hunting ability might also affect prey selection, with larger packs having higher success rates in capturing and killing formidable prey (MacNulty, Tallian, Stahler, & Smith, 2014), such as moose. The Dirty Shirt pack was the largest wolf pack (n = 7 - 13) with confirmed successful breeding pairs during the study period (April in 2015 - May in 2017) (Supplementary Table 2). Larger pack size could make wolves in the Dirty Shirt range more effective at preying on moose. Both pack-specific prey abundance and hunting-ability could affect prey consumption rates. The correlation between moose consumption rate and moose abundance in the Dirty Shirt pack range needs to be further investigated with the inclusion of prey abundance data in this ecosystem.

Coyote & Ungulate: Ungulate Neonate Predation or Scavenging?

It has been widely assumed that coyotes are not efficient predators on adult deer and are incapable of killing adult moose, but coyotes can occasionally prey on ungulate neonates (<3 months old) during the fawning season (mid-May to mid-June) (Benson & Patterson, 2013; Chitwood et al., 2015; Chitwood, Lashley, Moorman, & Deperno, 2014). Moose calves are vulnerable to coyote predation as well. Female ungulates in the late-gestation stage (April to early May) are also vulnerable targets for coyotes (Chitwood et al., 2014). Coyote pups are born in April, resulting in high lactation demands on females in the spring (Kilgo et al., 2012). This aspect of the coyote life cycle could result in higher pressure on ungulate neonates. The high

FOO of moose in the coyote spring diet in the Dirty Shirt range (66.67%) suggests that coyote might predate on moose calves. However, the ungulate neonate predation hypothesis cannot explain the high FOO of deer (60.00%) in the fall coyote diet in the Smackout range, when the deer consumption rate by coyotes in the spring was only 20.83%. Interestingly, moose consumption by wolves was highest in the Dirty Shirt range (71.43%) with no seasonal difference. Deer consumption by wolf was highest in the Smackout range (58.82%), especially in the fall (80.00%). Furthermore, the dietary overlap between these canid species was greatest in the Dirty Shirt range (0.70) in the spring and in the Smackout range in the fall (0.74). Overall, these multiple lines of evidence suggest that coyotes use ungulate carrion subsidies from wolves as a highly-valued food resource. The substantial deer consumption by wolf in the Smackout range in the fall (80%) could be due to severe weather or disease outbreak which might make deer more vulnerable to wolf predation. It could also be due to reduced interspecific competition with other ungulates in this area.

Consumption of Domestic Animals by Wolves and Coyotes

We detected the DNA of domestic animals in the diets of wolves and coyotes, including pigs, rabbits and domestic cow (Figure 3). Pig DNA was detected in three wolf samples in Goodman Meadows, including one in the fall and two in the spring. Rabbit DNA was detected in two coyote samples, including one in the Dirty Shirt in the fall and the other in the Smackout in the fall. The rabbit DNA was matched to European rabbit (*Oryctolagus cuniculus*). However, this could be from domestic pet rabbits since European rabbits are mainly found on the San Juan Islands in Washington state. In total, we found 18 samples containing cow DNA, including 16 wolf samples and 2 coyote samples. The occurrence of

domestic cow DNA in our samples was unlikely to be due to contamination, since none of the negative controls were found to contain cow DNA. Here we only focused on the domestic cow consumption by wolves. Domestic cow was the fourth most frequently occurring prey in the wolf diet, with a FOO of 16.16%. However, it is important to emphasize that the FOO method tends to overestimate the rare prey and underestimate the abundant prey. Indeed, RRA data indicated that the average read proportion of domestic cow in the wolf diet was quite low, only 3.73%. The 16 wolf samples with cow DNA were distributed among three different wolf pack ranges, different years and different seasons. If we assume that 1) all the samples we collected were relatively fresh (based on the high PCR amplification success rate), 2) consumption of any given cow was restricted by the same wolf pack range, in the same season of the same year, and 3) movement of domestic cows across the landscape was limited, we could estimate that there was a minimum of 7 domestic cow individuals involved: two in the Dirty Shirt range (2015 & 2016), two in the Goodman Meadows range in 2015 (fall & spring), and three in the Smackout range (2015, 2016, 2017). Based on Washington Gray Wolf Conservation and Management Annual Reports and gray wolf updates from WDFW, we could only find four reported wolf-cow conflicts that occurred in our study area during the study period, including one incident in Dirty Shirt on Oct 2nd, 2016 (confirmed wolf depredation which injured one cow), one incident in Smackout on September 21st, 2016 (a confirmed wolf depredation resulting in a dead calf), one incident in Smackout on September 28, 2016 (a probable wolf depredation resulting in a dead calf) and another in Smackout on September 29, 2016 (a confirmed wolf depredation resulting in an injured calf). These four incidents appear to correspond to three samples on the list of Supplementary Table 3, with sample ID 164077 (Dirty Shirt,

Fall 2016), 164007 and 164010 (both in Smackout, Fall, 2016). We could not find wolf-predation reports from WDFW that could represent matches of the rest of 16 wolf samples, making it difficult to establish the causes of domestic cow consumption. Though very promising, DNA metabarcoding technology cannot differentiate active predation from scavenging, partial prey consumption or fecal matter consumption. Therefore, caution is needed when interpreting the results from DNA metabarcoding. Conventional methods such as field necropsies and killing-bite wound examination are able to confirm predator identification. Camera trap provides great insights into the feeding behaviors of predators. DNA metabarcoding technology should supplement, not replace conventional methods. Local ranchers, wildlife biologists, and government agencies can work together to examine multiple lines of evidence and combine expertise from each stakeholder to achieve a better understanding of the impact of wolf recovery on the local ecosystem in Washington state.

Predator-Specific Blocking Primer is Not Necessary with High-Throughput Sequencing Platforms

In dietary studies with fecal DNA, samples contain higher amounts of predator DNA than prey DNA, which can cause PCR amplification being dominated by predator DNA, resulting in low sequencing depth for prey characterization. Predator-specific blocking primers can offer a solution by specifically reducing the amplification of predator DNA. However, with NGS technology becoming faster and cheaper, it might not be necessary to apply predator-specific blocking primer in the diet analyses of carnivores. Indeed, though the majority of sequence reads in our study were from the predator hosts, the amount of prey sequences generated was large enough to characterize the diet profile without the use of blocking

primers. Moreover, specific blocking oligos can block prey DNA along with the targeted predator (Piñol et al., 2014; Robeson et al., 2017) or cause amplifications to fail altogether (Shehzad et al., 2012), introducing additional bias into the analysis of diet composition. In our study, the use of blocking primers increased the proportion of prey sequences from 26.40% to 65.97%. However, all prey species were detected without adding the blocking primer and chipmunk was not detected when the blocking primer was applied. Given the above, we do not believe that predator-specific blocking primer is cost-effective in the diet analyses of carnivores, and this will likely become even more so as NGS technology continues to become faster and cheaper.

Recommendations for Future Research

It is important to include negative controls and sequence them along with samples for metabarcoding studies. A low amount of contamination is inevitable with NGS technologies, especially when using universal primers, despite good laboratory practices to minimize contamination risks. We found noticeable contamination in our negative controls with sources from human, striped skunk, wolf, coyotes, moose and deer. Negative controls should always be included to check for potential contamination (De Barba et al., 2013). These controls are often included during steps of DNA extraction and PCR, but they are not always sequenced and may only get checked using gel electrophoresis. Such practice can be misleading as most contaminating sequences cannot be visually detected via gel electrophoresis. By contrast, the series of filtering steps we conducted to remove the impacts of contaminations are very effective and provide valuable framework for contamination control. We also recommend the use of PCR replicates that are sequenced

independently as a way to help confirm the presence of taxa in a given sample and further remove false-positives (De Barba et al., 2013; Galan et al., 2018). Pooling PCR replicates prior to sequencing masks the variation among PCR replicates. Therefore, we recommend this multi-replicate approach that the presence of a prey item in a given sample is only confirmed if it occurs in at least 2 replicates.

The key advantage of DNA metabarcoding relative to traditional methods is its high taxonomic resolution. However, this method also has its limitations. Most MOTUs were assigned at the species level except for deer, ground squirrel, red-backed vole, flying squirrel, and chipmunk, which can only be assigned at the genus level. This was likely due to our use of a single short marker (12SV05F/R, ~100 bp). The degree of DNA degradation in fecal samples limits the length of fragments that can be successfully amplified. For this reason, the recommended fragment length is usually in the range of 100-250 bp, which inevitably reduces taxonomic resolution (Pompanon et al., 2011). The multigene approach (Gunther, Knebelsberger, Neumann, Laakmann, & Arbizu, 2018) and mitogenomics approach (Piñol et al., 2014; Tang et al., 2014) have been proposed as the next phase of the current single-locus metabarcoding method. As a PCR-free approach, the mitogenomics approach can alleviate the artifacts caused by PCR bias while expanding single-gene metabarcoding into whole mitochondria metagenomics (Taberlet et al., 2012). The growing mitogenome databases and the continuously decreasing cost of sequencing will eventually make the mitogenomics approach much more affordable and favorable over the single-marker DNA metabarcoding approach.

Acknowledgements

We thank all the conservation canines and dog handlers who have conducted sample collection for the study, including Heath Smith, Jennifer Hartman, Suzie Marlow, Will Chrisman, Caleb Stanek, Justin Broderick, Casey McCormack, Mairi Poisson, Collette Yee, Rachel Katz, Jake Lammi, Peter Dubyoski, Marlen Richmond and Julianne Ubigau. We thank the Burke Museum of Natural History for providing positive samples during the initial testing phase. We thank Noah Synder-Mackler, India Schneider-Crease, and Sierra Sams for their advice**s** on library prep and MiSeq sequencing. The MiSeq sequencing platform is funded by the Student Technology Fee at the University of Washington. We thank Pierre Taberlet for his advice with experiment design and Susanne Butschkau for her help with bioinformatic data analysis. The study was funded by the Johnson Foundation, the Dawkins Trust and the Maritz Family foundation. Yue Shi was funded by WRF Hall Fellowship from the University of Washington.

Data Accessibility

After peer review and prior to final publication, the following data will be deposited in Dryad: (i) raw sequence reads (*fastq* format), (ii) filtered abundance table including taxonomic affiliations.

Author Contributions

YS and SKW conceived the project. YS designed the experiments. YS, YH and ER performed the experiments. YS conducted the analyses and wrote the manuscript. SKW guided analyses and edited the manuscript. All authors declare no conflict of interests.

References

Benson, J. F., & Patterson, B. R. (2013). Moose (*Alces alces*) predation by eastern coyotes (*Canis latrans*) and eastern coyote × eastern wolf (*Canis latrans* × *Canis lycaon*) hybrids. *Canadian Journal of Zoology*, *91*(11), 837–841. http://doi.org/10.1139/cjz-2013-0160

Benson, J. F., Loveless, K. M., Rutledge, L. Y., & Patterson, B. R. (2017). Ungulate predation and ecological roles of wolves and coyotes in eastern North America. *Ecological Applications*, 1–17.

Berry, T. E., Osterrieder, S. K., Murray, D. C., Coghlan, M. L., Richardson, A. J., Grealy, A. K., et al. (2017). DNA metabarcoding for diet analysis and biodiversity: A case study using the endangered Australian sea lion (*Neophoca cinerea*). *Ecology and Evolution*, *7*(14), 5435–5453. http://doi.org/10.1002/ece3.3123

Boyer, F., Mercier, C., Bonin, A., Le Bras, Y., Taberlet, P., & Coissac, E. (2015). obitools: a unix-inspired software package for DNA metabarcoding. *Molecular Ecology Resources*, *16*(1), 176–182. http://doi.org/10.1111/1755-0998.12428

Buglione, M., Maselli, V., Rippa, D., de Filippo, G., Trapanese, M., & Fulgione, D. (2018). A pilot study on the application of DNA metabarcoding for non-invasive diet analysis in the Italian hare. *Mammalian Biology*, *88*, 31–42. http://doi.org/10.1016/j.mambio.2017.10.010

Carrera, R., Ballard, W., Gipson, P., Kelly, B. T., Krausman, P. R., Wallace, M. C., et al. (2008). Comparison of Mexican Wolf and Coyote Diets in Arizona and New Mexico. *Journal of Wildlife Management*, *72*(2), 376–381. http://doi.org/10.2193/2007-012

Chitwood, M. C., Lashley, M. A., Kilgo, J. C., Pollock, K. H., Moorman, C. E., & Deperno, C. S. (2015). Do Biological and Bedsite Characteristics Influence Survival of Neonatal White-Tailed Deer? *PLoS ONE*, *10*(3), e0119070–14. http://doi.org/10.1371/journal.pone.0119070

Chitwood, M. C., Lashley, M. A., Moorman, C. E., & Deperno, C. S. (2014). Confirmation of Coyote Predation on Adult Female White-Tailed Deer in the Southeastern United States. *Southeastern Naturalist*, *13*(3), N30–N32. http://doi.org/10.1656/058.013.0316

De Barba, M., Miquel, C., Boyer, F., Mercier, C., Rioux, D., Coissac, E., & Taberlet, P. (2013). DNA metabarcoding multiplexing and validation of data accuracy for diet assessment: application to omnivorous diet. *Molecular Ecology Resources*, *14*(2), 306–323. http://doi.org/10.1111/1755-0998.12188

Deagle, B. E., Kirkwood, R., & Jarman, S. N. (2009). Analysis of Australian fur seal diet by pyrosequencing prey DNA in faeces. *Molecular Ecology*, *18*(9), 2022–2038. http://doi.org/10.1111/j.1365-294X.2009.04158.x

Drouilly, M., Nattrass, N., & O'Riain, M. J. (2017). Dietary niche relationships among predators on farmland and a protected area. *The Journal of Wildlife Management*, *82*(3), 507–518. http://doi.org/10.1002/jwmg.21407

Estes, J. A., Terborgh, J., Brashares, J. S., Power, M. E., Berger, J., Bond, W. J., et al. (2011). Trophic downgrading of planet Earth. *Science*, *333*(6040), 301–306. http://doi.org/10.1126/science.1205106

Ficetola, G. F., Coissac, E., Zundel, S., Riaz, T., Shehzad, W., Bessiere, J., et al. (2010). An *In silico* approach for the evaluation of DNA barcodes. *BMC Genomics*, *11*, 434.

Gable, T. D., Windels, S. K., Bruggink, J. G., & Barber-Meyer, S. M. (2018). Weekly Summer Diet of Gray Wolves (*Canis lupus*) in Northeastern Minnesota. *The American Midland Naturalist*, *179*(1), 15–27. http://doi.org/10.1674/0003-0031-179.1.15

Galan, M., Pons, J.-B., Tournayre, O., Pierre, É., Leuchtmann, M., Pontier, D., & Charbonnel, N. (2018). Metabarcoding for the parallel identification of several hundred predators and their prey: Application to bat species diet analysis. *Molecular Ecology Resources*, *18*(3), 474–489. http://doi.org/10.1111/1755-0998.12749

Gallagher, A. J., Trull, P. F., Faherty, M. S., Freidenfelds, N., Heimbuch, J., & Cherry, M. J. (2019). Predatory behaviors of coyotes (*Canis latrans*) living in coastal ecosystems. *Ethology Ecology & Evolution*, *31*(2), 198–204. http://doi.org/10.1080/03949370.2018.1521874

Gunther, B., Knebelsberger, T., Neumann, H., Laakmann, S., & Arbizu, P. M. (2018). Metabarcoding of marine environmental DNA based on mitochondrial and nuclear genes. *Scientific Reports*, 1–13. http://doi.org/10.1038/s41598-018-32917-x

Hawlitschek, O., Fernández-González, A., Balmori-de la Puente, A., & Castresana, J. (2018). A pipeline for metabarcoding and diet analysis from fecal samples developed for a small semi-aquatic mammal. *PLoS ONE*, *13*(8), e0201763–19. http://doi.org/10.1371/journal.pone.0201763

Hody, J. W., & Kays, R. (2018). Mapping the expansion of coyotes (*Canis latrans*) across North and Central America. *ZooKeys*, *759*(4), 81–97. http://doi.org/10.3897/zookeys.759.15149

Kamenova, S., Bretagnolle, V., Plantegenest, M., & Canard, E. (2018). DNA metabarcoding diet analysis reveals dynamic feeding behaviour and biological control potential of carabid farmland communities. *bioRxiv*, 1–33. http://doi.org/10.1101/332312

Kartzinel, T. R., Chen, P. A., Coverdale, T. C., Erickson, D. L., Kress, W. J., Kuzmina, M. L., et al. (2015). DNA metabarcoding illuminates dietary niche partitioning by African large herbivores. *Proceedings of the National Academy of Sciences*, *112*(26), 8019–8024. http://doi.org/10.1073/pnas.1503283112

Kertson, B. N. (2018). *Job Progress Report Federal Aid in Wildlife Restoration: Washington carnivore research. Project #2. Progress Report.* (pp. 1–25). Olympia, WA, USA.

Kilgo, J. C., Ray, H. S., Vukovich, M., Goode, M. J., & Ruth, C. (2012). Predation by coyotes on white-tailed deer neonates in South Carolina. *The Journal of Wildlife Management*, *76*(7), 1420–1430. http://doi.org/10.1002/jwmg.393

Kilgo, J. C., Vukovich, M., Ray, H. S., Shaw, C. E., & Ruth, C. (2014). Coyote removal, understory cover, and survival of white-tailed deer neonates. *The Journal of Wildlife Management*, *78*(7), 1261–1271. http://doi.org/10.1002/jwmg.764

Latham, A. D. M., Latham, M. C., Knopff, K. H., Hebblewhite, M., & Boutin, S. (2013). Wolves, white-tailed deer, and beaver: implications of seasonal prey switching for woodland caribou declines. *Ecography*, *36*(12), 1276–1290. http://doi.org/10.1111/j.1600-0587.2013.00035.x

Latham, A. D. M., Latham, M. C., Mccutchen, N. A., & Boutin, S. (2011). Invading white-tailed deer change wolf-caribou dynamics in northeastern Alberta. *The Journal of Wildlife Management*, *75*(1), 204–212. http://doi.org/10.1002/jwmg.28

MacNulty, D. R., Tallian, A., Stahler, D. R., & Smith, D. W. (2014). Influence of Group Size on the Success of Wolves Hunting Bison. *PLoS ONE*, *9*(11), e112884–8. http://doi.org/10.1371/journal.pone.0112884

Marshall, K. N., Stier, A. C., Samhouri, J. F., Kelly, R. P., & Ward, E. J. (2015). Conservation Challenges of Predator Recovery. *Conservation Letters*, *9*(1), 70–78. http://doi.org/10.1111/conl.12186
Modave, E., MacDonald, A. J., & Sarre, S. D. (2017). A single mini-barcode test to screen for Australian mammalian predators from environmental samples. *GigaScience*, *6*, 1–13. http://doi.org/10.1093/gigascience/gix052
Morello, L., Braglia, L., Gavazzi, F., Gianì, S., & Breviario, D. (2019). Tubulin-Based DNA Barcode: Principle and Applications to Complex Food Matrices. *Genes*, *10*(3), 1–16. http://doi.org/10.3390/genes10030229
Moreno-Rueda, G., Melero, E., Reguera, S., Zamora-Camacho, F. J., & Álvarez-Benito, I. (2017). Prey availability, prey selection, and trophic niche width in the lizard *Psammodromus algirus* along an elevational gradient. *Current Zoology*, *64*(5), 603–613. http://doi.org/10.1093/cz/zox077
Nelson, M. A., Cherry, M. J., Howze, M. B., Warren, R. J., & Mike, C. L. (2015). Coyote and Bobcat Predation on White-tailed Deer Fawns in a Longleaf Pine Ecosystem in Southwestern Georgia. *Journal of the Southeastern Association of Fish and Wildlife Agencies*, *2*, 208–213.
Nordberg, E. J., & Schwarzkopf, L. (2019). Predation risk is a function of alternative prey availability rather than predator abundance in a tropical savanna woodland ecosystem. *Scientific Reports*, 1–11. http://doi.org/10.1038/s41598-019-44159-6
O'Donoghue, M., Boutin, S., Krebs, C. J., Zuleta, G., Murray, D. L., & Hofer, E. J. (1998). Functional Responses of Coyotes and Lynx to the Snowshoe Hare Cycle. *Ecology*, *79*, 1193–1208.
Patterson, B. R., & Messier, F. (2000). Factors Influencing Killing Rates of White-Tailed Deer by Coyotes in Eastern Canada. *Journal of Wildlife Management*, *64*, 721–732.
Pianka, E. R. (1973). The structure of lizard communities. *Annual Review of Ecology and Systematics*, *4*, 53–74.
Piñol, J., Mir, G., Gomez-Polo, P., & Agustí, N. (2014). Universal and blocking primer mismatches limit the use of high-throughput DNA sequencing for the quantitative metabarcoding of arthropods. *Molecular Ecology Resources*, *15*(4), 819–830. http://doi.org/10.1111/1755-0998.12355
Pompanon, F., Deagle, B. E., Symondson, W. O. C., Brown, D. S., Jarman, S. N., & Taberlet, P. (2011). Who is eating what: diet assessment using next generation sequencing. *Molecular Ecology*, *21*(8), 1931–1950. http://doi.org/10.1111/j.1365-294X.2011.05403.x
Randa, L. A., Cooper, D. M., Meserve, P. L., & Yunger, J. A. (2009). Prey Switching of Sympatric Canids in Response to Variable Prey Abundance. *Journal of Mammalogy*, *90*(3), 594–603.
Riaz, T., Shehzad, W., Viari, A., Pompanon, F., Taberlet, P., & Coissac, E. (2011). ecoPrimers: inference of new DNA barcode markers from whole genome sequence analysis. *Nucleic Acids Research*, *39*(21), e145–e145. http://doi.org/10.1093/nar/gkr732
Ripple, W. J., Wirsing, A. J., Beschta, R. L., & Buskirk, S. W. (2011). Can restoring wolves aid in lynx recovery? *Wildlife Society Bulletin*, *35*(4), 514–518. http://doi.org/10.1002/wsb.59
Robeson, M. S., II, Khanipov, K., Golovko, G., Wisely, S. M., White, M. D., Bodenchuck, M., et al. (2017). Assessing the utility of metabarcoding for diet analyses of the omnivorous wild

pig (S*us scrofa*). *Ecology and Evolution*, *8*(1), 185–196. http://doi.org/10.1002/ece3.3638
Rohland, N., & Reich, D. (2012). Cost-effective, high-throughput DNA sequencing libraries for multiplexed target capture. *Genome Research*, *22*(5), 939–946. http://doi.org/10.1101/gr.128124.111
Shehzad, W., Riaz, T., Nawaz, M. A., Miquel, C., Poillot, C., Shah, S. A., et al. (2012). Carnivore diet analysis based on next-generation sequencing: application to the leopard cat (*Prionailurus bengalensis*) in Pakistan. *Molecular Ecology*, *21*(8), 1951–1965. http://doi.org/10.1111/j.1365-294X.2011.05424.x
Sivy, K. J., Pozzanghera, C. B., Colson, K. E., Mumma, M. A., & Prugh, L. R. (2017). Apex predators and the facilitation of resource partitioning among mesopredators. *Oikos*, *127*(4), 607–621. http://doi.org/10.1111/oik.04647
Smith, J. A., Thomas, A. C., Levi, T., Wang, Y., & Wilmers, C. C. (2018). Human activity reduces niche partitioning among three widespread mesocarnivores. *Oikos*, *127*(6), 890–901. http://doi.org/10.1111/oik.04592
Stenseth, N. C., Falck, W., Bjornstad, O. N., & Krebs, C. J. (1997). Population regulation in snowshoe hare and Canadian lynx: Asymmetric food web configurations between hare and lynx. *Proceedings of the National Academy of Sciences*, *94*, 5147–5152.
Stier, A. C., Samhouri, J. F., Novak, M., Marshall, K. N., Ward, E. J., Holt, R. D., & Levin, P. S. (2016). Ecosystem context and historical contingency in apex predator recoveries. *Science Advances*, *2*(5), e1501769–14. http://doi.org/10.1126/sciadv.1501769
Sullins, D. S., Haukos, D. A., Craine, J. M., Lautenbach, J. M., Robinson, S. G., Lautenbach, J. D., et al. (2018). Identifying the diet of a declining prairie grouse using DNA metabarcoding. *The Auk*, *135*(3), 583–608. http://doi.org/10.1642/AUK-17-199.1
Taberlet, P., Coissac, E., Pompanon, F., Brochmann, C., & Willerslev, E. (2012). Towards next-generation biodiversity assessment using DNA metabarcoding. *Molecular Ecology*, *21*, 2045–2050.
Tang, M., Tan, M., Meng, G., Yang, S., Su, X., Liu, S., et al. (2014). Multiplex sequencing of pooled mitochondrial genomes—a crucial step toward biodiversity analysis using mito-metagenomics. *Nucleic Acids Research*, *42*(22), e166–e166. http://doi.org/10.1093/nar/gku917
Vestheim, H., & Jarman, S. N. (2008). Blocking primers to enhance PCR amplification of rare sequences in mixed samples – a case study on prey DNA in Antarctic krill stomachs. *Frontiers in Zoology*, *5*(1), 12–11. http://doi.org/10.1186/1742-9994-5-12
Wallach, A. D., Izhaki, I., Toms, J. D., Ripple, W. J., & Shanas, U. (2015). What is an apex predator? *Oikos*, *124*(11), 1453–1461. http://doi.org/10.1111/oik.01977
Washington Department of Fish and Wildlife. (2017). Wildlife Program 2015-2017 Ungulate Assessment, 1–186.
Wasser, S. K., Keim, J. L., Taper, M. L., & Lele, S. R. (2011). The influences of wolf predation, habitat loss, and human activity on caribou and moose in the Alberta oil sands. *Frontiers in Ecology and the Environment*, *9*(10), 546–551. http://doi.org/10.2307/41479958?ref=no-x-route:addb7ca5ae392d054664081ba69a3ef7
Wiles, G. J., Allen, H. L., & Hayes, G. E. (2011, January 23). Wolf Conservation and Management Plan for Washington. Olympia, Washington.

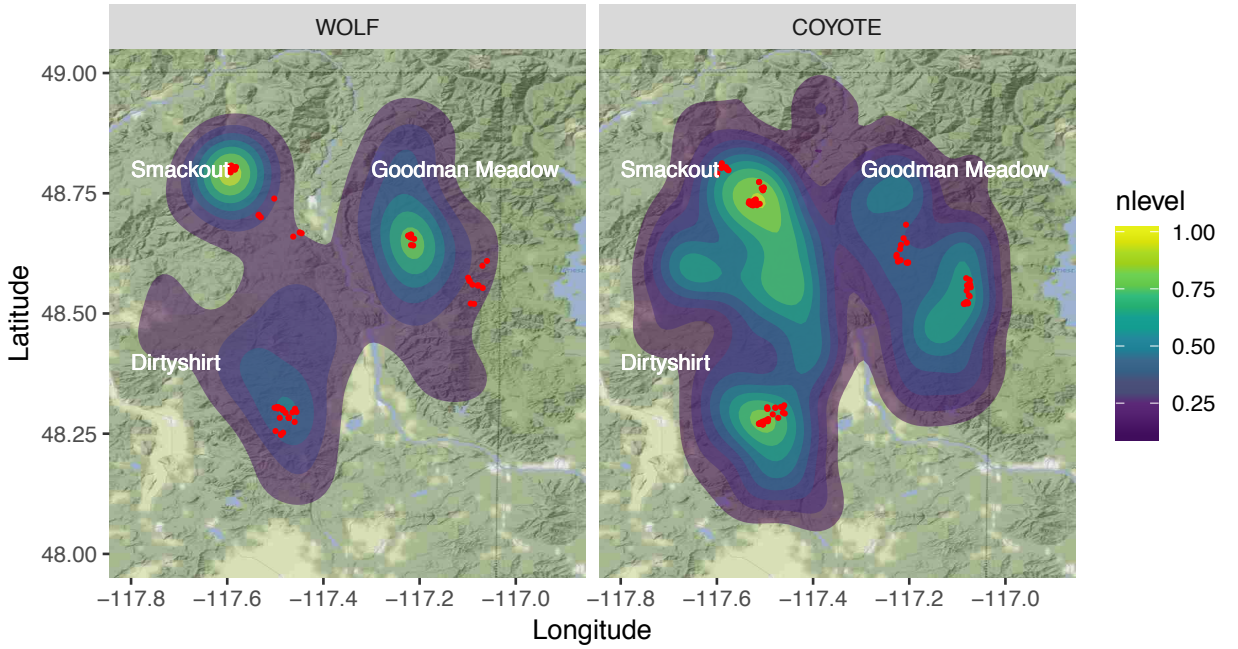

Figure 2 Sample selection based on relative kernel density (nlevel) map. Samples used in this study were selected from an ongoing project with 647 wolf fecal samples and 1893 coyote fecal samples. Kernel density was calculated using function *stat_density2d* in R *ggplot2*. Note: The color gradient indicates the relative density ranges from 0 to 1.

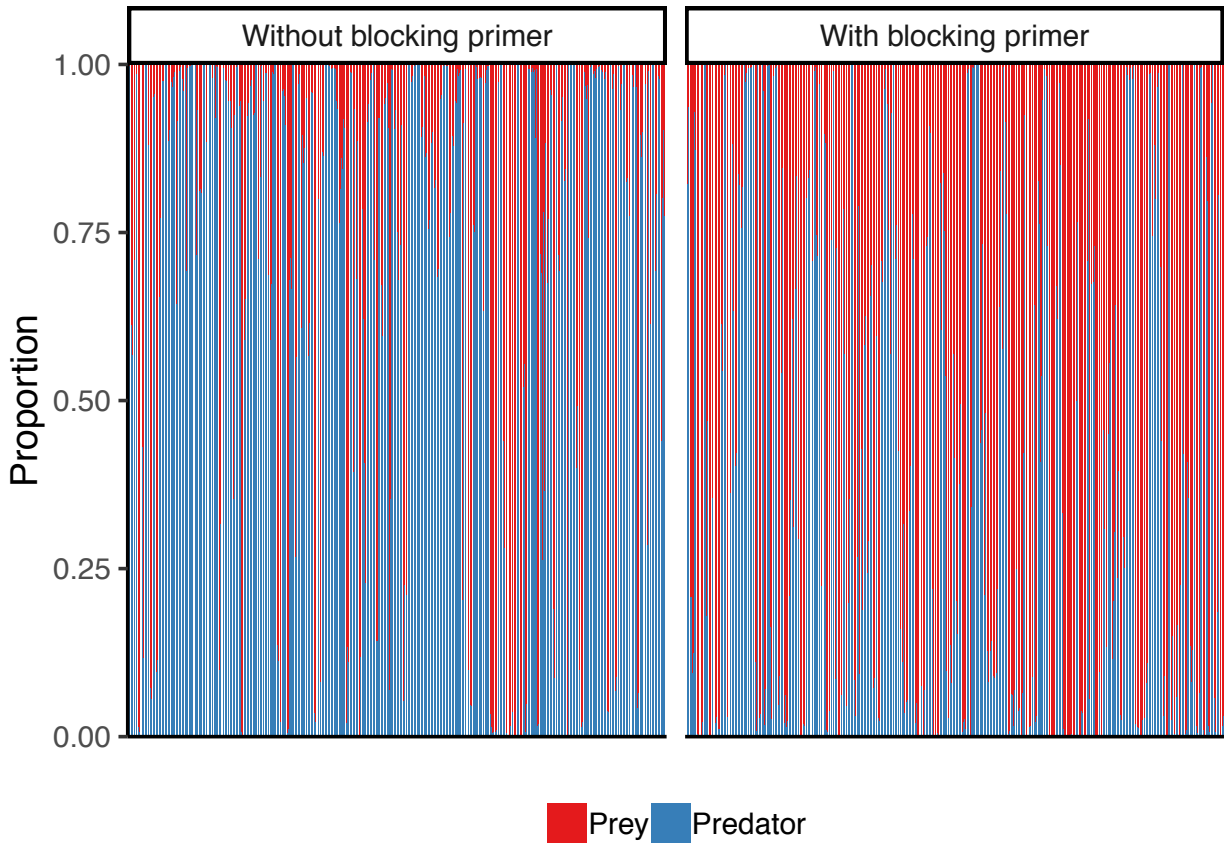

Figure 2 Effects of the predator-specific blocking primer on the proportion of reads mapped to the predators and preys.

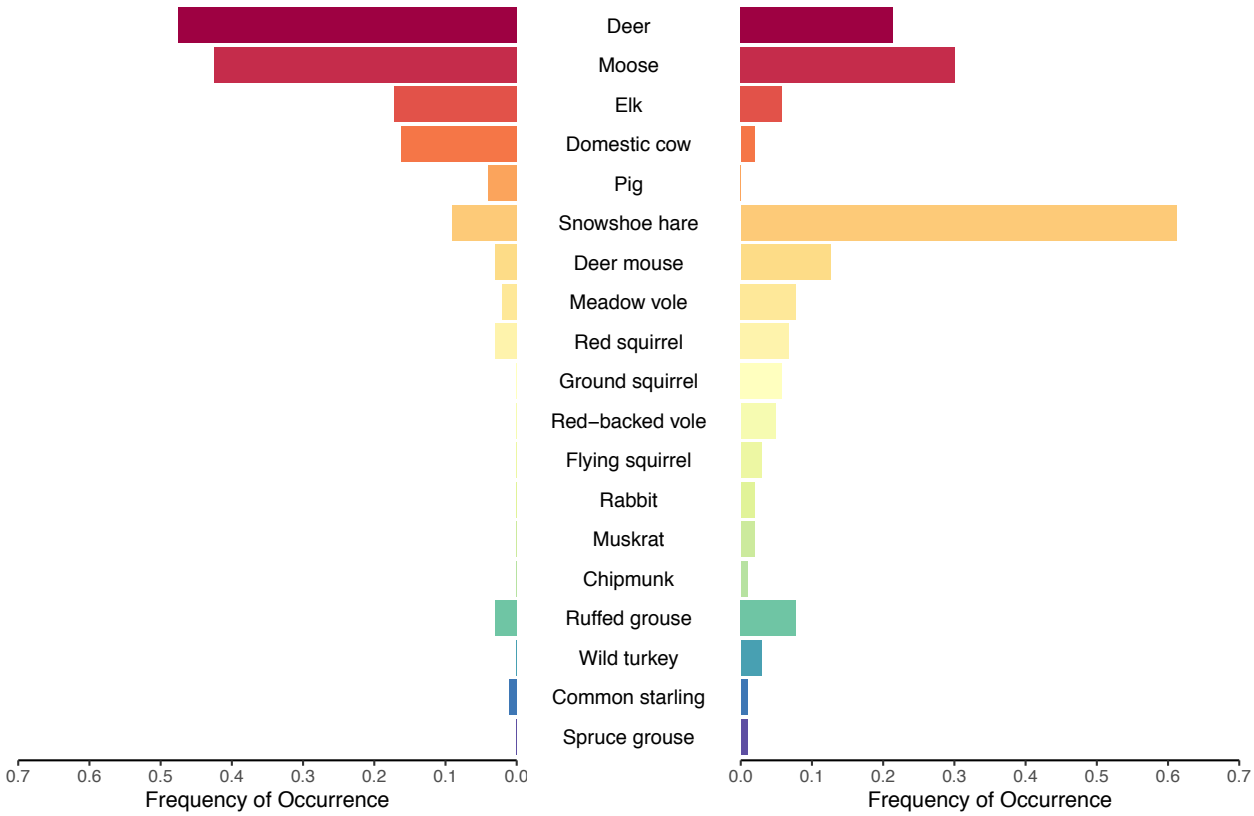

Figure 3 Diet profile of wolves ($N = 99$) and coyotes ($N = 103$) using the frequency of occurrence of 19 prey species. There was a significant difference in the diet profile between wolves and coyotes ($p = 0.001$).

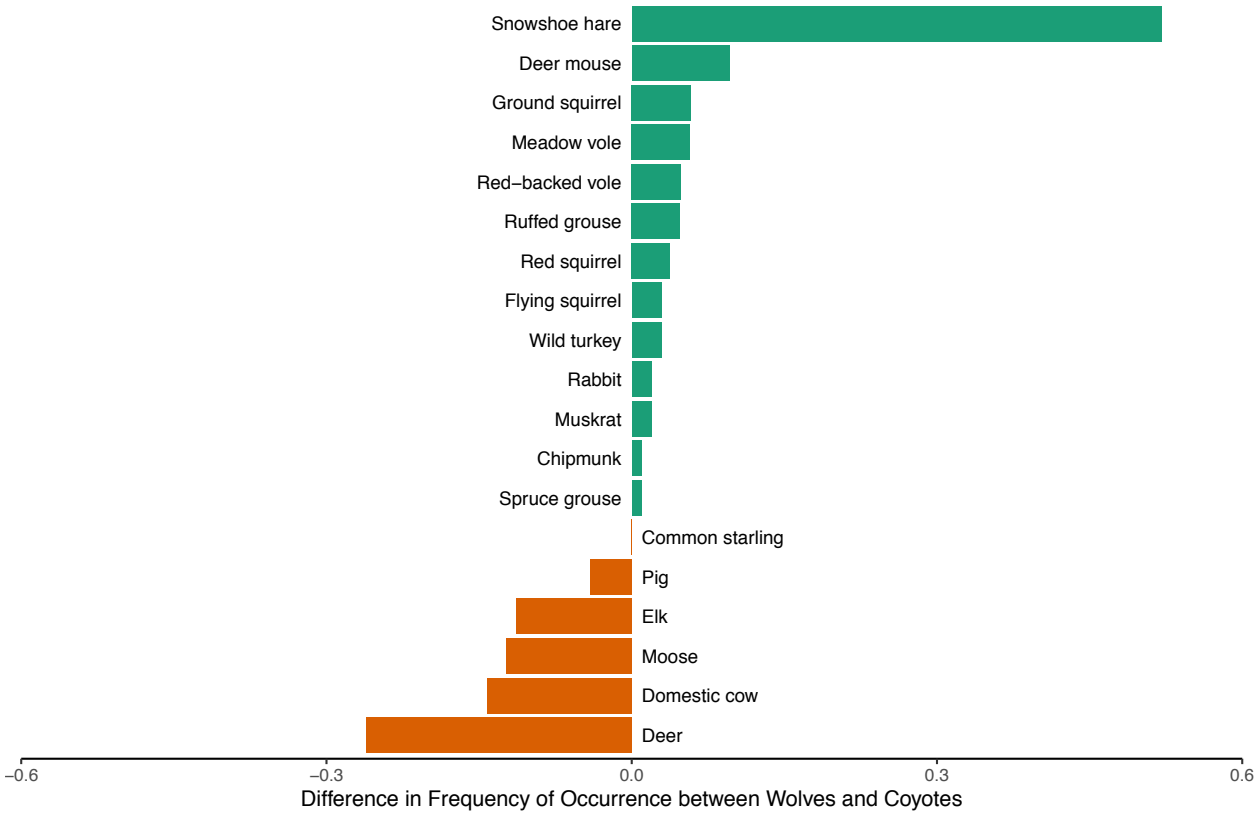

Figure 4 Differences in diet profile of wolves ($N = 99$) and coyotes ($N = 103$) using the frequency of occurrence of 19 prey species. Difference in the frequency of occurrence (FOO) of any prey species was calculated as FOO in wolf - FOO in coyote.

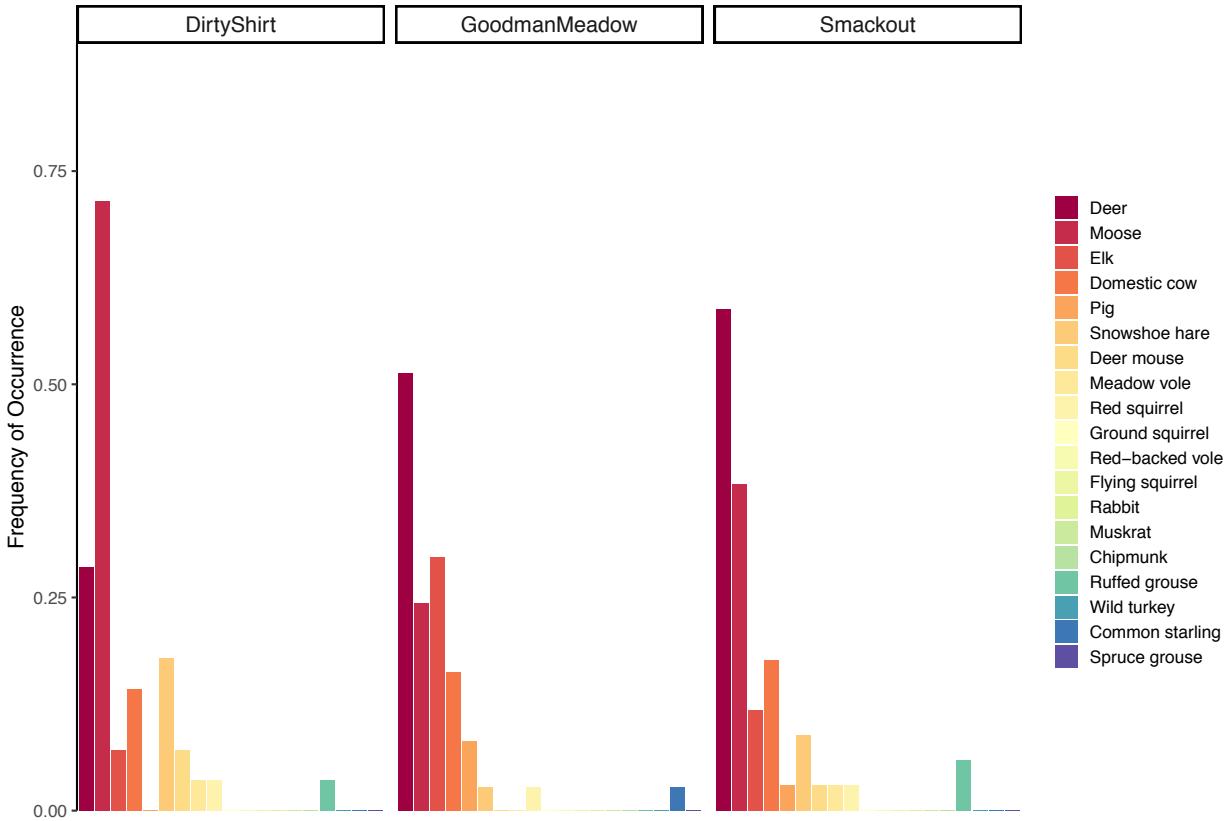

Figure 5 Significant spatial differences in the wolf diet profiles among three wolf pack ranges, using the frequency of occurrence of 19 prey species ($p = 0.001$).

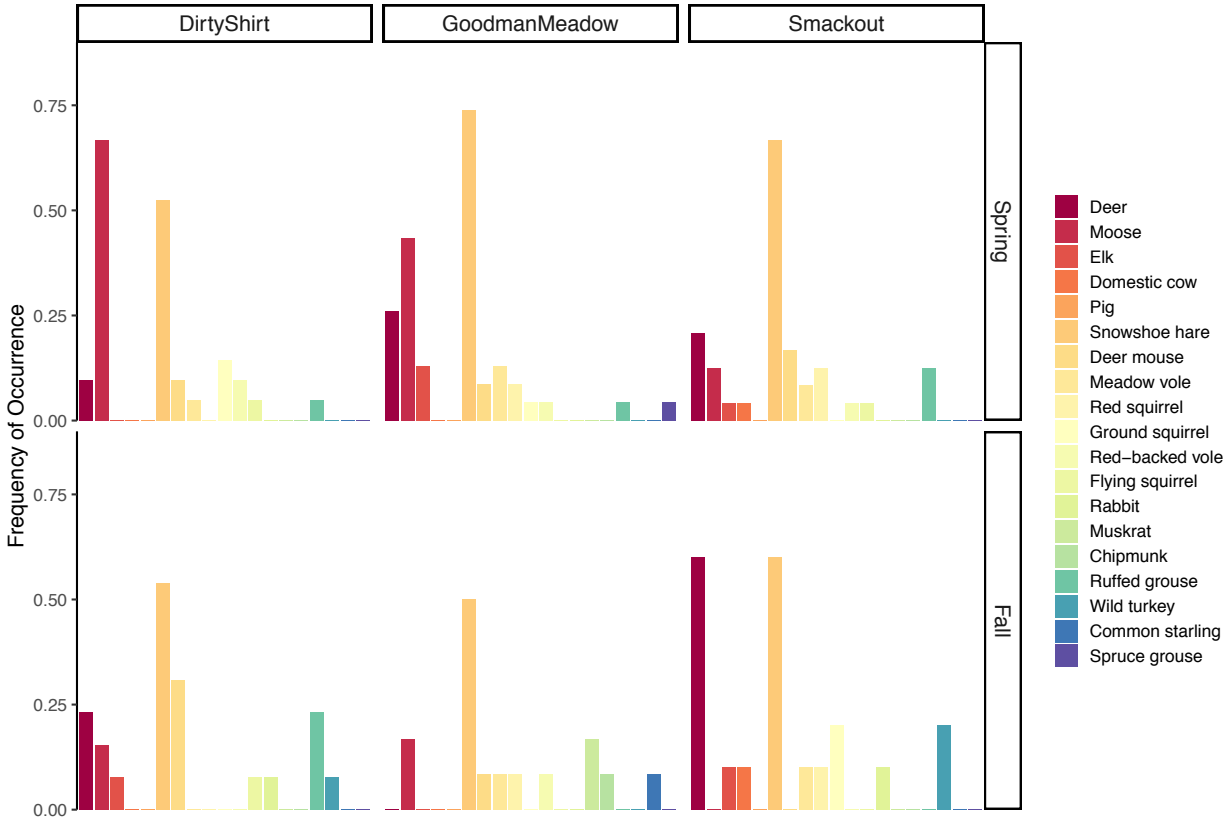

Figure 6 Spatiotemporal variations in the diet profile of coyotes, using the frequency of occurrence of 19 prey species. Both the main terms and the interaction term were significant based on perMANOVA analysis (season $p = 0.037$; Pack: $p = 0.003$; pack:season $p = 0.043$).

Table 1 Dietary overlap between wolves and coyotes in different seasons or wolf pack ranges. Dietary overlap was determined with Pianka's adaptation of the niche overlap (*O* metric), ranging from 0 (no overlap) to 1 (complete overlap). Sample size (N) for each predator in each season or wolf pack range was also given.

	Dirty Shirt		Goodman Meadows		Smackout	
	Spring	Fall	Spring	Fall	Spring	Fall
N (Wolf)	7	21	13	24	24	10
N (Coyote)	21	13	23	12	24	10
O metric	0.70	0.56	0.58	0.08	0.41	0.74

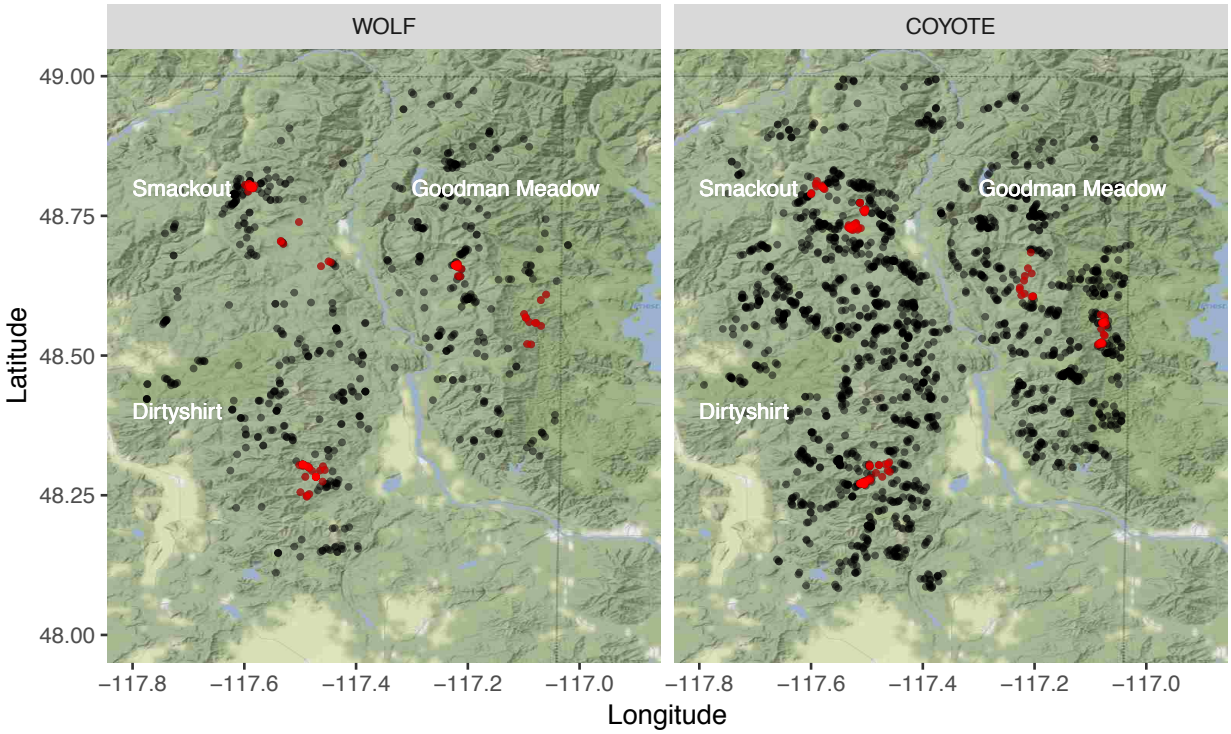

Supplementary Figure 3 Samples used in this study were selected from an ongoing project with 647 wolf fecal samples, and 1893 coyote fecal samples.

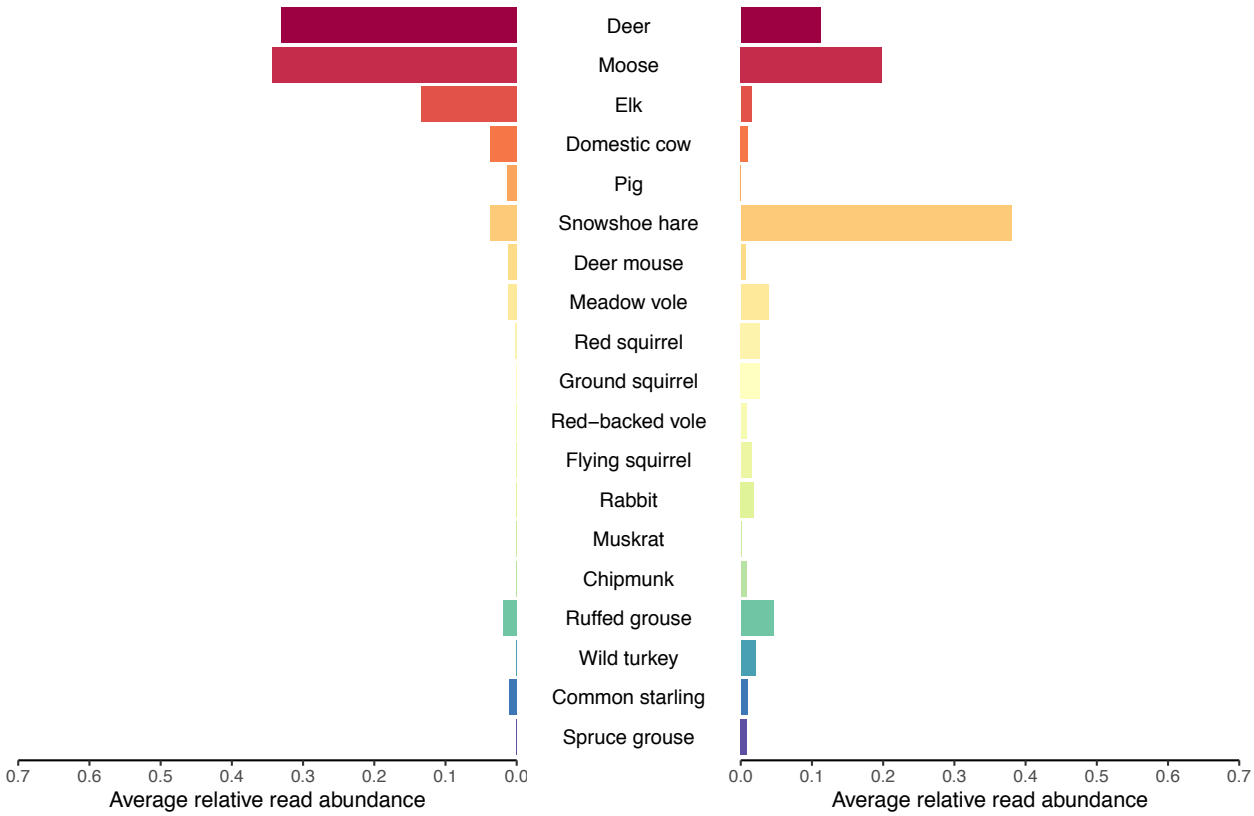

Supplementary Figure 2 Diet profiles of wolves ($N = 99$) and coyotes ($N = 103$) using the average relative read abundance of 19 prey species.

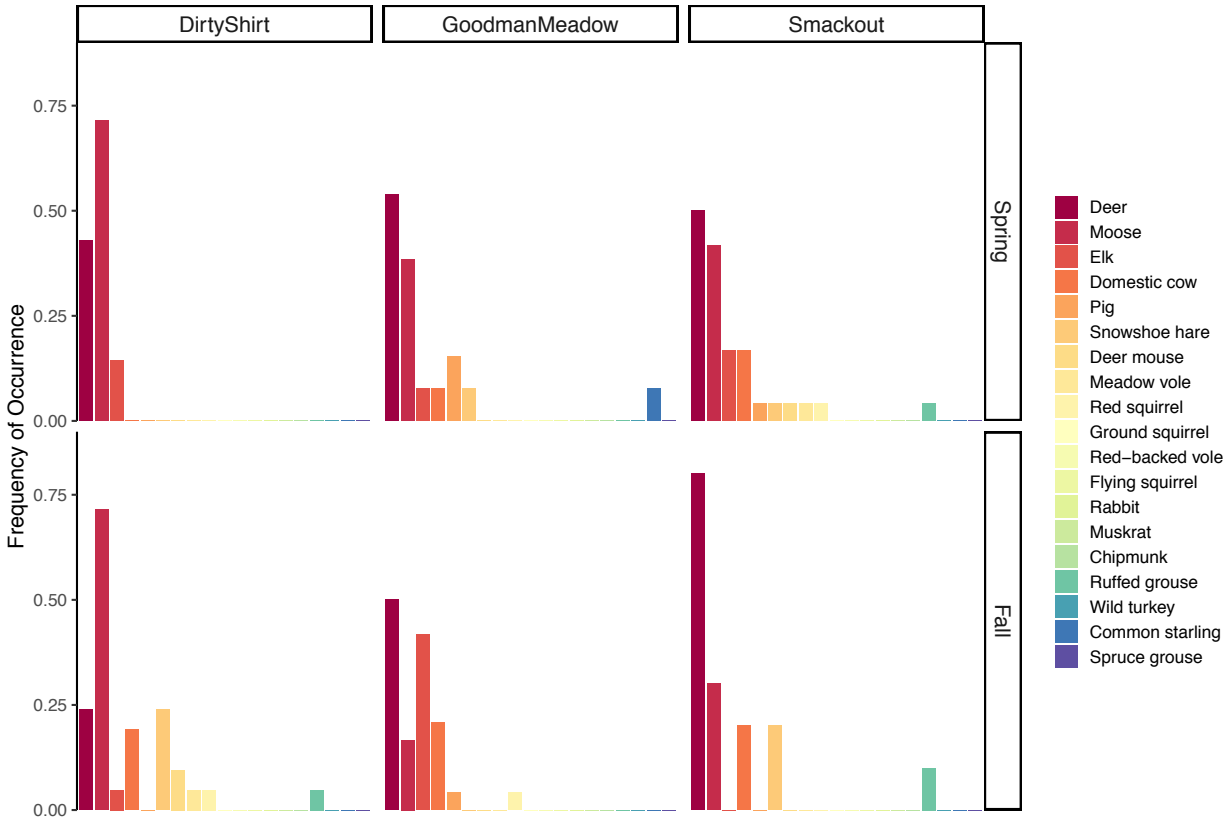

Supplementary Figure 3 Spatiotemporal variations in the wolf diet profile, using the frequency of occurrence of 19 prey species. The dietary differences among wolf pack ranges were significant (p = 0.001). There was no significant seasonal difference in wolf diet (p = 0.448) nor significant interaction between seasons and wolf pack ranges (p = 0.095).

Supplementary Table 1 Impacts of the predator-specific blocking primer on the occurrence of difference prey species.

Prey	Without blocking primer	With blocking primer
Chipmunk	1	0
Common starling	2	2
Deer	50	60
Deer mouse	8	15
Domestic cow	13	12
Elk	19	22
Flying squirrel	2	3
Ground squirrel	6	6
Meadow vole	8	10
Moose	60	62
Muskrat	2	1
Pig	4	3
Rabbit	2	2
Red squirrel	5	10
Red-backed vole	3	4
Ruffed grouse	6	11
Snowshoe hare	68	65
Spruce grouse	1	1
Wild turkey	3	3

Supplementary Table 2 Wolf pack size from 2015 to 2017 based on Washington Department of Fish and Wildlife Annual Report.

Pack	2015[1]	2016[2]	2017[3]
Dirty Shirt	8	13	7
Goodman Meadows	7	7	5
Smackout	8	8	6

Note: [1]: Washington Gray Wolf Conservation and Management 2015 Annual Report (https://wdfw.wa.gov/publications/01793); [2]: Washington Gray Wolf Conservation and Management 2016 Annual Report (https://wdfw.wa.gov/publications/01895); [3]: Washington Gray Wolf Conservation and Management 2017 Annual Repot (https://wdfw.wa.gov/publications/01979);

Supplementary Table 3 List of samples found to contain domestic cow DNA

Sample ID	Predator ID	Cow Read Count	Pack Range	Season	Year
9183	COYOTE	33	Smackout	Fall	2015
847	COYOTE	26	Smackout	Spring	2015
164077	WOLF	6	DirtyShirt	Fall	2016
9106	WOLF	32	DirtyShirt	Fall	2015
9107	WOLF	81	DirtyShirt	Fall	2015
9113	WOLF	220	DirtyShirt	Fall	2015
7190	WOLF	14	GoodmanMeadow	Fall	2015
7191	WOLF	528	GoodmanMeadow	Fall	2015
7193	WOLF	4	GoodmanMeadow	Fall	2015
7198	WOLF	17	GoodmanMeadow	Fall	2015
7204	WOLF	1585	GoodmanMeadow	Fall	2015
308	WOLF	56	GoodmanMeadow	Spring	2015
164007	WOLF	8	Smackout	Fall	2016
164010	WOLF	4	Smackout	Fall	2016
170859	WOLF	7	Smackout	Spring	2017
829	WOLF	127	Smackout	Spring	2015
831	WOLF	327	Smackout	Spring	2015
840	WOLF	158	Smackout	Spring	2015